6-1961

Operational Characteristics of a Fission Gas Detector

Raymond Curtis Lee
University of Tennessee - Knoxville

To the Graduate Council:

I am submitting herewith a dissertation written by Raymond Curtis Lee entitled "Operational Characteristics of a Fission Gas Detector." I have examined the final electronic copy of this dissertation for form and content and recommend that it be accepted in partial fulfillment of the requirements for the degree of Doctor of Philosophy, with a major in Chemistry.

George K. Schweitzer, Major Professor

We have read this dissertation and recommend its acceptance:

George T. Trammell, John A. Dean, William E. Bull, Hilton A. Smith

Accepted for the Council:
<u>Dixie L. Thompson</u>

Vice Provost and Dean of the Graduate School

(Original signatures are on file with official student records.)

May 20, 1961

To the Graduate Council:

     I am submitting herewith a thesis written by Raymond Curtis Lee entitled "Operational Characteristics of a Fission Gas Detector." I recommend that it be accepted in partial fulfillment of the requirements for the degree of Doctor of Philosophy, with a major in Chemistry.

_____
Major Professor

We have read this thesis and recommend its acceptance:

_____

_____

_____

_____

Accepted for the Council:

_____
Acting Dean of the Graduate School

OPERATIONAL CHARACTERISTICS OF A FISSION GAS DETECTOR

A Thesis

Presented to

the Graduate Council of

The University of Tennessee

In Partial Fulfillment

of the Requirements for the Degree

Doctor of Philosophy

by

Raymond Curtis Lee

June 1961

ACKNOWLEDGEMENT

TABLE OF CONTENTS

LIST OF TABLES

LIST OF FIGURES

CHAPTER I

INTRODUCTION

A. The Purpose of This Research

One of the major problems associated with the operation of nuclear
reactors is the radioactivity hazard caused by the release of fission
products from the fuel. In a solid-fuel reactor, the uranium is usually
present as an alloy or in the form of UO_2, either in the pure state or
mixed with other oxides which improve the thermal and mechanical properties
of the material. As the fuel material undergoes fission in the reactor,
radioactive fission products are produced. If they were not prevented
from doing so, these fission products would diffuse out of the fuel ma-
terial, enter the reactor coolant as it flows past the fuel, and be
carried from the reactor. The magnitude of the hazard thus created de-
pends on the type of reactor, the reactor power, shielding of the coolant
lines, and other factors. In a reactor where the coolant makes only a
single pass through the system, such as the air-cooled graphite reactors,
the fission products are discharged into the atmosphere or into some
coolant sink. This situation is usually unacceptable from a health stand-
point. If the coolant flows in a closed loop, as in most present day
water-cooled reactors, the fission products build up in the coolant, pro-
ducing a radiation hazard in the coolant loop.

In most reactors the fission product release is prevented by clad-
ding the fuel elements with a metal sheath impervious to fission products.
The fuel elements for the oldest operating reactor, the ORNL Graphite

Reactor, are natural uranium slugs clad with aluminum.[1] Many of the later gas-cooled and water-cooled reactors have utilized aluminum or aluminum alloy cladding over a central uranium-containing core.[2] Another metal widely used for cladding, both in the pure form and as an alloy, is zirconium.[3] However, no clad process has yet been found which is completely failure-proof; for this reason, a fission product detector of some kind is often placed in the exit coolant from a reactor. Any leak or failure in the cladding will be indicated by this detector; if the condition is serious, the defective fuel element can be located and replaced.

As requirements for higher temperature fuel elements have come about, advanced metallurgy and ceramic technology have been used to design new fuel elements. These prototype fuel elements are subjected to regular mechanical and physical integrity testing during the course of their development. If they prove satisfactory in these respects, they are usually operated in a test reactor (such as the Materials Testing Reactor, MTR, or the Oak Ridge Research Reactor, ORR) before they are finally considered reliable for reactor construction purposes.

The General Electric Company, Aircraft Nuclear Propulsion Department, has undertaken the responsibility for construction of a direct cycle, air cooled aircraft propulsion reactor.[4] In this reactor, heat is transferred directly from the fuel elements to the cooling air, which makes a single pass through the system. From a reactor standpoint, the development problems are similar to that of a gas-cooled power or research reactor. The principal difference is in the higher temperature requirement, and of course the severe weight limitations. In development of a gas-cooled

reactor, a large safety margin is maintained between fuel element operating temperature and fuel element failure (or cladding failure) temperature. In the ANP reactor, the temperature of the fuel elements will be kept as near the failure temperature as is feasible. In fact, a certain small release of fission products from such a reactor could probably be tolerated because of the military application of the powerplant. Development of high-temperature fuel elements has been underway continuously since the inception of the program.

A facility has been made available to the GE-ANP project by the Oak Ridge National Laboratory for dynamic testing of prototype fuel elements. One position in the Low Intensity Testing Reactor (LITR) and one in the Oak Ridge Research Reactor are in use. The Oak Ridge Research Reactor system utilizes hole F-2, a core position in the reactor lattice. Cooling air for fuel specimens tested in this position is furnished by large compressors, located just north of the ORR building. Depending on the fuel loading of the specimen under test and its heat transfer characteristics, the air flow can vary between 10 and 100 cubic feet per minute over the test. In order to evaluate properly the specimen being tested, it is desirable to know the fission product concentration in the exit air at all times. For this purpose, the F-2 test system incorporates several devices for monitoring the exit air activity, similar to the fission product detectors used in gas-cooled reactors. This research is an evaluation of one of those devices.

B. Measurement of Radioactivity in Gases

1. ### Counter Adaptations

The methods for detecting and measuring fission product concentrations, whether in liquid or gaseous media, nearly all depend on counting the emitted β and γ rays. Thus any of the usual counting methods can be adapted to detection of fission products. Since sampling of gaseous and liquid media present slightly different problems, only the methods useful in analysis of radioactivants in gas will be examined in detail.

Most of the work in adapting counters for measurement of radioactivity in gases has been for the purpose of determining the disintegration rate of weak beta emitters, principally carbon-14 and hydrogen-3 (tritium). A number of investigators have used Geiger-Mueller and proportional counters for this purpose. One of the earliest modifications to be used for quantitative work in radioactive gas analysis is described by Kummer.[6] This consisted of an end-window Geiger-Mueller tube of the usual type, with a very thin window. Attached directly to the end of this tube was a chamber through which the radioactive gas was passed. The Geiger-Mueller tube window was thin enough so that when carbon-14 was introduced into the chamber in the form of carbon monoxide, the weak carbon-14 beta would penetrate the window and produce counts in the tube. The self-adsorption of betas by the carbon dioxide gas is considerably less than in the most frequently used carbon-14 analysis method, the counting of solid barium carbonate; furthermore, the system could be easily adapted to continuous flow analysis of carbon-14 dioxide gas. Such a use of this counter is described in connection with gas chromatography studies by

Kokes, Tobin and Emmett.[7] These workers used the counter to detect the
various tracer-labeled components carried by the sweep gas as it passed
through the adsorption column.

The end-window Geiger-Mueller tube, although more sensitive for
carbon-14 analysis than solid barium carbonate counting, is quite fragile
and still absorbs a portion of the weak ($\sim$ 0.15 Mev maximum energy) carbon-
14 betas. For many years, windowless counters have been in use in which a
suitable counting gas environment in the active volume is provided by a
slow flow of a counting-gas mixture through the tube. These counters are
usually operated in the proportional region; the sample is customarily
introduced (as a solid) on a small planchet at the bottom of the tube.
Since it seemed reasonable that a radioactive gas could be mixed with or
replace the counting-gas to give increased sensitivity to weak beta parti-
cles, a number of counters employing this principle were constructed. A
proportional counter will function as a counting device with almost any
filling gas, but the counting characteristics of the tube are not as re-
producible and clear-cut with non-conventional gases unless adequate pre-
cautions are taken. One of the determinations of the half-life of carbon-
14 was made with a proportional counter filled with carbon-14 dioxide.[8]
Robinson[9] made full use of the sensitivity inherent in the design by
adapting it to hydrogen-3 counting. The very weak hydrogen-3 beta particles
(maximum energy 0.055 Mev) are extremely difficult to count accurately by
conventional methods. In this early counter, the glass counter walls con-
stituted a source of some difficulty.

A later modification using a metal-wall counter was described in
1955.[10] The hydrogen-3 is introduced into these counters as part of a

labeled methane molecule; since methane is a normal constituent of many counting-gas mixtures, a proper counting environment for the tube is easily provided.

Wolfgang and Rowland[11] used a direct-flow proportional counter for radioassay by gas chromatography of hydrogen-3 and carbon-14 labeled compounds. The sweep gas was helium, which passed through the counter with the chromatographic column effluent. In order to give the gas mixture the proper counting characteristics, methane was injected into the system between the column and the counter.

An excellent summary of the capabilities of this type of counter, along with details of counter construction, is given by Wolfgang and Mackay.[12] A proportional gas counter, used for non-continuous batch assay of gases, utilizes P-10* counting gas along with the radioactive gas introduced into the active volume of the counter. This counter is about 95 per cent efficient, and will give the disintegration rate of a sample directly when a few small corrections are applied. The counter is easily taken apart for decontamination. A gas flow counter, similar to the batch counter but for continuous flow applications such as gas chromatography, is also described. The counter is windowless and can therefore be used for carbon-14 and hydrogen-3 without calibration. A window flow counter can be used where there are no requirements for counting weak betas. The window counter comes in three sections; the center one is a long flat rectangular compartment having the windows, through which the sample flows. The other two sections are hollow semicylinders, each of which has a

---

*P-10 is a mixture of 10 per cent methane and 90 per cent argon.

collecting wire down the center. When these parts are clamped together, a counting gas such as P-10 is flowed through the counting sections. The window thickness can be adjusted to absorb all hydrogen-3 betas, but still pass carbon-14 betas so that carbon-14 can be assayed in the presence of hydrogen-3. Counters analogous to these three types have been used in a number of cases.[13-18]

As a device for counting the weak betas for which it was designed, the gas flow counter has no competitor except a very sensitive ion chamber. Although designed for weak betas, these counters work well for any beta emitter and could be readily adapted to assay of fission gases in air. There is one serious limitation to the use of these counters for this kind of work, and that is their inherent low maximum counting rate. Above about 4000 counts per second, most proportional counters begin to saturate, and the long dead-time makes large corrections necessary.

Scintillation counters are capable of much higher counting rates than Geiger-Mueller tubes, but they have found little application in gas analysis. The main reason for this is the low sensitivity of scintillators, caused by the poor geometry of a solid scintillator embedded in the wall of the gas container. Also, scintillators present certain difficulties in detection of weak betas, which have been the main concern of persons interested in gas analysis. However, scintillation counters have certain advantages not found in Geiger-Mueller tubes and ion chambers, principally the ability to resolve gamma-ray spectra.[19,20]

One method of using scintillators which provides an efficiency of about 75 per cent for alpha-counting is described by Van Dilla and Taysum.[21]

A glass gas chamber with a volume of 120 cm.^{3}, which was designed specifically for radon counting, was mounted directly on the end of a RCA-5819 or Dumont-6292 phototube. The entire inside surface of the container was coated with a film of zinc sulfide, and the outer surface (except for the bottom) was painted white. The gas was admitted through a valve; scintillations on the zinc sulfide are reflected back into the phototube giving nearly 2 π geometry.

Another ingenious method which improves the efficiency of scintillators for gas counting is the use of a gaseous scintillator in a container attached to the phototube. Considerable success had been obtained in the use of liquid scintillators; a weak β-emitter or other radioactivant was dissolved in a liquid scintillator such as solutions of an alkali halide,[22] then the mixture was poured into the counting chamber. Scintillations originating throughout the mixture were then counted by one or more phototubes mounted at the edges of the chamber. In analogy to this, a number of investigators have made use of scintillations in the rare gases to provide a means of radioassay. Eggler and Huddleston[23] first reported scintillations in gases detectable with photomultiplier tubes. They found that a wavelength-shifter between the scintillating gas and the photomultiplier was necessary to provide light of the correct frequency to initiate phototube action. In a counter they developed,[24] argon was used as the scintillating gas to detect alphas and other heavy particles, such as fission recoil nuclei (from a fission event occurring within the chamber). Other counters used xenon as the scintillator[25] or a mixture of gases including at least one noble gas.[26] These counters were all quite insensitive to

beta and gamma rays, and therefore unsuitable for fission product assay, although future developments in this field may erase these limitations.

Another solution to the sensitivity problem is the use of high-pressure gases in the chamber attached to the phototube. Drickamer[27,28] and his co-workers developed methods for the determination of the activity of high-pressure gases, by a batch-wise process. Their gas chamber was under such high pressure that a light-pipe of considerable length had to connect the scintillator to the phototube. Their experiments involved tagged carbon-14 and sulfur-35 atoms. Another counting system has been developed which monitors a flowing gas continuously.[29] This utilizes an anthracene crystal to detect the betas given off by sulfur-35, which is incorporated into hydrogen sulfide gas. The tagged hydrogen sulfide, in a mixture of water vapor, carbon dioxide, and hydrogen sulfide, was counted as it passed over the crystal and the result interpreted, with other measurements, to give the exact composition of the vapor at all times.

A direct approach to gaseous flow counting was used by Evans and Willard.[30] They used a thin wall, 1 ml. glass thimble in a sodium iodide (thallium activated) scintillation well crystal. The effluent gas from a gas chromatograph flowed directly through the thimble; gamma-emitting tagged compounds gave peaks in count-rate as they were eluted from the column. Embedding the thimble in a well crystal improves the geometry considerably. Actually, the high efficiencies and favorable geometries which most investigators have sought in developing scintillation gas counters would probably not be necessary or even desirable in monitoring

air containing fission products from a reactor or fuel test. The count rates for almost any gas coming from a reactor will be considerably higher than the activities normally used in tracer gas, even if no fission products are being released into the gas stream.

The third method in common use in determining the radioactivity of gases employs ion chambers. These versatile electronic devices have been used over the entire range of radioactivity measurement from thousands of roentgens per hour to a few disintegrations per minute.[31,32] In fact, single instruments can be made to cover several decades of counting rate by appropriate switching arrangements. One of the early applications of ion chambers was in measuring the weak carbon-14 betas. Since the volume of the ion chamber can be filled with the radioactive gas, and all of the ionization produced by the radioactive particles collected and measured, ion chambers are quite suitable for measurement of weak betas and alphas. In the ion chamber of Henriques and Margnetti,[33] carbon-14 dioxide was used to fill the spherical chamber; a voltage was applied and the current produced was measured by a Lauritzen electroscope. This apparatus is very sensitive. A more convenient way of measuring ion chamber currents is with the vibrating reed electrometer. Jesse, Hannum, Forstat and Hart[34] used the vibrating reed and Lindemann electrometers in their measurement of carbon-14 dioxide activity. Their ion chamber had a volume of 150 cc., which is about the size of most chambers used in tracer work, and was operated at atmospheric pressure.

One of the most sensitive ion chambers reported was used for measuring the disintegration rate of hydrogen-3.[35] Currents down to 10^{-13} ampere were measured directly; lower currents were detected by charging a condenser,

then measuring the charge on the condenser. Voltages between 90 and 450 volts were used with little change in relative current over this range, unless saturation occurred. When the activity inside the chamber produces ions at such a rate that an appreciable fraction will recombine before they can be collected, then the chamber is saturated. The upper voltage cannot be raised much higher because electron multiplication starts. The lower limit of sensitivity was $\sim 5 \times 10^{-16}$ ampere, which corresponded to 25 counts per second. With care in calibration, a tritium analysis was accurate to better than ± 1 per cent.

Janney and Moyer[36] give procedures for routine carbon-14 dioxide analysis, and give an error analysis of ion chamber measurements. Carbon-14 dioxide is usually made from solid barium carbonate by reaction with sulfuric or other acid. The circuitry for ion chambers used in carbon-14 analysis is treated extensively by Brownell and Lockhart,[37] who also give a procedure for gas counting by ion chambers. The measurement of gamma-rays in gas-filled ion chambers is somewhat different than beta measurements; for good sensitivity and reproducibility, it is desirable to have the emitted radiation completely adsorbed in the volume of the chamber and all of the ions collected. Because of the long range of gamma rays, many of the gammas in a gas-filled chamber will escape and not be counted. However, gamma-sensitive ion chambers have been made. Bullen[38] describes an ion chamber used in radioassay work, which is sensitive to betas and gamma emitters over the range of 20 microcuries to 400 millicuries. High-pressure ion chambers for counting solid or liquid gamma sources, inserted into a well in the chamber, are common; they do not encounter the gamma-

escape problem of a gamma-emitting gas filled chamber. In general, any
ion chamber must be calibrated with the particular isotope to be counted
in order to give accurate disintegration rates since the number of ions
formed varies with the energy and type of emitted radiation.

Ion chambers have also been used in continuous flow experiments.
Riesz and Wilzbach[39] used an ionization chamber in the effluent line of a
vapor chromatograph. Wilson and Calvin[40] used a continuous flow ion
chamber to monitor and record carbon-14 dioxide activity. The carbon
dioxide pressure in the chamber was also recorded and a correction made,
so that the disintegration rate could be accurately obtained. An ion
chamber which has found some application in detection of radiogases was
invented by Kanne.[41] This chamber was evaluated by Fitzgerald and
Borelli.[42] The Kanne chamber is quite large, having a volume of about
16 liters, and is used for radioanalysis of air. A de-ionizer removes ions
and dust-borne radioactive material before the air enters the sensitive
volume of the chamber. The air follows a folded-flow path within the
chamber before it is discharged; only disintegrations taking place during
this time are counted. The chamber is sensitive primarily to beta rays;
it must be calibrated for each beta-emitting gas to be assayed.

A valuable summary of ionization chamber assay of radioactive gases
is found in UCRL-3499, by Tolbert.[43] Construction of the Borkowski[44] and
Tolbert-Carey ion chambers is described, and the general operating char-
acteristics of ion chambers is discussed. The author states that an
accuracy of $\pm$ 0.2 per cent in ion chamber measurements on radioactive gases
can be obtained. Procedures in carbon-14 dioxide and hydrogen-3 continuous

assay are given; the output of the ion chamber is amplified and recorded directly on a strip-chart recorder. Ion chamber calibration, an important phase of quantitative work, is explained in detail.

Other methods of radioassay of gases, not directly involving counters, have been tried. None of these methods have proven useful for fission product measurement.

2. Air Sampling

Although the term "fission gas" should strictly apply only to the fission-produced xenon and krypton isotopes, nearly any of the fission products released by a fuel element into a moving stream of air will be entrained by the air and carried out of the reactor. These radioactive atoms or molecules either are adsorbed on dust particles in the air, or form colloidal agglomerates which are easily suspended in the air. The amount and nature of the activity, with the velocity and temperature of the air determine how well the material will remain in suspension; some of the less-volatile fission products are entrained in hot air and then plate out along the exit air ducting when a cooler region is reached.

A variety of equipment and techniques is used in sampling the atmosphere for radioactive contaminants.[45] Most of these techniques were developed for health-physics monitoring of the air, but can be adapted to situations in which the activity levels are much higher. Even the noble gases xenon, krypton and radon are sometimes present, adsorbed on particulate matter in the air, especially at low concentrations, and they can be sampled by some methods. Since the amount of radioactivity in the atmosphere is usually small, the radioactivants are first separated out

and concentrated by some means, and then counted.

A method for detecting hydrogen-3 in the atmosphere by continuous monitoring has been worked out at Los Alamos.[46] This method does not depend on separation of the activity; it is analogous to certain of the gas-analysis methods discussed in the last section. A motor-driven blower pulls air continually through an ion chamber, where the ions present from hydrogen-3 disintegrations are collected. On the most sensitive scale, 80 microcuries of hydrogen-3 per cubic meter of air give a full reading. This "tritium sniffer" was hooked up to a system which sounded an alarm when a dangerous concentration level was reached. One difficulty with this instrument is that any source of ionization near the monitor, i.e., flames, will set the monitor off.

The separation of dusts and mists from air has been under study for many years. The Chemical Engineer's Handbook[47] gives a summary of several separators used industrially; some of these systems have also been used to clean up the effluent from gas cooled reactors. The Radiation Hygiene Handbook[45] lists a number of separation methods which have been used for air sampling. These include filters, charcoal trapping, impingers, impactors, thermal precipitators, and electrostatic precipitators. The most common of these aerosol separation methods is air filtration.

One of the first theoretical approaches to air filtration was developed by Langmuir.[48] His theories were investigated and modified slightly by Ramskill and Anderson.[49] A more complete approach to air filtration has been worked out by Chen.[50] He discusses the filtering efficiency for various particle sizes and the pressure drop for air flowing through a

fibrous filter. There is a size of particle which penetrates any filter best; particles both larger and smaller are trapped more easily. Relations between air flow and this particle size are given.

Portable and permanent air monitors in common use near reactors and fuel-element recovery plants employ filters through which air is drawn by motor-operated blowers. A portable-disc sampler (PDS) is used by the Oak Ridge National Laboratories for spot checks of air activity, in such places as hot cells and stack areas.[51] A disc of filter paper about one inch in diameter is used; air is drawn through the filter paper at a rate of one cubic foot per minute. Sampling periods are usually 15-20 minutes long. A flexible extension tube several feet long can be used on the inlet side to sample air to which there is no easy access, such as a highly-contaminated hot cell. The filter paper is removed from the sampler and counting done in the regular manner, for alpha, beta and gamma emissions.

A permanent constant air monitor (CAM) is also used in reactor buildings and other potentially hazardous areas. The sensitive element in this machine is a cylindrical Geiger-Mueller probe. This is held in a wire cage slightly larger than the probe; a piece of filter paper is wrapped around this cage and taped into place. A blower pulls air through the filter at a rate of five cubic feet per minute. The probe and cage are inserted in a lead shield to protect against direct radiation, i.e., the opening of a reactor beam hole. Filters are changed daily; as air is drawn through the filter, the count rate rises continuously during the 24-hour period. The count rate is recorded on a strip-chart recorder attached to the instrument, and an alarm is provided which sounds if the

air activity gets too high. This instrument is sensitive to beta and gamma activity.

A continuous air monitor for alpha activity has been developed by Sawle.[52] This uses a filter paper 4-3/4 inches in diameter; a flow of 16 cubic feet per minute is pulled through the filter. The trapped alpha activity is counted continuously with scintillation counters. This monitor is designed to discriminate against alpha counts due to natural radioactivity (radon and its daughters), and count only the dangerous plutonium, thorium and uranium isotopes. This is done by biasing one counter so that only the 7.68 Mev polonium-214 alpha, which constitutes 94 per cent of the naturally occurring alpha activity, is counted. This count rate is subtracted from the total activity to give the plutonium, thorium and uranium counts; alphas from these isotopes are all 30 per cent or more lower in energy than the polonium-214 alpha.

A number of people have built air monitors on the principle of a moving strip or tape of filter paper. Kuper, Foster and Bernstein[53] used a strip of paper which moved at 1 inch per hour across an aperture through which air was drawn. The air flow was about 5 cubic feet per minute. After the dust and activity had been collected, the strip passed in front of beta and alpha counters and was counted. By varying the distance between the collector and detectors, decay times of from one-half to 18 hours were possible. A single roll of paper lasted 6 months; sections could be cut from the exposed roll for decay determinations, gamma spectrum determinations, and other studies. A similar system with shorter decay time was designed by Mansfield.[54] The filter strip was drawn over two holes,

each 2 inches in diameter. Velocity of air through the filter paper could be varied between 100 and 500 feet per minute; the filter paper velocity was normally 3.7 inches per hour, but this could be varied by a factor of 4 in either direction. The alpha and beta counters used were mounted directly over the air-flow holes; a response time of only 2 or 3 minutes could be realized through this arrangement. Another moving-filter system[55] had a flow of 3 cubic feet per minute through the paper; filter tape speed was 1 inch per hour. The tape was monitored with two beta-gamma Geiger-Mueller tubes and two alpha scintillation counters, so spaced that the decay of the two kinds of activities could be measured. The results were recorded on a strip-chart multiplex recorder. Recently, a windowless flow counter suitable for either alphas or betas has been developed for paper filter strip counting.[56]

Special types of filter papers have been developed for air monitoring.[45] Most filters are counted directly, without processing, but some filters can be dissolved and a more suitable counting sample prepared. Columns or tubes loaded with lead shot, sand, glass fibers, etc. have been used for special applications. The so-called "millipore" filters, which are much more efficient in removing small particles than fibrous filters, have been used.

The use of filters for entrapment of aerosols is simple and inexpensive; however, filters cannot hold the noble gases such as krypton and xenon. The best trapping method for these gases appears to be activated charcoal. The use of charcoal involves certain difficulties, notably in reducing the trapped activity to a form in which it can be counted. Applications of radiochemical techniques are often required to separate con-

stituents when a mixture of radioactive gases, such as is released by fuel element irradiations, is trapped on the charcoal. A typical example of the use of charcoal is described by Hursh.[56] A charcoal trap was attached to a gas-mask apparatus; a subject breathed into the mask and the radon in his breath was trapped by the charcoal. After a suitable collection period, the charcoal was removed from the mask and placed in a container, where it was heated to drive off the radon. A sweep gas was passed through the container and the radon carried to an alpha-particle detector. The detector used was a modified ion chamber;[57] each alpha produced enough ionization for a current pulse, even though the voltage applied to the chamber was too low for any electron multiplication.

Extensive work on the use of charcoal for trapping fission products has been carried on by W. E. Browning and co-workers[58-63] at Oak Ridge. Most of these reports are concerned with the use of charcoal filters to clean up reactor, nuclear-fuel processing and in-pile experiment effluent gases. In one instance,[62] however, the charcoal traps were used to detect the release of fission products in an in-pile loop. This experiment involved the operation of a fuel-element specimen in a high pressure system containing NaK as a coolant. Periodically, the gases present in equilibrium with the NaK system were bled off through a charcoal trap. The trap was counted, and any leak of fission products was determined.

The characteristics of charcoal adsorbant for krypton and xenon have been carefully determined by Adams and Browning.[58-63] A theoretical expression for holdup time of these gases was derived and verified. Xenon has a much longer holdup time in charcoal than krypton. Holdup time de-

creases logarithmically as temperature increases; the presence of other gases such as water vapor in the air stream also decreases holdup time. For the less volatile fission products such as iodine and bromine, holdup time is essentially infinite for reasonable amounts of charcoal and reasonable flow velocities. Adsorbants other than charcoal were studied; these included silica gel, activated alumina and molecular sieves. None of these was as good as charcoal.

Charcoal traps have been used to measure the exit-air activity of Low Intensity Testing Reactor tests for several years.[64] These traps are immersed in a bath of trichloroethylene and dry ice; at this low temperature (-61°) the noble gases are retained quite well in the trap. Traps are normally run for a few hours during a test, then removed. A radio-chemical separation of the entrapped activity is necessary before counting for the various constituents is carried out; gamma spectroscopy is used as an aid in determining specific isotope activities.

Impingers provide another means of collecting aerosols. An impinger consists of a jet which discharges against a flat plate under water (or other liquid); mists and dust in the air stream are trapped in the liquid or on the plate. The impinger is not efficient for fine dust and fumes, and has been little used for collecting radioactive samples. Impactors use no liquid; the jet discharges directly against a flat plate which traps the particles. A sticky substance, such as vaseline or glycerine, is often smeared on the collection plate to improve collecting efficiency. The sample collected can usually be counted directly. High-flow-velocities yield better efficiencies (i.e., collect smaller particles). Even for high

velocities, the small size of the nozzle used limits the flow rate, so a high concentration of material or a long sampling time is needed for good results. Impaction on a moving plate or strip has not worked well because the radioactive dust concentration is not usually high enough.

One application of the impactor to health-physics work has been made by Tait.[65] He used an impactor to sample air for plutonium dust. The air flow was 500 to 1000 liters per minute through the impactor, with a corresponding linear velocity at the nozzle of 60 to 75 meters per second. The air stream impacted on a vaseline-covered plate. The dimensions of the nozzle and flow velocity were adjusted so that particles of one micron or greater diameter were impacted on the plate; these particles carried attached plutonium dust. Particles less than one micron in diameter remained in the air; radon and its decay products were primarily attached to particles of this size. Thus, a separation was effected. After a sampling time of 2-5 minutes, the collection plates were taken up and counted. A more elaborate impactor with 4 stages is described by May.[66] This impactor actually separates particles into 4 groups of different sizes. A general description of impactors and centrifugal separators (not used for air sampling) is found in an article by Johnstone and Roberts.[67]

Thermal precipitators employ a hot wire near a cold plate; particles agitated to rapid thermal motion by the wire impact against the plate and stick. This device is almost 100 per cent efficient, even for small particles. However, only very slow sampling rates are possible; air flows in many cases are only a few milliliters per minute, and the highest practical flows approach one liter per minute. Further, the activity tends to

collect directly under the wire. An oscillating precipitator has been described[67] which deposits particles in a uniform band across the collection plate. These devices are used mostly for research and highly accurate work.

The last method of air sampling to be considered is electrostatic precipitation. The use of electrostatic methods of aerosol precipitation has been widespread since the discovery of the Cottrell precipitator; electrostatic precipitation can be used on a large scale for reactor effluent cleanup and on a small scale in air sampling instruments. An instrument using high voltage AC current for precipitation has been built.[69] Most of the devices, however, use DC voltage for their operation. The typical air sampler consists of a can with a wire down the center of it; high voltage is applied between the wire and the can and air is drawn continuously through the can with a blower. The suspended particulate matter is precipitated on the inner wall of the can, on a liner of cellophane, paper or metal. After the sampling period is over, the liner is removed and counted. Some liners can be flattened and counted directly. Electrostatic precipitation is very efficient (∼98 per cent) but the equipment is difficult to maintain and has not found extensive use in sampling for radioactive dusts.

One electrostatic sampler which has worked well utilizes a collector can with no liner.[70] A potential of 15,000 volts is applied to the central wire electrode; particles collect on the inner wall of the can from air passing through the system. After sampling is completed, the can is removed from the system and placed over an ion-chamber probe. Three

hundred volts are applied between the probe and can; the current is measured with a vibrating reed electrometer. After counting, the can is washed in nitric acid and used again. Sampling times in the experiments performed varied between 0.5 and 180 minutes; only alpha activities were assayed.

A precipitator which can be used on either large or small scale has been developed in Great Britain.[71] This device is a special Cottrell precipitator which has a moving film of water for the receiving electrode. A 3-inch diameter tube, from 3 to 8 feet long was used. A swirler at the top of the tube directed water down the inside surface of the tube. A central wire running down the center of the tube had a potential of 18.5 kilovolts. Air was drawn through the tube at velocities between 3 and 10 feet per second. Under these conditions, precipitation was better than 99.9 per cent efficient for removing industrial dust pollution. This type of precipitator has these advantages: (a) it has a very high efficiency; (b) it precipitates small, widely dispersed particles; (c) there is a very low pressure drop; and (d) the precipitator is continuously self-cleaning.

CHAPTER II

DETECTION OF FISSION PRODUCTS IN REACTOR EFFLUENTS

A. Water Cooled Reactors

Nearly every reactor which operates at a significant power level has some system for detecting cladding failures in the reactor fuel elements. Some of the cladding failure detection systems used in liquid cooled reactors are worthy of consideration for possible use in gas cooled reactors.

Most fuel element failure detection systems provide some method of detecting fission products in the presence of radiation from the coolant produced by neutron activation. One proposal which provides a unique solution to the failure problem without the need for fission product counting was advanced by Pobereskin and Sunderman, et al.[72] They suggested that each fuel element of a water cooled reactor should have a different tracer isotope added to it during manufacture; when a leak occurred, the faulty fuel element could be located by radiochemical analysis of the effluent water. This is the only system thus far proposed for water cooled reactors which both detects a leak and locates it.

One of the methods for detecting fission product leakage involves the counting of delayed neutrons emitted by the fission products bromine-87 and iodine-137. Calculations have been made on the sensitivity of this system.[73] There is some interference with the fission product neutrons from neutrons produced by the photodisintegration of deuterium in the water.

High-energy gamma rays, such as those from 7-second nitrogen-16, are able to cause this reaction. Also, some neutrons are produced in the decay of oxygen-17. This method was also proposed for a liquid-metal cooled reactor, where there should be less interference from coolant-produced neutrons.[74]

Another means of counting fission products in the presence of other radioactive species involved the use of a Cerenkov detector.[75] This consisted of a phototube looking directly at the coolant water; high energy beta particles emitted by the fission products produce light pulses as they are slowed by the water. This light pulse is counted by the phototube. By adjusting the bias of the counter so that only pulses from betas with 5 Mev of energy or greater are counted, it is possible to discriminate against non-fission product activity. There are a few short half-life fission products, such as bromine-87 and iodine-136, which have betas of more than 5 Mev and these are the ones detected.

Probably the most elaborate activity monitor for a water cooled reactor is used in surveying the Columbia river activity at Hanford.[76,77] An automatic analysis is made for neutron activation products, but not for fission products. A water sample is taken; sodium-24 and manganese-56 are determined by gamma-ray spectrometry on the untreated sample. After a 24-hour period to allow the sodium-24 and manganese-56 to decay, the sample is counted by gamma spectrometry again for neptunium-239. Copper-64 is determined by gamma-gamma coincidence counting. Another water sample is passed through a cation exchange column, which removes interfering substances and allows arsenic-76 to be counted by a gamma spectrometer. Some

samples are chemically treated to separate phosphorus-32 and silicon-31 from the other activities. The combined beta activity is determined, then the sample is recounted after 24 hours when only phosphorus-32 remains. Subtraction gives the silicon-31 activity. All of the processes are carried out automatically and the results recorded. In addition, another instrument measures the gross beta count rate. Water samples are pipetted automatically into depressions on an aluminum tape; the water is dried and the sample moved under a beta counter.

Another system almost as complicated is in use at the Materials Testing Reactor in Idaho for detection of fission products in the coolant water.[78,79] This system performs a continuous separation of fission product iodine on an ion exchange resin; by using gamma-ray energy discrimination, only iodine-136, iodine-134 and iodine-135 are counted. A small flow of water from the main reactor coolant loop is passed through a glass wool filter to remove particulate matter, then through a cation exchange column. This removes most normal radioactive contaminants and many fission products from the water, leaving only molybdenum, technetium, tellurium, bromine, iodine and rare gases. The cation column is followed by an anion resin, which retains the iodine. The gamma activity of the column is monitored by a scintillation detector. A similar system based on isotope exchange has been developed by Battelle Memorial Institute.[80] These investigators used a column of solid silver halide salt crystals and passed the aqueous fission-product-containing sample through the column. The radiohalides in the sample exchanged with halide ions in the column and were retained in the column. Then the radiohalide activity of

the column could be determined either by counting the delayed neutrons
from the bromine-87 and iodine-137, or by direct gamma monitoring of the
column.

A delayed-neutron counter and a direct-gamma monitor have also been
evaluated at the Materials Testing Reactor. The gamma monitor uses two
gamma spectrometers; one counts the nitrogen-16 activity, which is the
principle contributor to the background. The other channel counts fission
products in the 0.7-1.5 Mev range. This energy range gives the highest
signal-to-noise ratio for fission-product activity against the reactor
coolant background. The net fission-product count rate is obtained from
a difference circuit. The main objection to this direct method was the
high complexity of the electronic equipment needed to perform the counting
operations.

The use of direct gamma monitoring for in-pile test loops is common.
In one fuel test run in the Materials Testing Reactor,[81] fuel element
leakage was suspected when high activity readings were obtained in the
loop, and the presence of fission products was confirmed by identification
of cesium-138 in a water sample from the loop. These investigators noticed
that the gas above the water sample taken from the loop was quite radio-
active, and proposed that in future tests a device be built to degassify
the water and count the gas. This approach to fission product separation
from water had earlier attracted the attention of experimenters running a
fuel test loop in the Chalk River NRX Reactor.[82]

The problem of stripping radioactive gas from the NRX loop coolant
was complicated by the fact that the coolant (deuterium oxide) was pres-
surized. It was necessary to reduce the pressure on a sample from the

loop to one atmosphere before passing the helium stripping gas through it. Direct monitoring of the radioactive gas was found to be sufficiently sensitive for detection of fuel ruptures.[83] However, two other techniques for counting the gas were tried. One involved delayed-neutron counting and the other utilized precipitation of the fission gases on a charged wire followed by counting of the wire. The wire precipitation method was found to be more sensitive, especially to longer half-life isotopes. The gas was passed into a chamber through which a negatively-charged collecting wire moved. The wire formed a continuous loop moving through the chamber, past a counter and then back to the collecting chamber. Positively-charged particles created by the beta decay of fission products and other nuclides were drawn to the wire, which was kept at a negative potential of 1000 volts. Subsequent decays when the wire was at the counter were detected. Thus two decays are required for detection: the first creates a positive ion which is drawn to the wire, and the second is detected. Since fission products often decay by a series of consecutive beta emissions while most other radionuclides decay to the ground state in a single step, this system will be sensitive primarily to fission products.

A Geiger-Mueller tube was used for counting the wire. The wire speed used was 2.5 inches per minute, which gave a cycle time of 2 hours. During this time activity picked up in the chamber had nearly all decayed; there was no appreciable buildup of background wire activity with time. The half-lives of some of the isotopes trapped on the wire were determined by stopping the wire and following the decays. Half-lives of 15 and 32 minutes were found and identified as rubidium-89 and cesium-138. The decay

of gas activity in the collecting chamber was also followed by halting the gas flow; 2.6- and 17-minute activities were found and identified as krypton-89 and xenon-138, the predecessors of the isotopes found on the wire. A 2.8-hour component, krypton-88 was also found in the gas. The decay of the gas as measured by direct monitoring was found to be closely approximated by a total decay curve for the xenon and krypton radio-isotopes based on the fission yield and half-life of each isotope.

Kinchin[74] proposed the use of gas stripping to detect fission gases in a sodium-cooled reactor. A similar system was investigated for use with the Pressurized Water Reactor[84] but was not recommended because of the problems involved in depressurizing a water sample. A British patent[85,86] has been issued on a spray tower for stripping radioactive gas from water coolants. A summary of the methods thus far advanced for burst slug (or cladding failure) detection in water-cooled reactors is given by Aliaga-Kelly.[87] He considers: (1) the pressure drop in the fuel channels, caused by expansion of the fuel specimen during rupture; (2) the use of tracers incorporated into each fuel element which can be detected after rupture; (3) direct monitoring of the coolant; (4) delayed neutron counting; (5) ion exchange columns for trapping the activity; and (6) electrostatic precipitation methods. He concludes that the electrostatic-precipitation method, collecting krypton and xenon gas from a scrubbed or stripped water sample, is best.

B. Gas Cooled Reactors

The methods used for detection of fission leakage in gas-cooled reactors parallel those employed for water cooled reactors. The oldest gas-cooled reactor, the Oak Ridge National Laboratory Graphite Reactor, uses an oil-soaked rag in the exit-air duct to pick up fission products.[88] The rag is pulled from the exit air plenum about once every eight hours and the activity is measured. If the activity becomes abnormally high, then the reactor is shut down, and the bad fuel slug is located by visual inspection. Experience has shown that the thermocouple temperatures in this reactor often give an indication of fuel-cladding failure.[89]

Direct monitoring of the effluent coolant has been used for gas-cooled reactors. An ion chamber for this purpose was designed by Kanne.[90] This is a large-volume folded-flow chamber, adapted to batch or continuous analysis, which is sensitive primarily to beta emissions. The French gas-cooled reactors at Saclay use 1.6-liter chambers to collect gas samples for analysis.[91] A Geiger-Mueller tube in the center of the chamber determines the activity. A number of analyzers are needed to locate the fuel channel where failure occurs; one reactor with 2600 channels has 135 channels tied into each analyzer. The channels are sampled individually by operation of a complicated valving arrangement.

A more precise system used on an in-pile test trapped the fission products on charcoal.[92] A uranium dioxide fuel sample was cooled by a flow of helium gas. The gas coming from the test contained a mixture of fission products; non-volatile components were removed in a dry ice trap. Then the gaseous products were trapped in activated charcoal cooled by

liquid nitrogen. After a suitable sampling period the charcoal trap was removed from the system and the fission gases desorbed by heating the charcoal to 400°. The activity of the desorbed gas was monitored by a gamma spectrometer.

A combination of methods is used at the air-cooled Brookhaven Graphite Research Reactor to detect leaks in the fuel cartridges.[93] The exhaust air is monitored by an ion chamber; in addition a probe similar to that used at the Oak Ridge National Laboratory Graphite Reactor is employed. This consists of an oil-soaked steel wool mass inserted into the air stream. The air is passed through a filter before going to the stack; this filter is monitored for high activity which might indicate fuel element failure. However, first warning of a fuel cartridge leak is provided by a pressurized helium system built into the cartridges at manufacture.[94,95] Thirty-three uranium slugs are loaded into a single can 11 feet long; helium gas is used to fill void spaces in the can. A long capillary tube is attached to the cartridge; when the cartridge is loaded into the reactor, this capillary extends through the shielding to the outside of the reactor. The helium pressure in the cartridge is measured; a leak in the can causes the helium pressure to drop. This system has worked quite well, although loading the reactor with fuel is complicated by the presence of the capillaries.

The continuous analysis of gas streams without counting the gas directly is possible if the radioactive particles are collected from the gas by some means. One design[77] accomplishes this by pulling the air through a moving strip of filter paper, then through a scrubber filled

with 0.2 Normal sodium hydroxide. The filter paper is then drawn past a gamma detector and counted; the sodium hydroxide solution is analyzed separately. This analyzer has not been used on a reactor, but has been applied to the waste gas stream from a fuel reprocessing plant. A similar concept was used by Fenning and Jackson.[96] They patented a device to monitor the radioactivity of dust coming from a gas cooled reactor by collecting it on an adsorbent cord drawn past a counting head.

The original patent application for a charged, moving wire fission gas detector was filed in 1949 by Livingston and Levy.[97] Their design is essentially the same as that in use today at the NRX Reactor[92] and other places. The most extensive use of the charged wire detector has been in the British gas-cooled reactors.[98-103] A continuous wire is used in their detectors; the recycling is slow enough so that only 3 per cent of the peak activity is retained by the wire. The wire does not move continuously; it is held in the precipitation or collecting chamber for a short while, then moved quickly into the counter. This method of operation increases the sensitivity of the detector as compared to continuous wire operation.

The British reactors have a large number of channels to be sampled; the Calder Hall Reactor, for example, has 1696 channels. In order that each channel might be scanned individually, a complicated system of sample lines and valves has been installed permitting the channels to be sampled in sequence. The large number of channels to be sampled introduces a problem in handling the counting data provided by the detectors; a data-processing system has been developed to cope with this problem.[100]

A summary of the methods presently in use for cladding failure detection in gas-cooled reactors has been given by Kaufman.[104] The charged, moving-wire detector enjoys the widest use at the present, although little work has been done on quantitative measurements of its potentialities. Barr and Ralfe[103] have predicted the performance of the intermittent wire-movement detector used by the British. The characteristics of a fission gas detector used on a fuel loop in this country have been discussed by Collins, Conn and Trice.[105] Reference will be made to these results in a later section.

C. Proposed Problem

A survey of the literature on detection of fission products in reactor effluents has indicated the utility of a wire-precipitation type Fission Gas Detector (FGD). It might be well at this point to review what is known about the operation of these devices. Air (or some other gas) containing fresh fission products is conducted through a Fission Gas Detector collection chamber. A negatively charged wire moves through this chamber. When the fission products undergo beta decay, positive ions are formed. These positive ions migrate to the wire and are carried out of the chamber. The wire moves to a radiation detector, where subsequent decays of nuclei on the wire are counted. Thus, two decays are required for detection: the first decay creates a positive ion which is collected by the wire, and the second decay is detected. This effectively separates the fission products from other positive ions which might have adhered to the wire; the neutron-rich fission product nuclei often

undergo two or more decays before reaching a stable configuration, while other radioactive species likely to be found in reactor effluents decay to the ground state with a single emission.

The Fission Gas Detector has been in use for some time as a cladding failure detection device. For applications of this nature, the qualitative information now available on the operation of the FGD is sufficient. However, there are many fuel development programs of both practical and theoretical interest which require quantitative measurement of the fission product release from the material under irradiation. To adapt the FGD to quantitative use, all variables such as air flow, wire voltage and wire speed which could affect the count rate must be investigated. From the results of measurements on the FGD operational variables, optimum conditions for routine measurements can be specified. Likewise, a procedure for calibration of the instrument for routine use should be worked out. Also, an attempt will be made to explain theoretically the empirical results obtained from the measurements of the FGD operational characteristics. This attempt, if successful, will provide information useful in the future design of wire precipitation detectors.

There are several features of the Fission Gas Detector operation which are not easily altered for experimental purposes. One design variable which is fixed in these experiments is the size of the FGD collection chamber; changing the dimensions of this chamber will almost certainly have an effect on the count rate. Another factor beyond easy experimental control is the fission product concentration of the exit air stream. However, direct measurement as well as previous experience has shown that for

the kind of samples being irradiated during these investigations, the fission product concentration is essentially constant for periods of at least 12 hours at a time. This fortunate circumstance makes it possible to measure the variation of count rate with wire voltage, air flow and wire speed by assuming a constant source concentration. A third factor beyond experimental control is the delay between the time a fission product nucleus is formed and the time it enters the collection chamber. This delay depends primarily on the total air flow over the test; this also varies very slowly and can be considered constant during a series of measurements. Another area where clarification is required is the identification of the specific isotopes to which the FGD is sensitive. Tunnicliffe and Whittier[82] made a tentative identification of certain isotopes in their system from a measurement of their half-lives. Collins, Conn and Trice[105] used a gamma-ray spectrometer to help identify the radioactive constituents picked up by their detector. However, the poor resolution of their spectrometer made identification of gamma peaks difficult. Also, little information is presently available on the gamma energies emitted by short half-life fission products. For this reason, identification of the specific radioactive species involved in the FGD has not yet been put on a firm basis.

By the use of a gamma spectrometer with better resolution and the application of theoretical considerations, such as were worked out by Barr and Ralfe[103] from fission yields and decay schemes, the fission products which are preferentially counted by the FGD should be identified. Further, the prominent gamma energies of these species should be identi-

fiable if certain peaks in the gamma scan can be shown to correspond with certain half-lives. The complete unscrambling of the gamma spectra obtained through a multi-component scan is a complex mathematical problem, beyond the scope of this work.[106,107]

CHAPTER III

EQUIPMENT

A. The Oak Ridge Research Reactor System

The Fission Gas Detector utilized in this study is a moving charged-wire detector similar to that described by Tunnicliffe and Whittier.[82] It is incorporated in a fuel element test system at the Oak Ridge Research Reactor, maintained by the General Electric Aircraft Nuclear Propulsion Division for the irradiation of air-cooled fuel test specimens. The entire test system, with its associated controls and instrumentation, is quite complicated. Those features which are important in influencing the operation of the FGD are shown in Figure 1.

The Oak Ridge Research Reactor is a water cooled and moderated, enriched-fuel reactor very similar in core construction to the Materials Testing Reactor and the Low Intensity Testing Reactor.[108] Observed from the top, the core is a rectangular array of fuel and moderator elements. The core positions are numbered from 1 through 9 down one side, and from A through G down the other side. Each fuel element, moderator piece or experiment is located by a letter-number designation. The General Electric Aircraft Nuclear Propulsion test system utilizes position F-2 of the reactor core. A fuel element has been removed from this position and replaced with a core insert piece having a 2-13/16 inch diameter hole in it. Access to the position is from the top, through a flange in the reactor pressure vessel. An access tube is inserted into the core piece
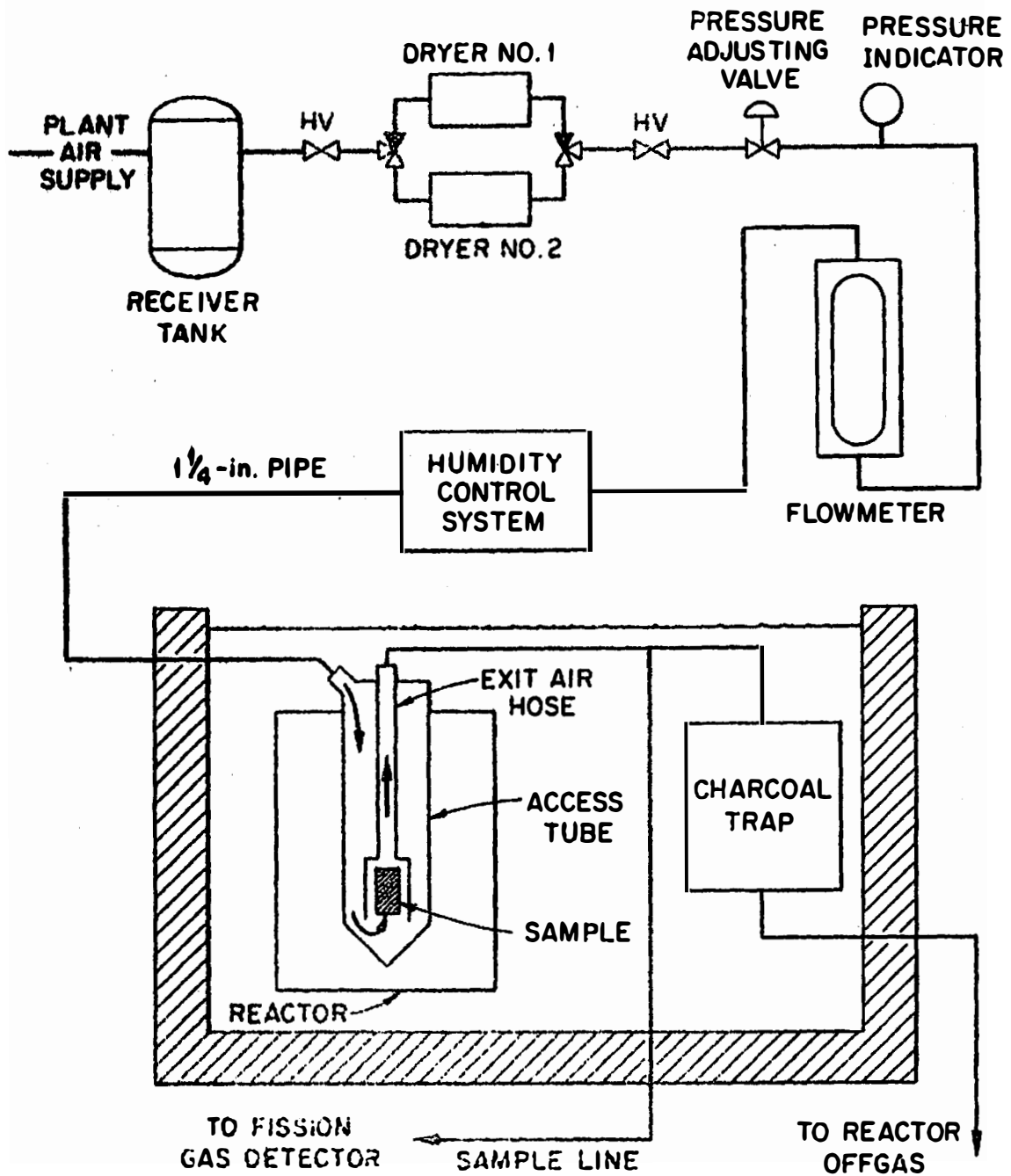
Fig. 1. The ORR Test System.

and extends up through the reactor pressure vessel, opening into the re-
actor pool about 5 feet beneath the surface. The maximum unperturbed
neutron flux in this facility is 9×10^{13} neutrons/cm.^{2}/sec. at 20 mega-
watts.

The flow of cooling air through the system can be followed by
reference to Figure 1. Air is supplied at 90 pounds per square inch from
a plant air supply main. It then passes through dryers to a pressure re-
ducing valve which maintains the pressure at the value required for a
given test. For some tests, moisture is added to the air and the humidity
controlled at a dewpoint of 25°F; other tests are run in dry air. The
air flows up to the reactor tank and enters the reactor pool at the balcony
level through a flange in the side of the pool. Inside the pool the
permanently installed piping connects to a flexible metal hose, 1 inch
inside diameter and 16 feet 3 inches long, to which the sample capsule
is attached. This hose with the sample capsule at the lower end is in-
serted into the reactor through the F-2 access tube. The top of the hose
fits into a flange which serves as a cap for the access tube, making it
an air-tight unit.

Air flows through the permanent piping and into the access tube,
pressurizing it. It then flows down the access tube and into the test
capsule through holes in the bottom of the capsule. The specimens are
cooled as air passes up over them and into the flexible hose, which
serves as the exit air line. At the top of the access tube the contami-
nated air re-enters the permanently installed piping and is passed through
a large charcoal-filled pot located at the bottom of the reactor pool.

Most of the fission products entrained in the air during its passage
over the fuel test specimens will be removed by the charcoal filter.
The air then leaves the pool through the flange by which it entered.
Air flow through the system is regulated by a flow-control valve located
just outside the reactor pool in a lead-shielded cubicle on the balcony.
It is only a few feet from this control valve to the discharge in the
main reactor off-gas line, which operates at a slight vacuum at all times.

An air sampling line branches from the exit air line ahead of the
charcoal pots, about 15 feet from the connection between the permanent
and temporary piping. This sample line, which is 3/8 inch stainless
steel tubing, leads from the pool to the lead shielded cubicle on the
balcony. The Fission Gas Detector and a glove box for charcoal-trap
sampling are located here. A diagram of the Fission Gas Detector piping
in the cubicle is shown in Figure 2.* The operation of nearly all equip-
ment in the cubicle is remotely controlled from an instrument console,
located on the first floor of the Oak Ridge Research Reactor building.
Many of the valves are pneumatically operated; air for this purpose is
supplied from a plant air line on the balcony through a hand valve (HV-36)
located just outside the cubicle. The pressure is reduced to 18 pounds
per square inch by a self-operated pressure reducing valve, and indicated
on a gauge (PI-45). The instrument air flows through a 3-way solenoid

---

*The notation is taken from a complete blueprint of the Oak Ridge
Research Reactor F-2 test system and is consistent with instructions in
ORNL Central File No. 57-2-1, "Instrumentation Flow Plan Symbols and
Recommended Drawings - A Standard System for ORNL Instrumentation Appli-
cation Work".
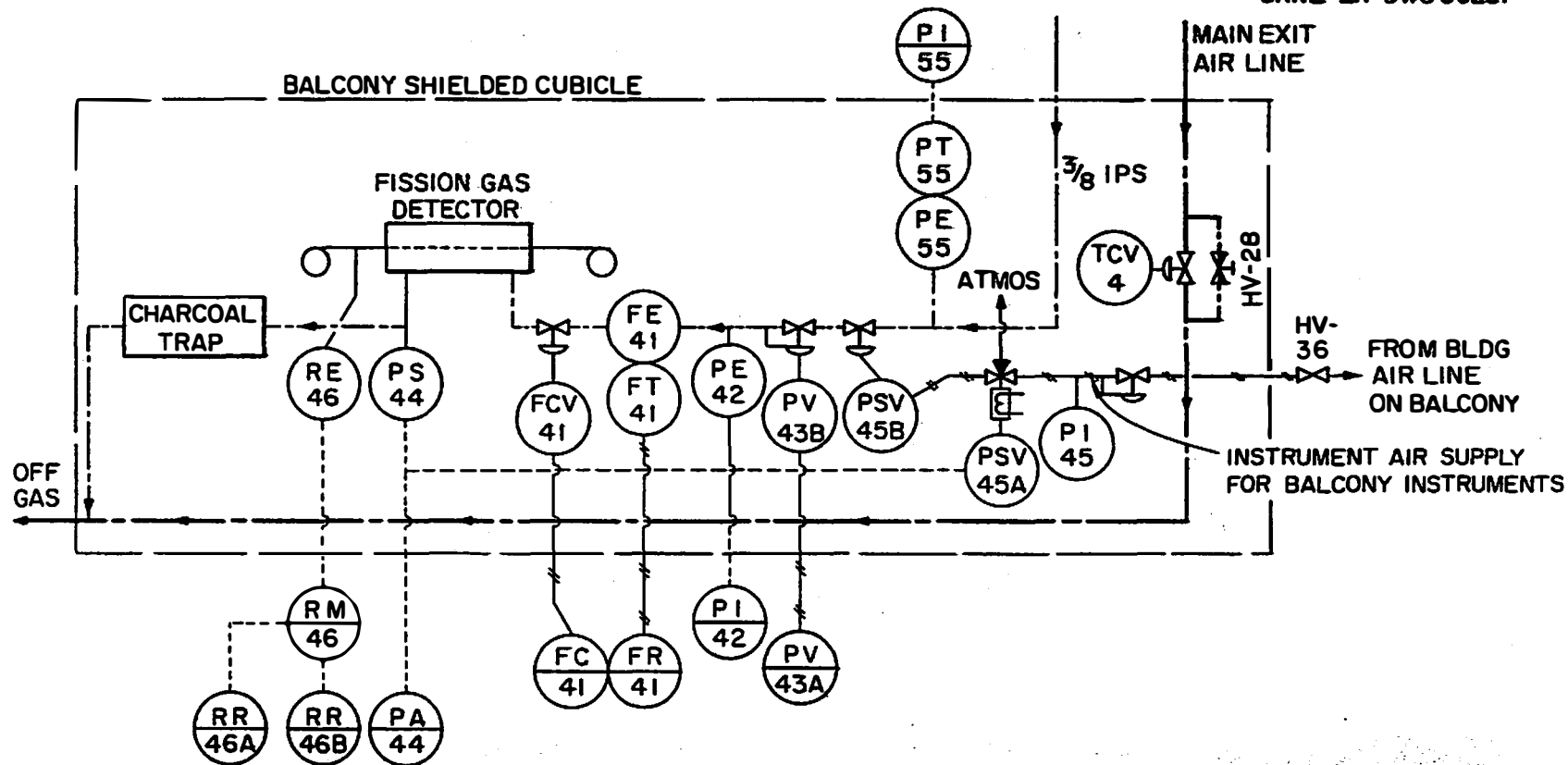
Fig. 2 Piping for the Fission Gas Detector in the Lead-Shielded Balcony Cubicule, Notation is Taken From ORNL CF-57-2-1.

40

valve, normally closed to the atmosphere, and supplies pressure to hold valve PSV-45B, on the FGD line, in the open position. This solenoid valve, and through it valve PSV-45B, can be opened and closed by a switch on the instrument console. However, if a signal is received by the 3-way valve (PSV-45A) from the pressure switch PS-44, the instrument air supply to PSV-45B is shut off and the trapped air in the valve vented to the atmosphere, causing the valve to close and shut off the FGD flow. When this occurs, the flow cannot be started again by using the open-close switch on the console until the signal from PS-44 has been cleared. The function of PS-44 will be described later.

The pressure on the FGD line ahead of any valves or constrictions is measured by a pressure element (PE-55) and a signal transmitted (by PT-55) to the instrument console, where it is read on a pressure indicator (PI-55). A Foxboro Dynaformer is used for this measurement. The pressure usually runs between 40 and 60 pounds per square inch in actual tests.

Pressure to the FGD is regulated by a remotely-operated pressure-reducing valve, PV-43B. A knob on the console, PV-43A, transmits a pneumatic signal to PV-43B. The pressure downstream from the pressure-reducing valve is sensed by a pressure element (PE-42) and transmitted to the console where it is read on indicator PI-42. This pressure measurement is also made with a Foxboro Dynaformer. Pressures can be adjusted between 0 and about 30 pounds per square inch; at higher flow rates, the maximum operating pressure must be reduced. Air flow is measured by a Fischer and Porter Rotameter (FE-41) and transmitted to the console via a flow transmitter (FT-41). At the console, the flow is recorded on a Fischer and Porter Rotagraphic recorder-controller (FR-41

and FC-41). When the desired flow rate is set with a pointer on the con-
troller, a pneumatic signal is transmitted to the flow control valve
FCV-41. The flow can be regulated quite accurately ($\pm$ 2 per cent) with
this instrumentation.

With the Rotameter reading and a knowledge of the pressure at the
Rotameter (from PI-42) the air flow can be calculated. The air flow is
measured as standard cubic feet per minute (SCFM). A standard cubic foot,
for engineering purposes, is the amount of air in 1 cubic foot at 1 atmos-
phere (14.7 pounds per square inch) and at 70°F.* The variation in the
amount of air in a given volume with temperature is small and the air
temperature remains fairly constant near 75°F, so no correction is made
for air temperature. However, a pressure correction must be made. The
pressure read on PI-42 is gauge pressure (above atmospheric). Figure 3
is a graph showing the correction factor _versus_ pressure up to 35 pounds
per square inch gauge.

The FGD Rotameter is calibrated for flows between 0.2 and 2 SCFM.
The recorder-controller indicator reads directly in SCFM, but the chart
is calibrated between 0 and 100 per cent flow. The chart reading is
normally used; to convert to SCFM, it is necessary to multiply by 2 and
divide by 100. The lowest reading on the Rotameter, when no flow is
going through the system, is 0.26 SCFM; at this point, the float in the
Rotameter is resting on the float stop. To obtain the actual air flow
for any indicated flow above 0.26 SCFM, the Rotameter reading is multiplied

---

*One standard cubic foot of air is equivalent to 34.01 grams or
26.15 liters of air at 760 mm. and 0°C.
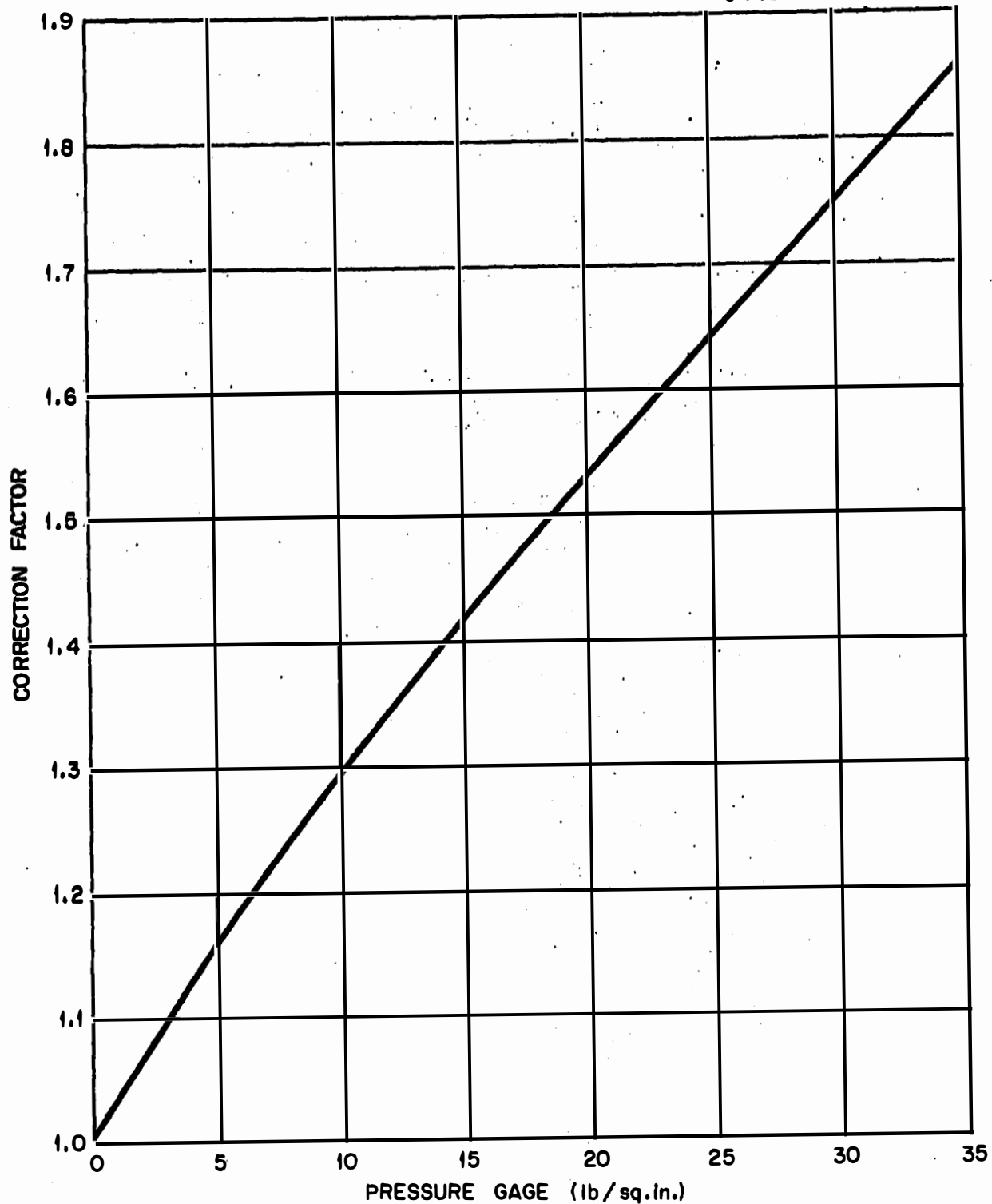
Fig. 3. Rotameter Reading Correction Factor for Operation Above Atmospheric Pressure.

by the proper correction factor for the pressure being used.

The pressure downstream from the flow control valve (FCF-41) is always kept slightly less than atmospheric pressure. This is necessary since the FGD barrel is not air-tight, and leaks of contaminated air into the Oak Ridge Research Reactor building cannot be tolerated. The air flows through the FGD and out through a small charcoal filter pot into the main reactor off-gas line, which is the source of the vacuum required by the FGD. A pressure switch, PS-44, acts as a safety device by cutting off the FGD flow, in a manner already described, when the FGD loses vacuum. A visible alarm on the console (PA-44) signals loss of vacuum. The pressure sensor, which is a Mettron vacuum-actuated switch, is set to trip when the difference between the FGD vacuum and atmospheric pressure is less than 15 inches of water. High pressure and flow rate through the FGD (as well as loss of off-gas vacuum) can cause a vacuum alarm.

RE-46, RM-46, RR-46A and RR-46B serve to identify the radiation detector, associated electronics, and the two radiation recorders associated with the FGD. These will be discussed in Section C of this chapter.

B. The Fisson Gas Detector

The Fission Gas Detector consists of four separate parts: (1) the FGD barrel, or collection chamber, through which the air to be monitored passes; (2) the feed spool mechanism, where the wire voltage is applied; (3) the detector and its shield; (4) the take-up mechanism. Figure 4 is a scale drawing of the Oak Ridge Research Reactor Fission Gas Detector, showing the dimensions of various parts of the system. The barrel and
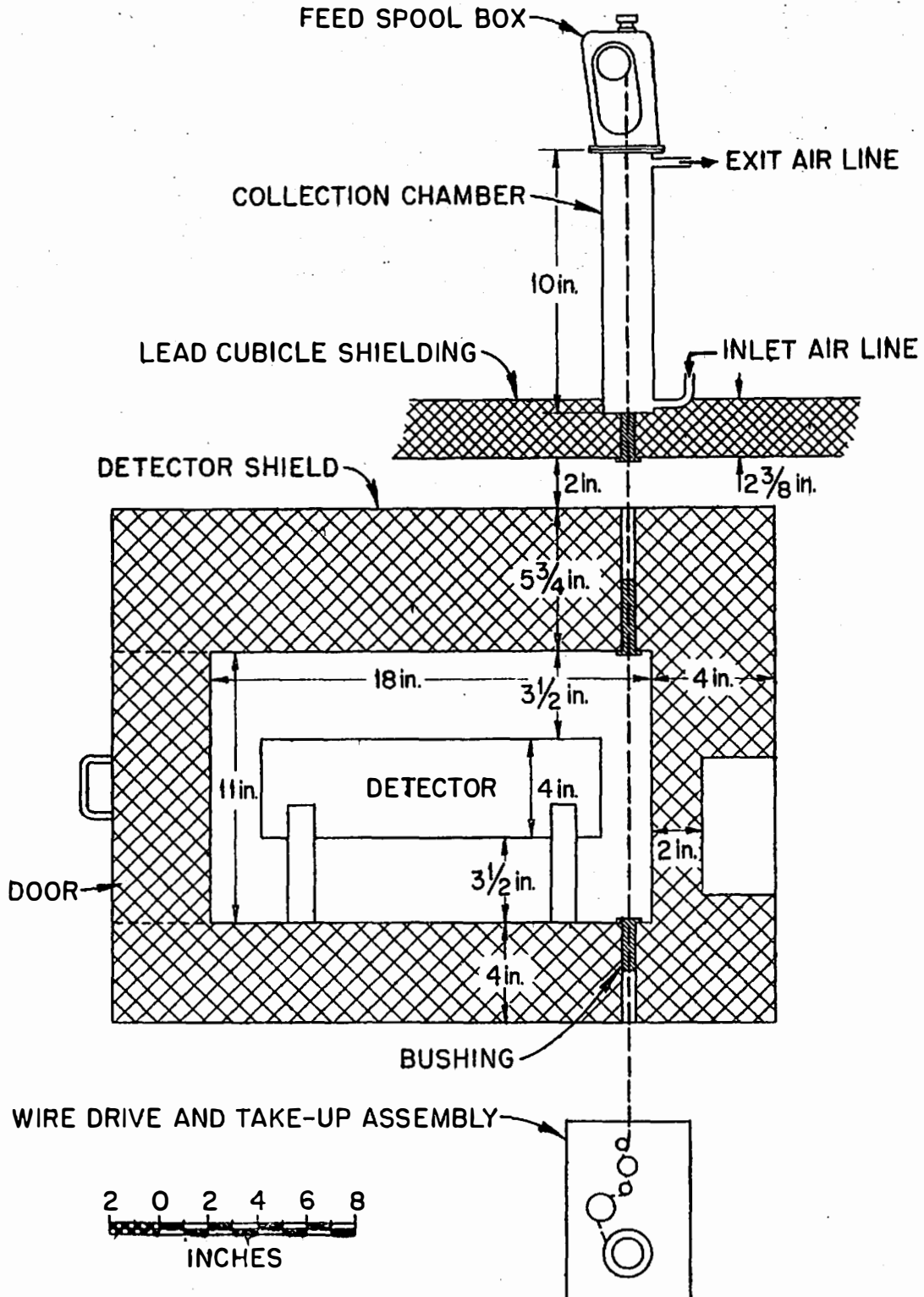
Fig. 4. The ORR Fission Gas Detector

feed spool are located inside the shielded lead cubicle in a vertical position; the detector shield and take-up mechanism are located beneath the cubicle.

The FGD barrel is made from a piece of brass tubing, 10 inches long and 2 inches outside diameter, 1.75 inches inside diameter. Air enters the chamber near the bottom and exits at the top. At each end of the chamber there is a screw-out bushing about 3 inches long through which the FGD wire passes. This bushing is made by drilling a hole in a 3/4 inch bolt and cementing a piece of pyrex capillary in the hole. The FGD wire is threaded through the capillary, which insulates the wire from the barrel. Since the capillary is slightly larger than the wire, air can enter or leave the FGD barrel through the capillary; for this reason, the FGD is operated slightly below atmospheric pressure.

The feed spool mechanism shown in Figure 5 is a box mounted atop the FGD barrel which holds a single spool of wire-recorder wire. The wire is used only once; after it has passed through the FGD barrel and onto the take-up spool, it is discarded. Many of the other wire precipitation machines now in use employ a continuous, recirculating wire.[82,101] The feed spool is mounted on an insulated holder; a pointed metal rod presses into a depression in the center of the feed spool holder. This rod, which is spring loaded, is mounted in a removable plexiglas cover for the feed spool box. The voltage for the FGD wire is applied via this rod; the barrel is grounded. The pressure of the rod on the feed-spool holder acts as a friction brake on the wire. A microswitch, through which the wire is threaded, halts the wire take-up mechanism when the wire has run out; a piece of plastic tape at the end of the roll trips the switch.

¾-in. PLUG

FEED SPOOL
HOLDER

WIRE FEED
ASSEMBLY

FEED SPOOL

VOLTAGE LEAD

FEED SPOOL BOX

FEED SPOOL

PLEXIGLASS COVER

BUSHING

FRONT VIEW

SIDE VIEW
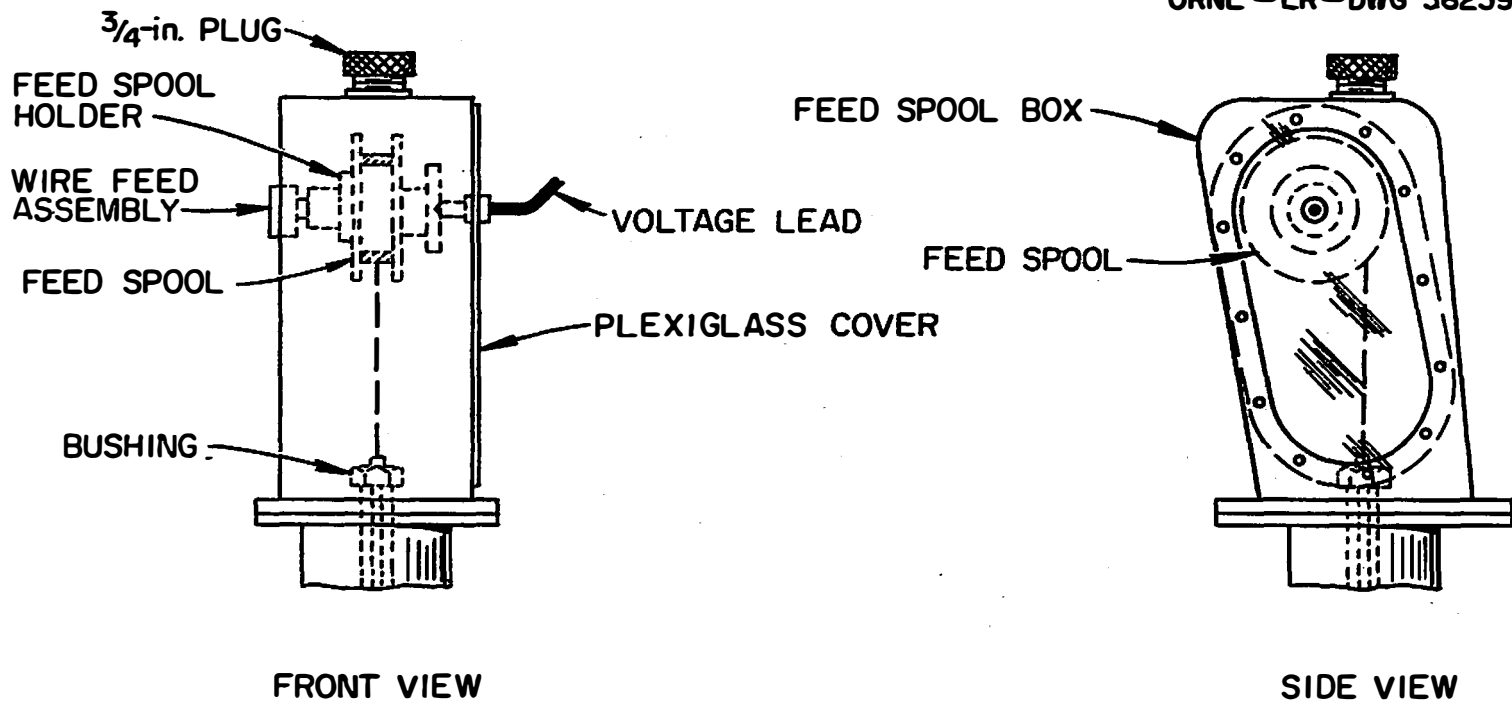
Fig. 5. Feed Spool Mechanism.

47

The bottom of the FGD barrel is partially embedded in the lead shielding of the balcony cubicle. The lower bushing is inserted from beneath the cubicle. The wire passes out the bushing and through the detector shield to the wire take-up mechanism. It is insulated from the detector shield by two bushings identical to those used in the FGD barrel. The take-up mechanism, shown in Figure 6, is mounted on a thick piece of plexiglas. The drive motor is insulated from the take-up spool by a non-conducting shaft. Thus, the FGD wire is isolated from ground at all points. When the Oak Ridge Research Reactor FGD was first put into operation, a low-resistance (50,000 Ω) path to ground developed through the feed-spool holder. This part of the holder was replaced with a similar part made from Teflon. After this change, the resistance between the wire and ground was found to be greater than 50 megaohms.

The wire used in the FGD is stainless steel wire-recorder wire with a diameter of 0.004 inches. The wire speed under the original conditions was 27 feet 9 inches per hour. At this speed, a roll of wire (1 hour size) would last for several hundred hours of continuous operation.

C. The Detector and Associated Electronics

The sensitive element of the FGD radiation detector was a 3-inch diameter by 3-inch long thallium-activated sodium iodide crystal. This crystal was mounted on a Dumont 6363 phototube, using a procedure similar to that described by P. R. Bell.[109] The energy resolution of the crystal

TOP VIEW

DRIVE SHAFT

IDLER

CAPSTAN

WIRE GUIDE

IDLER

FGD WIRE

TAKE UP SPOOL HOLDER

TAKE UP SPOOL

FRONT VIEW

TAKE UP SPOOL

FGD WIRE

WIRE GUIDE

IDLER

IDLER

CAPSTAN

TAKE UP SPOOL HOLDER
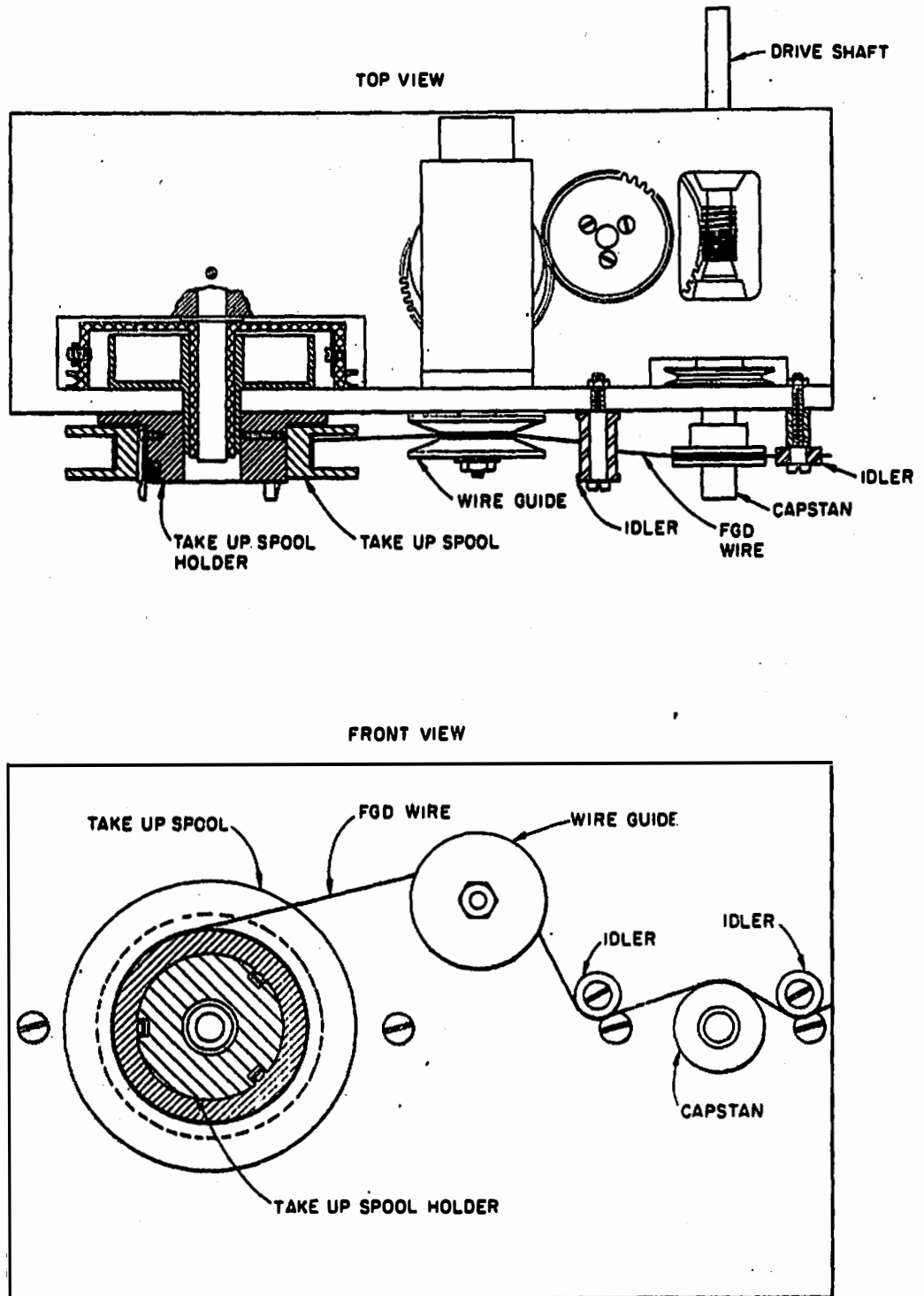
Fig.6. Wire Take Up Mechanism for the Fission Gas Detector.

was checked and found to be about 7.5 per cent.[*] The high voltage for the phototube was supplied by an Atomic Instrument Company Super Stable High Voltage Power Supply, Model 312. A block diagram of the electronics associated with the detector is shown in Figure 7. All instruments were located in the General Electric instrument console on the ground floor of the Oak Ridge Research Reactor building, while the detector and shield were at the balcony level. The use of long leads to connect a detector with its amplifier is known to attenuate the signal from the phototube significantly. To overcome this difficulty, a small pre-amplifier was installed beside the detector shield to boost the signal to the amplifier.

The amplifier was a Victoreen DD2 Linear Amplifier, Model 851A. The characteristics of this amplifier have been described by the designer, Edward Fairstein.[110] The total count rate from the amplifier was fed into an Oak Ridge National Laboratory Logarithmic Count Rate Meter, Model Q-1454 B. The output from this count rate meter was recorded on a 4-cycle log Brown recorder.

A second output from the amplifier was fed into a pulse height analyzer which was a modular unit of the amplifier. The analyzer accepts pulses from the amplifier which are between 0 and 100 volts in height. By adjusting the gain of the amplifier, a 100 volt pulse can be made to correspond to incident gamma energies from a few Kev to more than 10 Mev. When the pulse height analyzer is operated in the Integral position, all

---

[*]The energy resolution of a gamma detector is defined as the width of a gamma peak at half height, in Mev, divided by the gamma ray energy in Mev. This resolution varies with the energy of the gamma being measured; the usual value quoted is for the cesium-137 gamma at 0.662 Mev.
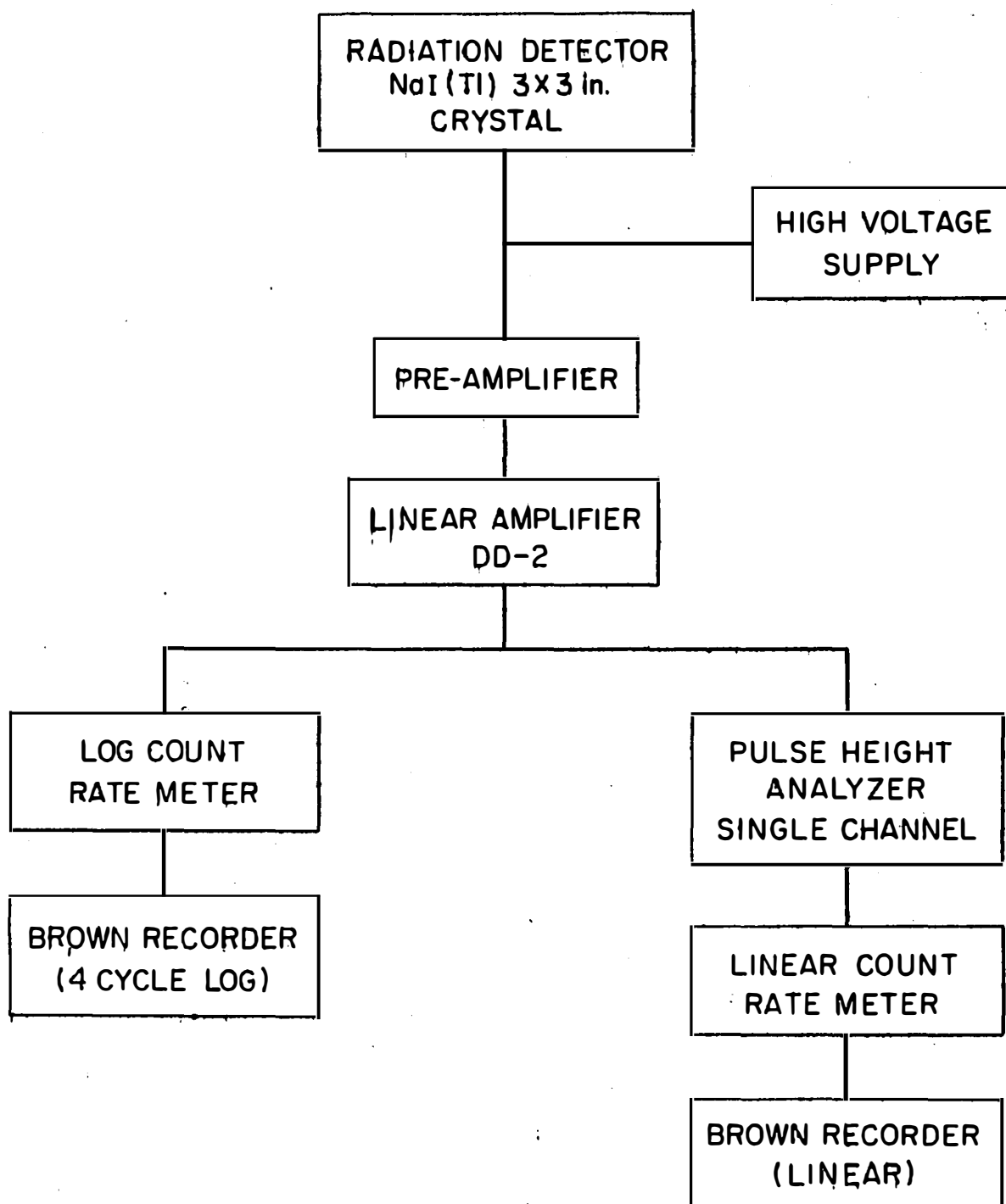
Fig. 7. Block Diagram of Counting Equipment for the Fission Gas Detector.

gammas up to the energy corresponding to a 100 volt pulse can be counted. In addition the minimum energy, or base line, can be changed so that only pulses above a certain voltage are counted. The common procedure was to set the base line slightly above 0 so that "noise" from the instrument would not be counted.

When the pulse analyzer was operated in the <u>Differential</u> position, only those pulses falling within a certain small voltage range were counted. The size of this "window" could be varied between 0 and 10 volts. The base line of the window determined the minimum voltage of the pulses counted; the maximum voltage was greater than this by the window width. The base line could be set with dials on the amplifier, or it could be changed externally. In making a gamma scan, the base line was moved at a uniform rate over the 0 to 100 volt pulse height range. Movement of the base line was externally produced by an auxiliary unit tied into the chart drive of the Brown recorder which recorded the count rate.

The output from the pulse-height analyzer was fed into a Radiation Counting Laboratory Linear Count Rate Meter, Model 20400.[*] The count rate was recorded on a linear Brown recorder using a chart graduated from 0 to 100 divisions. This recorder also had the scan mechanism attached to the chart drive, as mentioned above. The gear ratio of the scanner was such that a complete scan required 10 inches of chart, regardless of chart speed. An adjustment was provided on the linear count rate meter to vary

---

[*]A linear count rate meter was chosen instead of a log count rate meter for the gamma scans because it emphasizes small gamma peaks relative to a log plot.

the standard deviation of the counting output. When the standard devia-
tion was low, the pen movement of the Brown recorder was fast and there
was too much "wiggle" in the pen movement. If the standard deviation was
high, the pen movement of the Brown was slow; at fast chart speeds, the
pen could not move fast enough on scans to keep up with the changes in
count rate. After some experimentation, a chart speed of 1/2 inch per
minute was established as being slow enough to permit use of high standard
deviation without loss of accuracy, without being so slow that scanning
became tedious. A complete scan required 20 minutes.

The log count rate meter covers a count rate change of from 10^2 to
10^6 counts per minute, in 4 cycles. The linear count rate meter covers
a range of from 200 to 2×10^6 counts per minute by switching ranges.
Range changes can be made in steps with either a factor of 2 or 5 change
at each step. At a gross count rate of 2×10^6 counts per minute, there
is a very small coincidence correction for the NaI crystal, but this is
negligible compared to other counting errors in the system.

The detector shield was made of sheet iron filled with poured
molten lead. The dimensions are shown in Figure 8. Although there are
4 inches or more of lead in the shield on all sides except the back, the
background is moderately high inside the shield because of its proximity
to experimental lines containing radioactivity. When an air flow is
started through the FGD lines, the background increases about 100 per
cent, depending on the flow rate and amount of contamination in the air.

The internal cavity in the shield was 11 inches high, 14 inches
wide and 18 inches long. The detector is supported in the shield on an
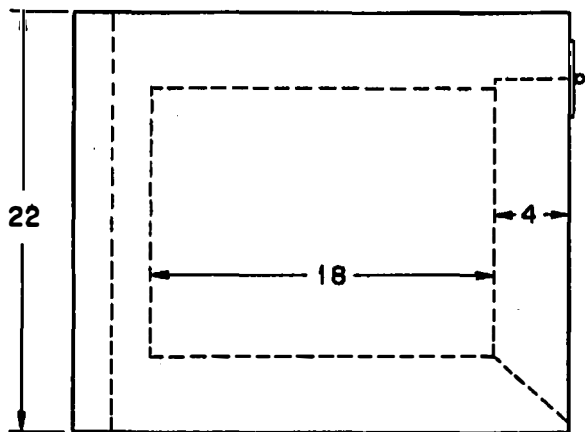
ALL DIMENSIONS ARE IN INCHES

22

18

4

TOP VIEW

HINGED DOOR

6

2

6½

11

12

26

SIDE VIEW

21

14

22
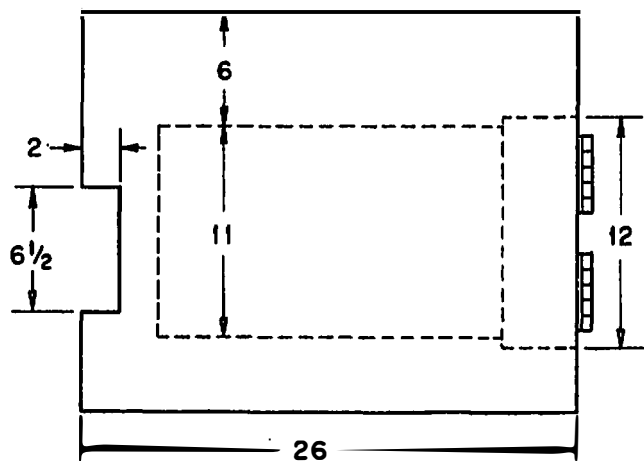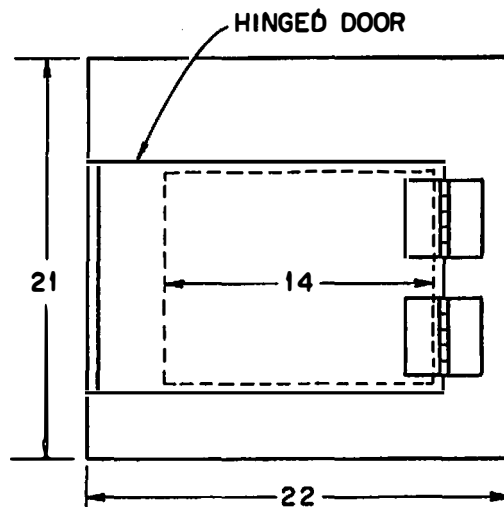
FRONT VIEW

Fig. 8. Fission Gas Detector Shield Dimensions.

aluminum stand; it is centered vertically and horizontally, as viewed
through the door, and positioned about 1 inch from the FGD wire. The
shield stands $9\frac{1}{2}$ inches above the floor; the wire takeup mechanism beneath
the shield rests directly on the floor.

D. Calibration of the Detector

Before the Fission Gas Detector equipment was put in use for actual
measurements, the performance was checked and calibration procedures
worked out. The measured count rate of any counting system is a function
of the 3 components of the system: first, the source disintegration rate,
energy and geometry; second, the detector response; and third, the char-
acteristics of the electronic circuitry. The detector response for a
properly prepared and mounted scintillation crystal should vary only slow-
ly with time, if at all; furthermore, any changes in the detector can be
at least partially compensated for by adjusting the electronics. The
first phase of the counter calibration was to determine the system response
to sources of various count rates and geometries. Then a procedure was
worked out using a long half-life source so that equivalent conditions
could be maintained for repeated measurements. The technique for doing
this will now be described.

For a given long half-life source in a fixed geometry, the number
of gamma rays entering the crystal per minute will be constant (within
the limits of statistical variation). If the detector response is con-
stant, then the count rate can be varied only by changes in the electronics.
The response of scintillation crystals and photomultipliers is known to be

a function of temperature;[111-113] however the FGD was operated in an air-conditioned building, and the temperature variations were small enough so that the detector sensitivity should not have been affected appreciably. There are 4 ways that the electronics could have affected the count rate:

1. The count rate changes when the high voltage to the phototube is varied.[114] Some instruments are calibrated by changing this voltage with a continuously variable high voltage supply;[115] however most modern counters, including the FGD system, use stepwise-variable high voltage supplies. The photomultiplier voltage remains at one setting in these systems.

2. The count rate meter characteristics can change. Count-rate variations from this source are prevented by calibrating the count-rate meters against the 60 cycles per second signal from the AC line voltage.

3. An amplifier gain change causes a change in count rate. Calibration of most counters is accomplished by changing the gain to produce the proper count rate for a standard source and geometry. A variation of this method was used for the FGD. A cesium-137 standard was chosen for the FGD calibration. Cesium-137 has a 33-year half-life, so decay of the standard could be neglected during the period these measurements were being made (about 1 year). Cesium-137 has two gammas; one at 0.032 Mev (actually due to barium-137m) and one at 0.662 Mev. The calibration procedure will be described below.

4. The count rate will change if the gamma energy interval being counted changes. On both the linear and log count rate meters, very low voltage pulses corresponding to low energy gamma rays were not counted. This eliminated errors due to amplifier and photomultiplier noise, bremsstrahlung and other random pulses. This low energy cutoff must remain constant if the count rate is consistent. When the amplifier gain is properly set, as described below, then the low energy cutoff can be accurately known.

There are two ways the amplifier gain can be set to give reproducible count rates. One method involves adjusting the gain to give a specified gross count rate with a standard sample in a fixed geometry. This can be done with either the log count rate meter or with the linear count rate meter set in the Integral position. The geometry of the source must be invariant, and the same standard should be used every time. The other method of setting the gain involves the use of the pulse height analyzer with the linear count rate meter. The gain is set so that the gamma scan covers a certain specified energy range, which for the FGD was 0 to 1.0 Mev. This method is much more sensitive than using the gross count rate. The counting standard does not have to be in a specified geometry, and its disintegration rate does not have to be known. This means that sample decay does not influence the calibration. Also, the FGD scan energy range is set when the calibration is performed, making any additional calibration for use of the scanner unnecessary.

The calibration procedure was as follows:

1. The high voltage supply was left at the same setting continuously.

2. The linear and log count rate meters were calibrated by comparing the count rate output, as shown on the Brown recorders, with the 60 cycles per second input line frequency.

3. Occasionally, the Pulse Height Analyzer linearity, zero point and slit width were checked and set using a test pulse generator.

4. A cesium-137 standard source was placed in a sample holder attached to the scintillation detector. This source was evaporated onto a 1-inch diameter watch glass, mounted in a 2-3/4 inch by 3-3/4 inch aluminum card with cellophane tape.

5. The Pulse Height Setting (PHS) dial on the Pulse Height Analyzer was set at 662, the energy of the cesium-137 gamma peak. The slit width was set at 1 volt. The linear count rate meter was set on the Internal, Differential position.

6. The coarse and fine gain controls on the amplifier were adjusted to produce the maximum count rate on the linear count rate meter. This corresponds to the top of the cesium-137 peak. When the amplifier has been set, then a PHS dial setting of 1000 corresponds to 1.0 Mev.

7. The linear count rate meter was switched to Internal, Integral. The PHS dial was set so that gammas above 0.05 Mev were counted.

8. The gross count rates on the log and linear count rate meters were compared with previously determined values for the same

standard in the same position. This provided a check on the
accuracy of the calibration.

The performance of the gamma scan was evaluated by scanning several
gamma standards and comparing the scans with the gamma spectra published
by Heath.[116] The standards were obtained from Mr. H. L. Parker of the
ORNL Isotope Division. The following isotopes were used:

sodium-24	antimony-124
cobalt-58	cesium-134
cobalt-60	cesium-137
silver-110	gold-198

The curves obtained from the FGD scan are on a linear scale, whereas the
curves in Heath are plotted on semi-log graph paper and must be replotted
for an accurate comparison. The agreement, when this is done, is quite
close. Figure 9 is a plot of a sodium-24 scan taken on the 3 inch x 3 inch
FGD crystal in a lead shield with an internal cavity of 11 inches x 14
inches x 18 inches, compared to a curve from Heath using a 3 inch x 3 inch
beveled crystal in a 12 inch x 12 inch x 24 inch shield.

The absolute efficiency of the counting equipment for cobalt-60
was also determined. A length of cobalt wire was irradiated in hole 10
of the ORNL Graphite Reactor. This wire was then cut to exactly 11 inches
long, so that it would fit inside the FGD shield in the same position
occupied by the FGD wire. This wire was coiled up and counted on the Oak
Ridge National Laboratory Isotope Division high pressure gamma ion chamber.
This ion chamber has been calibrated using standard cobalt solutions and
the calibration is checked daily with radium standards. The absolute
cobalt-60 disintegration rate of a sample can be determined with an
accuracy of ± 2 per cent. The disintegration rate for the cobalt wire
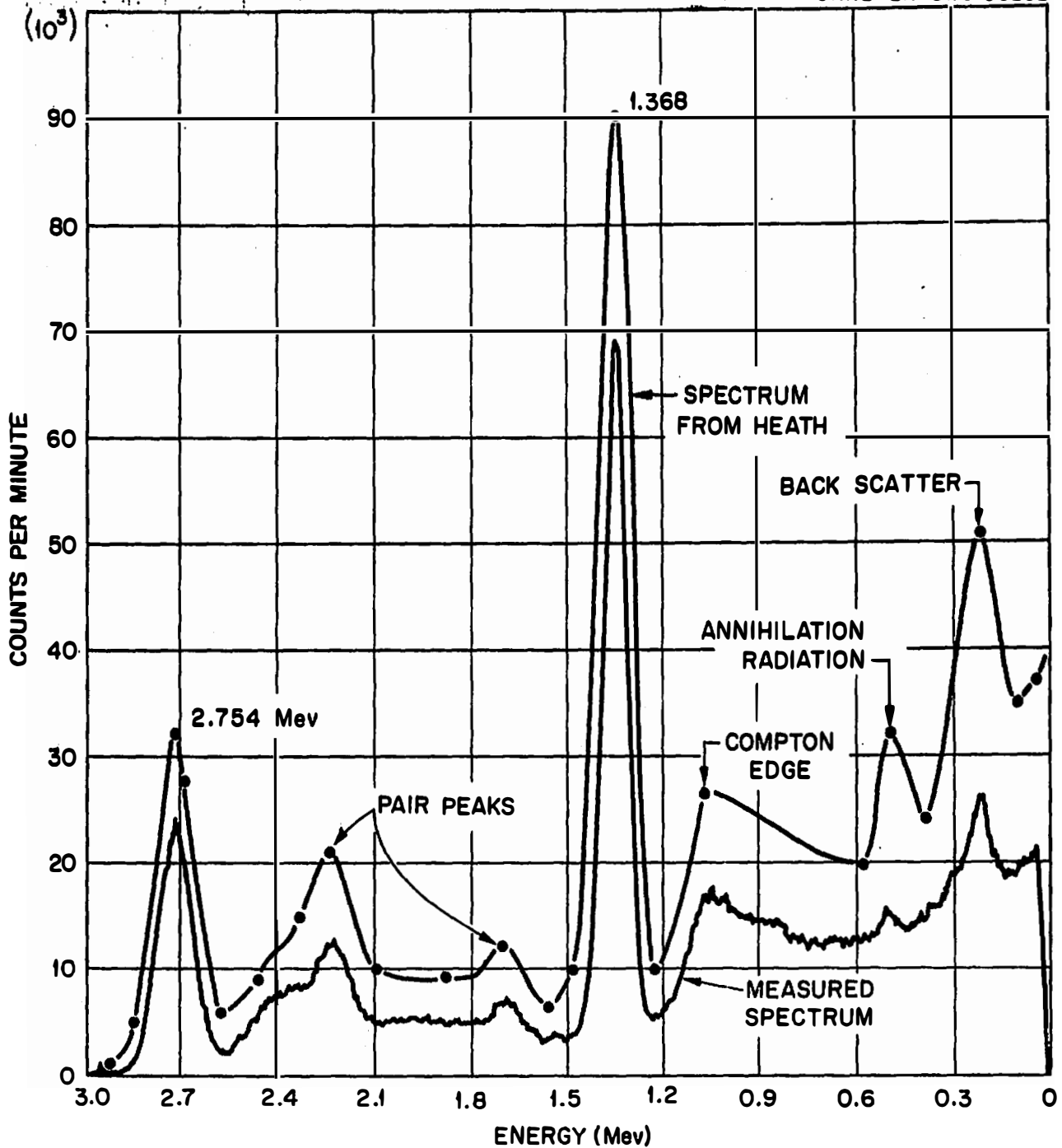
Fig.9. Comparison of FGD Scan with a Curve from Heath. Bottom Curve — Measured with FGD Equipment. Top Curve — Copied from R. L. Heath,"Scintillation Spectrometry Gamma-Ray Spectrum Catalog", IDO-16408, p.11-24-2. The Curve from Heath was Taken with a 3×3 In. Beveled NaI Crystal in a 12×12×24 In. (Inside Dimensions) Shield.

was determined to be 7.94 x 10^6 disintegrations per minute.

The cobalt wire was taped into place inside the shield and counted. With the amplifier gain set for a 0-2.0 Mev scan, the count rate on the log count rate meter was 4.60 $\pm$ 0.20 x 10^5 counts per minute, which corresponds to 4.88 x 10^5 counts per minute for a 0-1.0 Mev gain setting. Thus the ratio of disintegrations of cobalt-60 to counts is $\dfrac{7.94 \times 10^6}{4.88 \times 10^5} = 16.3$ disintegrations/count at the usual amplifier gain setting. By comparing the count rate of the other standards with the cobalt-60 standard count rate, a ratio of disintegrations per count can be obtained for the other standards counted (listed above). This ratio of disintegrations per count, of course, is only valid for the geometry presented by the FGD wire as it passes through the shield.

CHAPTER IV

EXPERIMENTAL RESULTS

A. Variation of Count Rate with Wire Voltage

The two variables which are easiest to change in the Fission Gas Detector are wire voltage and air flow. Both of these quantities can be regulated remotely from the control console. The variation of count rate with wire voltage was measured for several conditions of air flow and wire speed. Nearly all measurements were made at a wire speed of 5.55 inches per minute, and those results will be presented here. The effect of wire speed will be considered later. All the data to be discussed was taken on the linear count-rate meter, using it in the Integral position. The data from the log count-rate meter paralleled that from the linear meter, but differed slightly in magnitude. The log count-rate meter consistently ran about 25 per cent lower than the linear count rate meter; this was attributed to a difference in low-energy cut-off between the two count-rate meters. This difference in count rate introduced no practical difficulties, since the two count-rate meters were calibrated independently of each other.

The precision and reproducibility of the wire voltage versus count rate measurements was a very encouraging indication of the possibility of quantitative use for the Fission Gas Detector. A Tripplet Model 630 multimeter was used to measure the wire voltage. The accuracy of the Tripplet was checked with a standard voltmeter belonging to the Oak Ridge

National Laboratory Instrument Department; agreement between the meters was within 1 per cent on the scales checked. A plot of count rate versus wire voltage for low voltages is shown in Figure 10. Notice that zero voltage is in the center of the page and that negative voltage increases to the right. This convention will be followed in all succeeding plots and the minus sign will be omitted. As long as the wire was positive, few ions adhered to the wire; the total count rate is about twice background in this region. As the wire became negative, the count rate increased up to the voltage limit of this run (35 volts). The portion of the graph from 0 to 10 volts is quite linear; a similar linear region has been observed in all runs at low voltages. An anomalous high count rate was observed at zero applied volts when the FGD wire was not grounded. No DC voltage was observed between the wire and ground under these conditions with a vacuum tube volt-meter. This high count rate was at first attributed to the differential in migration speed between positive ions and electrons. However, later measure-ments showed that there was an AC pickup, amounting to 18.5 volts, present in the circuit when the wire was not grounded. Apparently, it was this AC voltage which caused some ions to adhere to the wire. This AC pickup was not present when a voltage source or voltmeter, other than a vacuum tube voltmeter, was connected in the circuit.

A count rate versus voltage curve taken over a wider voltage range is shown in Figure 11. Three regions can be distinguished on this plot: (1) the linear low-voltage region; (2) the count rate plateau at high voltages; and (3) a connecting region. The plateau at high wire voltage may readily be interpreted as a region of saturation, where all of the
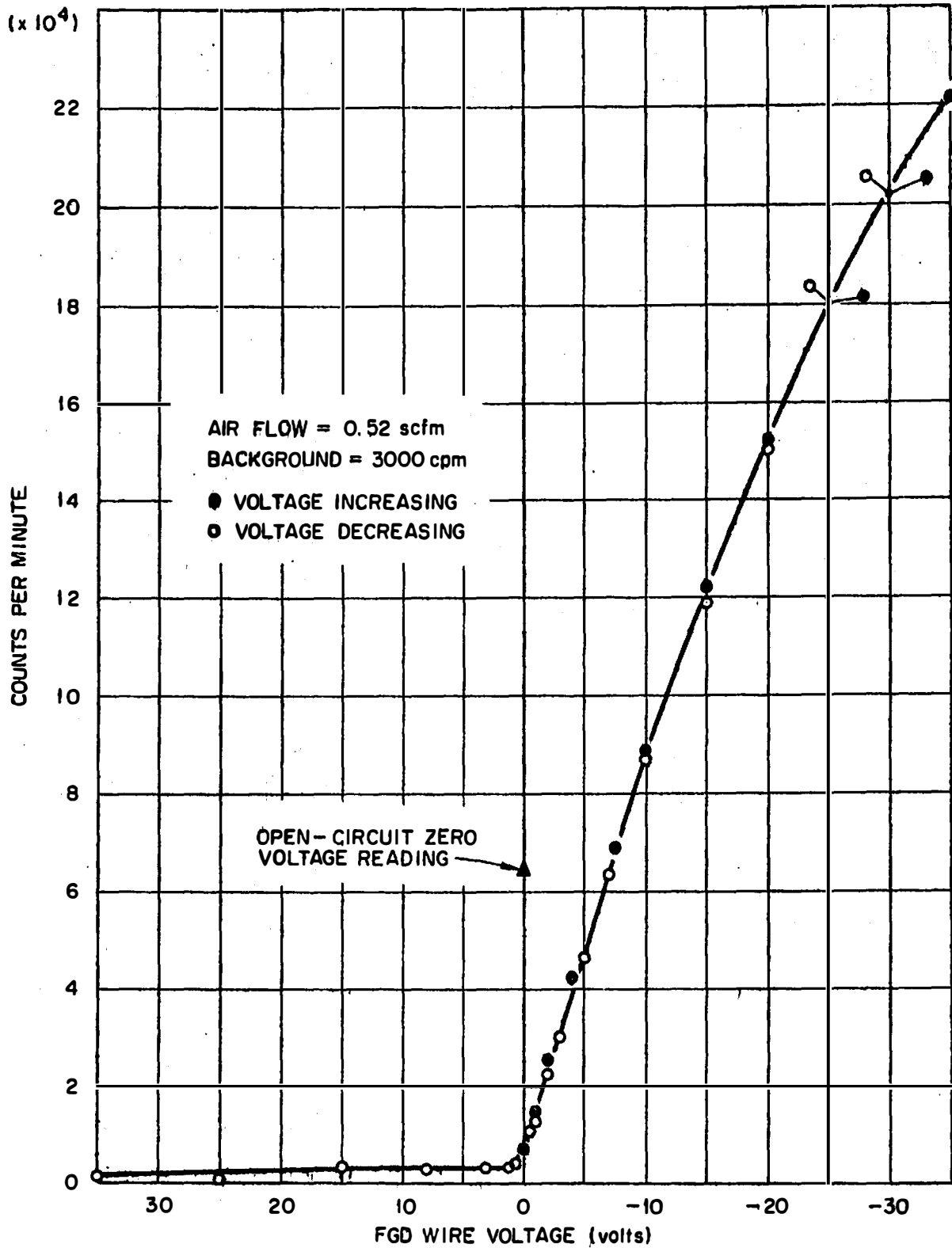
Fig. 10, Count Rate vs Voltage at Constant Air Flow. Negative Wire Voltage Increases to the Right. Background, 3000 Counts per Minute, Has Been Subtracted.
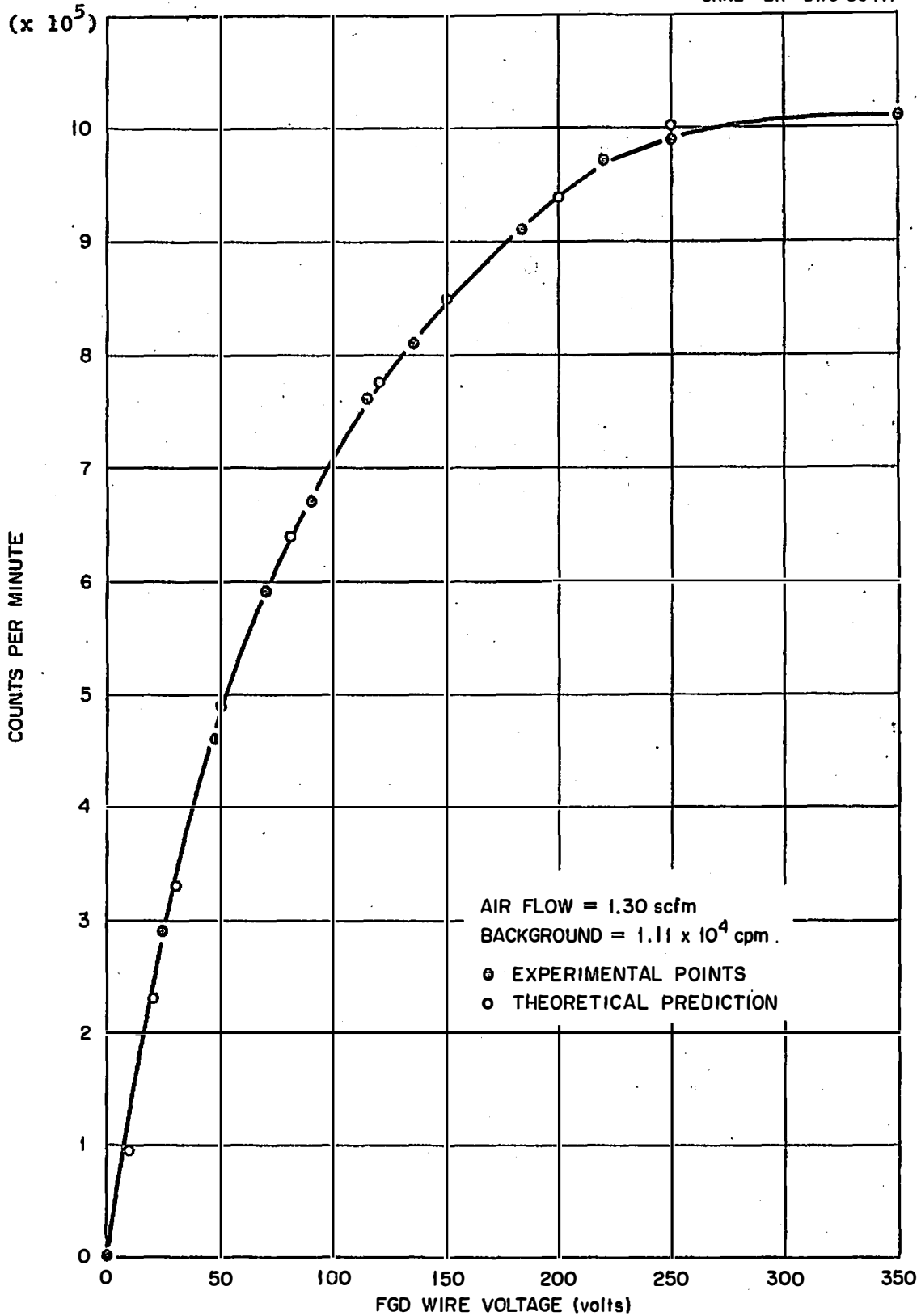
Fig. 11. Count Rate vs Voltage at Constant Air Flow. Background, 1.11 x 10⁴ Counts per Minute, has Been Subtracted.

ions introduced to the chamber or produced in the chamber are being drawn to the wire. This plateau is seen better in Figure 12 where the voltage is extended to 500 volts and data for several air flow rates is plotted. The linear region of the graph at low potential can be predicted from a consideration of ion migration velocities in an electrostatic field. However, before this is worked out it is necessary to know something about the transit time of a fission product nucleus from the fuel specimen to the collection chamber.

The Oak Ridge Research Reactor test system had 31.5 feet of 1 inch inside diameter piping from the fuel specimen to the junction with the FGD sample line. The FGD sample line is 3/8-inch tubing; it was 16 feet from the junction with the main air line to the FGD collection chamber. The collection chamber itself was 10 inches long and 1.75 inches inside diameter. Now, the time for a particle to get from the fuel specimen to the sample line junction is independent of the FGD flow, while the time from the sample line junction to the chamber and the time spent in the chamber will be flow-dependent. The main line pressure during the run of Figure 10 was about 45 PSIG downstream from the test; air flow at this pressure was 70 SCFM. The actual volume of air flowing through the system at 45 PSIG can be calculated from the perfect gas law if the temperature is known; the average exit-air temperature will be estimated at 200°F in order to make a rough calculation. Then, actual volume of air = 70 SCFM x $\frac{14.5}{59.5}$ x $\frac{659^*}{529}$ = 20.3 cubic feet per minute. Thus the linear velocity of the

---

*Atmospheric pressure is about 14.5 psi. Recall that standard conditions for SCFM include a temperature of 70°F.
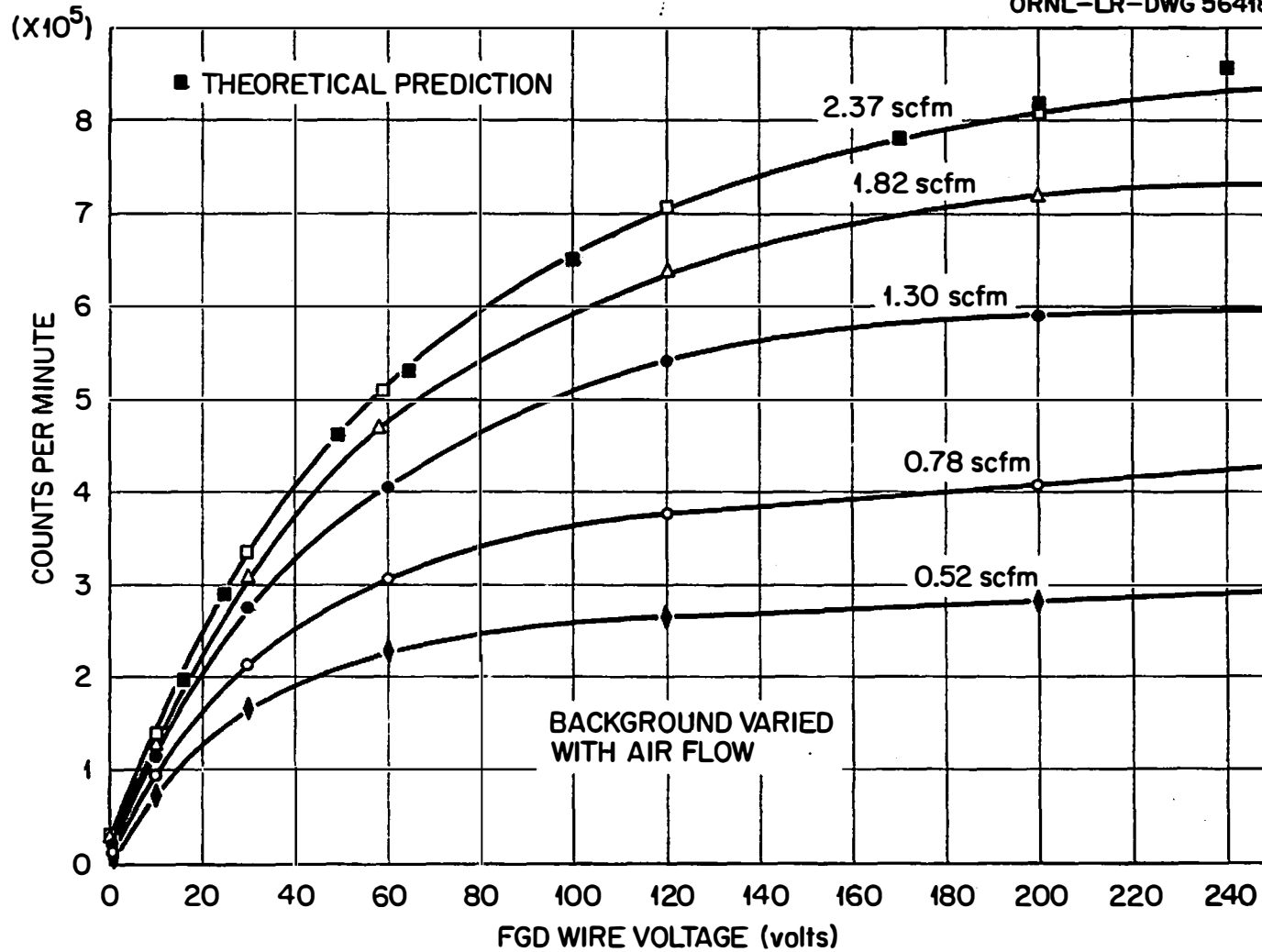
Fig. 12. Count Rate vs Voltage at Several Different Air Flows. The Background Has Been Subtracted for Each Curve. Fission Product Concentration Was Constant.

air through a 1-inch pipe (area 0.786 in.^{2}) would be $\dfrac{20.3 \times 144}{0.786}$ = 3.7 x

10^3 feet per minute = 62 feet per second. Since the distance from the

fuel specimen to the sample line junction is 31.5 feet, the air required

0.5 seconds to travel this distance.

The same pressure of 45 PSIG at a temperature of 70°F exists in

the FGD sample almost up to the collection chamber. The travel time for

a particle in this line depends on the flow; Figure 13 is a graph showing

this relation, computed as before. The pressure within the chamber is

slightly below atmospheric; this pressure was assumed to be 14 PSIG and

the time a particle remains in the chamber was calculated. This is also

shown on Figure 13 and in Table I. With this information we will examine

the curve in Figure 10.

Consider air entering the 10-inch long collection chamber, flowing

upward through it and out the top. As the air moves upward, ions in the

air will migrate to the central wire with the ions nearest the wire being

collected first. Reference to Table I shows that the air spends approxi-

mately 4 times as long getting to the chamber as it does in the chamber

for all flow rates. Also, the number of decays per second decreases with

time, so that most of the ions collected by the wire will have been formed

outside the chamber.[*] Thus the collection pattern will approximate a cone,

as illustrated in Figure 14. If we assume a uniform fission product

concentration in the air, then the count rate will be proportional to the

volume of the cone from which collection occurs. This volume will increase

---

[*]Assuming recombination is not rapid, which is a valid assumption
for the low ion concentrations and short times being considered.
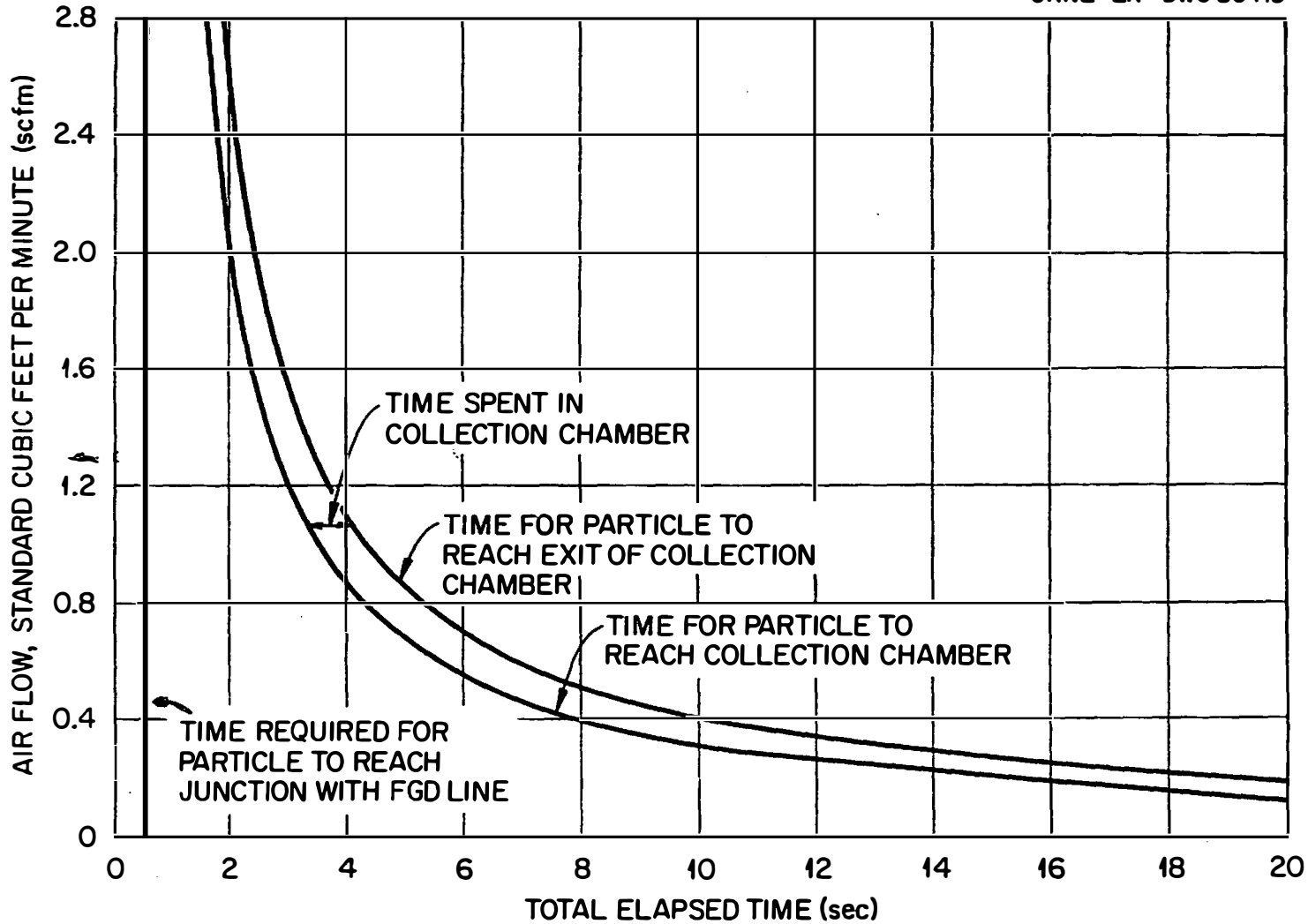
Fig. 13. Flow Time vs FGD Air Flow Rate for the ORNL Research Reactor Fission Gas Detector. Air Pressure, 45 lb per Square Inch.

TABLE I

AIR FLOW IN THE FISSION GAS DETECTOR SYSTEM

Air Flow (SCFM)	Time in FGD Lead Line (Seconds)	Total Time in Transit[a] (Seconds)	Time in FGD Chamber (Seconds)	Total Time in FGD System (Seconds)	Ratio of Time in Chamber to Total Transit Time
0.2	15	15.50	4.17	19.7	0.212
0.4	7.5	8.00	2.08	10.1	0.206
0.6	5.0	5.50	1.39	6.9	0.202
0.8	3.75	4.25	1.04	5.3	0.196
1.0	3.0	3.50	0.833	4.3	0.193
1.2	2.5	3.00	0.694	3.7	0.189
1.4	2.14	2.64	0.595	3.24	0.184
1.6	1.88	2.38	0.521	2.90	0.180
1.8	1.67	2.17	0.463	2.63	0.176
2.0	1.50	2.00	0.417	2.42	0.172
2.2	1.36	1.86	0.379	2.24	0.169
2.4	1.25	1.75	0.347	2.10	0.165
2.6	1.15	1.65	0.320	1.97	0.162
2.8	1.07	1.57	0.298	1.87	0.159

[a]Time in main exit line = 0.5 seconds.
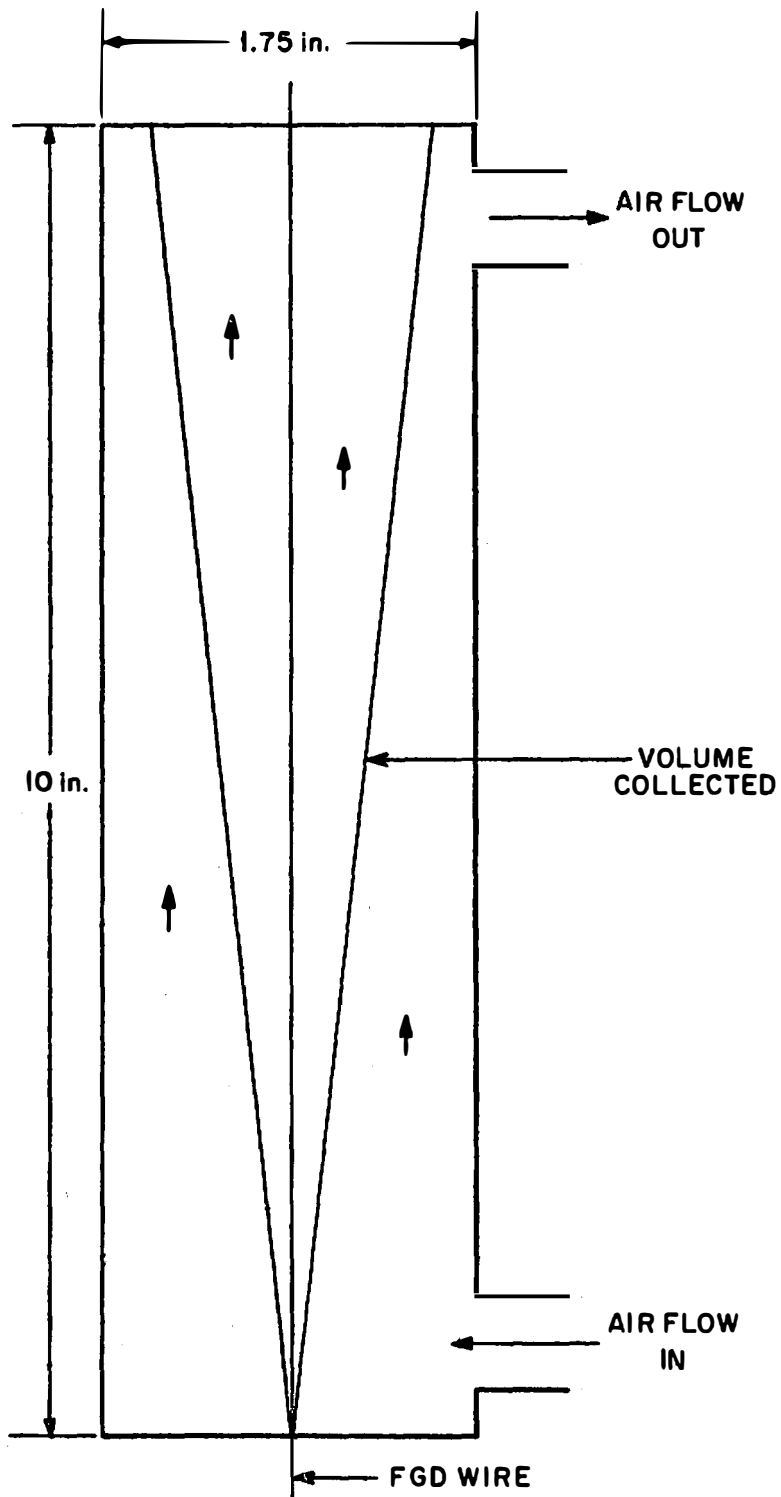
Fig. 14. Ion Collection Volume in the FGD Collect-
ion Chamber at Low Voltages.

as the voltage increases, until it reaches a limit when the radius of the base of the cone becomes 2.22 cm., the radius of the collection chamber. The volume of this cone is 1/3 πr_o^2 h where h = height of collection chamber = 25.4 cm. and r_o = radius of base of cone $\leq$ 2.21 cm.

The migration velocity of positive ions in an electrostatic field is given by,[117] $\frac{dr}{dt} = \mu E$ where $\frac{dr}{dt}$ = ion velocity, cm./sec.; μ = mobility, cm./sec./volt/cm.; and E = electric field strength, volts/cm. For a charged wire passing through a cylinder, the field strength E can be calculated from the relation,[118]

$$E = \frac{V}{r \ln (b/a)}$$

where

V = volts

r = distance from center of central wire

b = diameter of cylinder = 1.75 inches

a = diameter of central wire = 0.004 inches.

This reduces to E = $\frac{V}{6.08\ r}$ when the values for b and a are inserted. Then, $\frac{dr}{dt} = \frac{\mu V}{6.08\ r}$. Let t_o be the length of time a particle is inside the collection chamber. Then at t = t_o, r = r_o. Integrating the above equation gives, $\int_0^{r_o} 6.08\ r\ d r = \int_0^{t_o} \mu V dt$ so

$$3.04\ r_o^2 = \mu V t_o \qquad r_o^2 = \frac{\mu V t_o}{3.04}$$

Volume of cone collected from = 1/3 πr_o^2 h = 1/3 π x 25.4 x $\frac{\mu V t_o}{3.04}$

or, volume = const. x V at constant flow (and t_o). From this we conclude that the count rate, which is proportional to this volume, is proportional to the wire voltage: Count rate = const. x V, which is the linear relationship that was observed at low voltages.

It is possible to obtain an estimate of the length of this linear region from a knowledge of μ, the ionic mobility. When the mobility of an ion such as krypton or xenon is measured in carefully purified air or nitrogen, the value is higher than that found in ordinary atmospheric air.[119] The value of μ that has been found for large positive ions migrating in ordinary air is 1.3 to 1.4 cm./sec./volt/cm.[120] Now, the data plotted in Figure 10 were obtained at a flow rate of 0.52 SCFM; an ion at this flow rate would remain in the collection chamber for 1.6 seconds. This is the time t_0 which an ion at the very outside of the chamber has to migrate the distance r_0 and adhere to the wire, before being swept out of the chamber. To calculate the voltage V which is just sufficient to do this, we substitute in the equation $r_0^2 = \dfrac{\mu \, V t_0}{3.04}$ where t_0 = 1.6 sec., r_0 = 2.21 cm., and μ = 1.3 cm./sec./volt/cm. This gives V = 7.1 volts, which is in reasonably good agreement with the observed 10 volt linear region, considering the simplifications involved in these calculations. Another low-voltage measurement at a flow of 0.32 SCFM had a measured linear region of 7.0 volts and a calculated linear region from 0 to 4.4 volts, as shown in Figure 15. This demonstrates another prediction of this theory, namely that as the flow increases and t_0 decreases, the length of the linear portion of the count rate _versus_ voltage curve should become greater. This can be seen from the measurements at different flows shown in Figure 12. The curve at 2.37 SCFM is linear up to at least 30 volts, while the lowest curve at a flow of 0.52 SCFM has a linear region of less than 10 volts. The predicted linear voltage range at 2.37 SCFM is 32 volts.
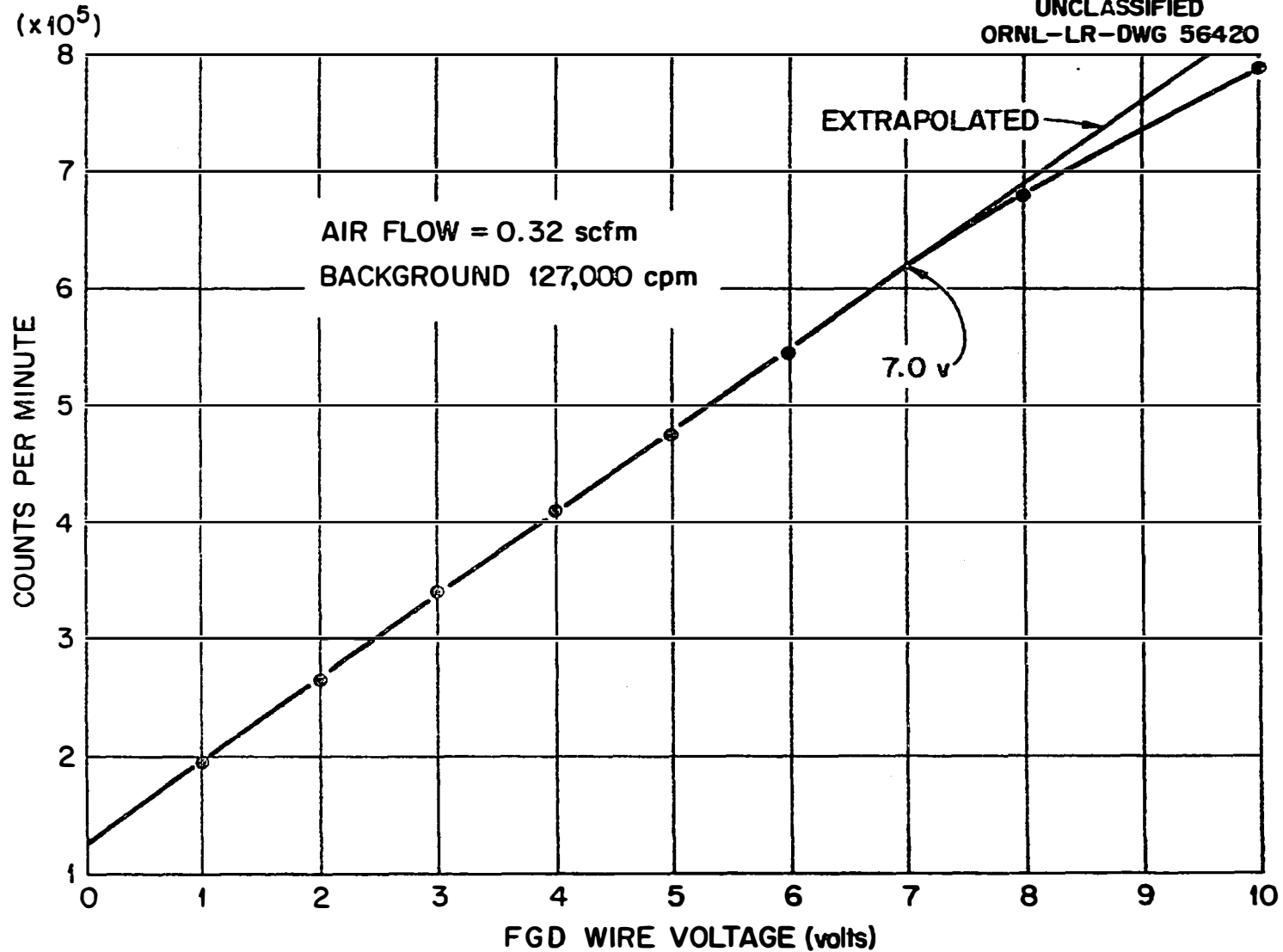
Fig. 15. Count Rate vs Voltage for Low Voltage and Air Flow, Showing Deviation from Linearity Above 7.0 Volts. Background has not been Subtracted.

If the analysis just presented is correct, than at the end of the linear count rate region nearly all of the fission products are being collected by the wire. An argument can be advanced to explain the continued count rate increase beyond this point, up to the saturation value. This is as follows: If we assume that most of the ions are generated outside the collection chamber, then as the voltage increases more of the ions will be collected on the lower part of the wire. Then the decay of these ions will be less before they reach the counter, and the count rate will be higher. At a wire speed of 5.55 inches per minute, the wire requires 1.87 minutes to get from the bottom of the chamber to inside the shield; from the top of the chamber this time is 3.67 minutes. For short half-life isotopes, this difference of 1.8 minutes could be significant.

Let h be the length of wire in the chamber on which no collection takes place (see Figure 16). The length of the chamber is 25.4 cm. and the wire speed is 14.1 cm. per minute. Now, a particle which can migrate 2.21 cm. in time t, where t is the length of time a particle has been in the chamber, can migrate r_0 cm. in time t_0. By simple geometry:

$$\frac{25.4-h}{2.21} = \frac{25.4}{r_0}$$

solving for h gives

$$h = 25.4 - \frac{25.4 \times 2.21}{r_0} ,$$

but r_0 was related to the wire voltage V by the formula,

$$r_0^2 = \frac{\mu \, V \, t_0}{3.04} .$$

At constant flow, t_0 (and μ) are constant, so that $r_0 = $ const. x $\sqrt{V}$. Thus, $h = 25.4 - \frac{\text{const.}}{\sqrt{V}}$. Since all particles are collected by time t,
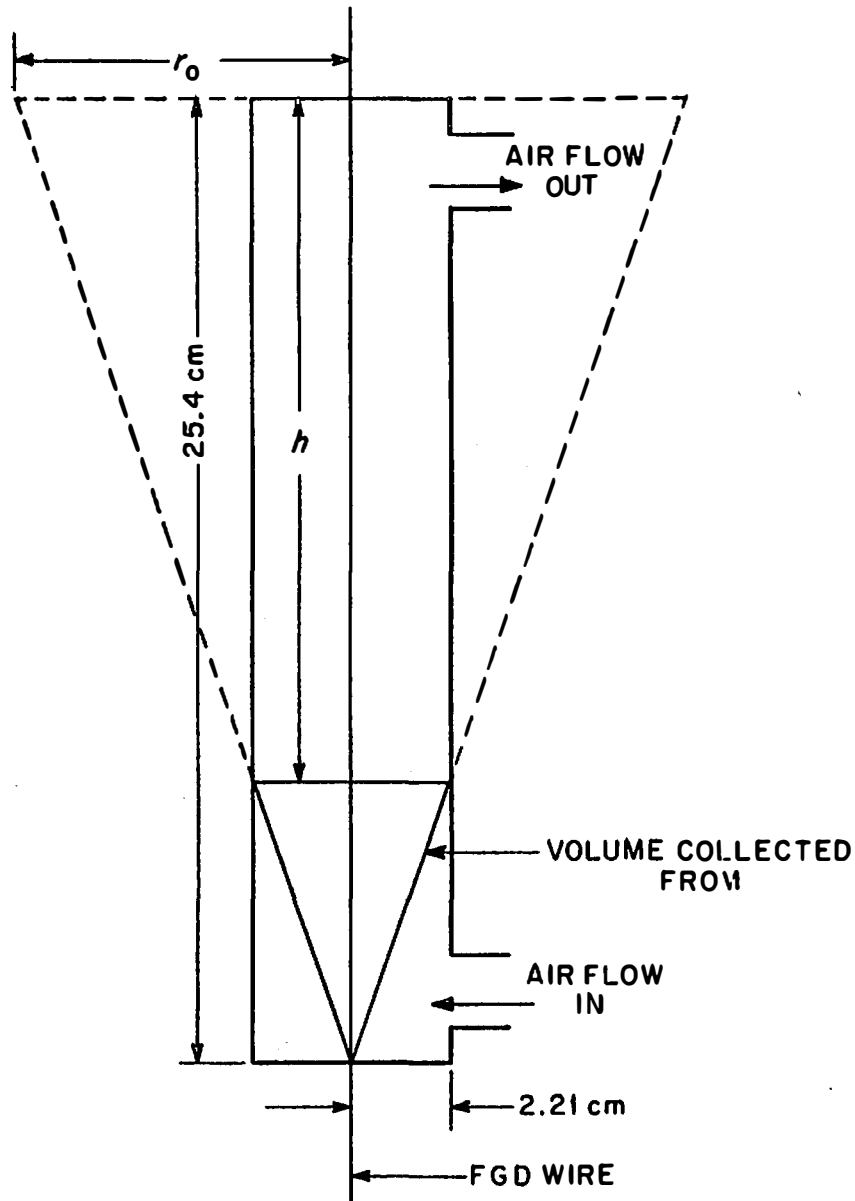
Fig. 16. The FGD Collection Chamber, Showing
Collection Volume at Moderate Voltage.

we shall assume the average particle is collected at time $t/2$.[*] Then the average time T to the counter is $1.87 + t/2$ minutes. Expressing t in terms of h and the wire speed, 14.1 cm./min., gives $t = \dfrac{25.4-h}{14.1}$. Thus, $T = 1.87 + \dfrac{25.4-h}{28.2}$. Substituting for h gives $T = 1.87 + \dfrac{const.}{\sqrt{V}} =$ decay time. Now let us assume that the fission products are decaying with decay constant λ. Let A_0 be the activity with no decay and A be the observed count rate. Then, $A = A_o e^{-\lambda T} = A_o e^{-1.87\lambda - \lambda K/\sqrt{V}}$ which reduces to $A = K_1 e^{-K_2/\sqrt{V}}$. This equation should give the count rate in the transition region of the count rate <u>versus</u> voltage curve when K_1 and K_2 are determined.

Referring to Figure 11 again, we shall use the count rate at 80 and 200 volts to determine, with two simultaneous equations, the values of K_1 and K_2. This gives $A = 182 \times 10^3 e^{-\frac{9.34}{\sqrt{V}}}$. This curve is also plotted on Figure 11. As can be seen, it gives a good fit from 15 to 240 volts. Above 240 volts, the saturation plateau begins and a further voltage increase produces only a small count-rate increase. The saturation plateau is not flat because of such factors as ion generation within the chamber and ion collection from outside the chamber. At high voltages, the wire will be able to attract, against the air flow, ions which are generated part of the way down the exit line.

---

[*]This is not strictly correct since there are more particles at large r, but the final equation will not be altered by this assumption.

B. Variation of Count Rate with Air Flow

Before discussing the count rate versus flow curves, the effects of changing the air flow on the count rate versus voltage curves should be considered. Several curves of count rate versus voltage at various flow rates are shown in Figure 12. One effect of flow rate has already been pointed out: the linear portion of the curve at low voltage is longer at high flow rates. This characteristic is emphasized by a replot of the data at low voltages in Figure 17. Another consequence of changing the flow rate is that, as the flow increases, the initial voltage at which saturation occurs becomes greater. Thus, the plateau begins at around 60 volts at 0.52 SCFM but does not start until over 200 volts at 2.37 SCFM. This means that the connecting region of the curves, fitted by the formula $A = K_1 e^{-K_2/\sqrt{V}}$, will also be shorter at low flow rates. For the curves shown in Figure 12, the 2.37 SCFM curve is fitted by the equation $A = 14.1 \times 10^5 e^{-7.86/\sqrt{V}}$ from 16 to 250 volts. A more accurately determined curve at 0.425 SCFM is shown in Figure 18. The theoretical curve $A = 4.8 \times 10^4 e^{-5.84/\sqrt{V}}$ fits these measured values from 6 to 60 volts, as shown. This result is the one that would be predicted from the change in flow velocity in the collection chamber; saturation should occur at a much lower voltage when the air velocity is small.

Turning now to the influence of flow on the count rate at constant voltage, we shall first examine the effect of changing the pressure of the system. A change in the pressure of the system affects the flow rate according to the relation shown in Figure 3. The pressure actually measured is the pressure at the Rotameter; the collection chamber, as previously
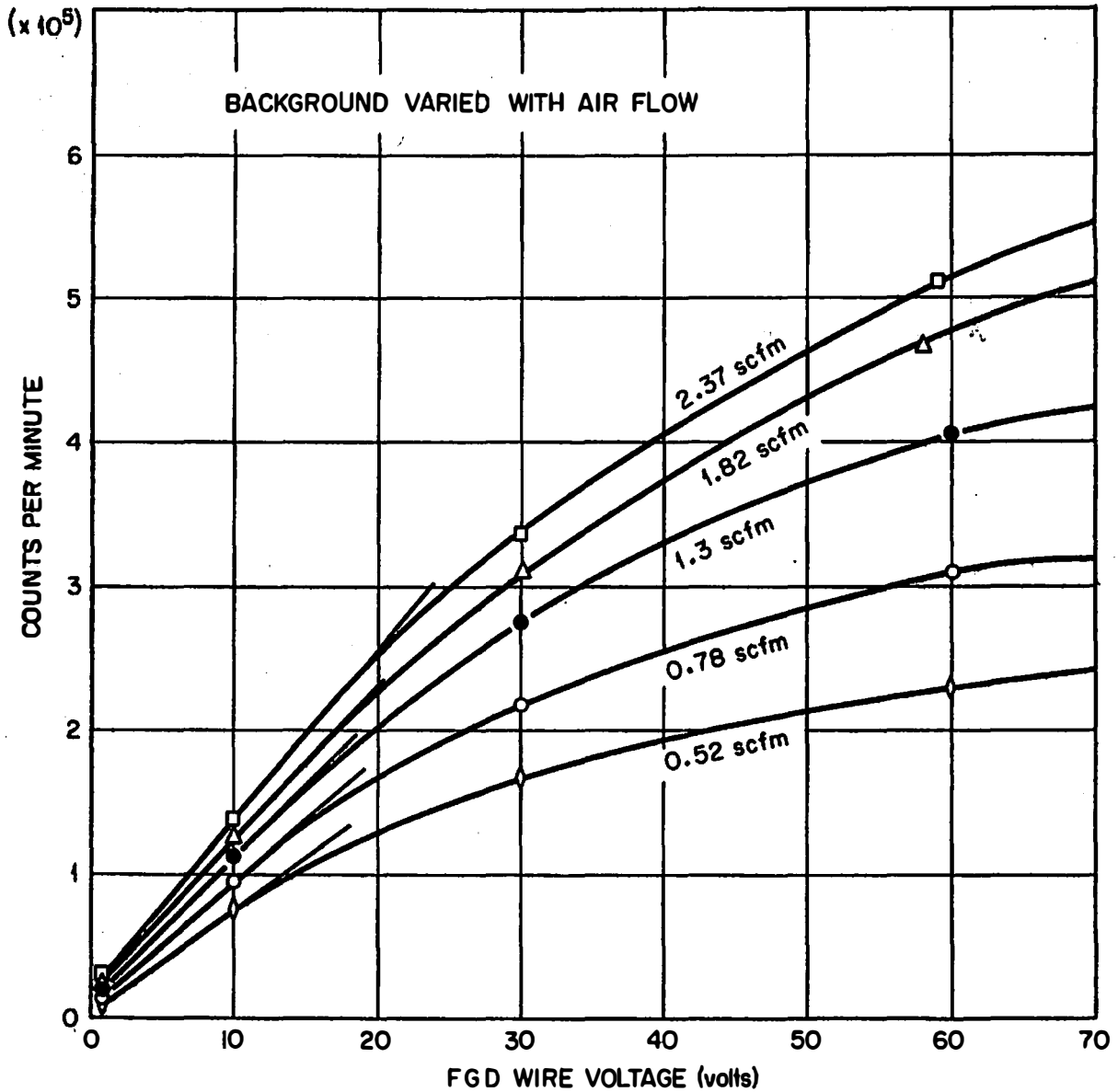
Fig.17. Linearity of Count Rate vs Voltage Curves at Low Voltage. Back — ground has been Subtracted. Fission Product Concentration was Constant.

AIR FLOW = 0.425 scfm
x EXPERIMENTAL POINTS
o THEORETICAL PREDICTION
BACKGROUND = 3200 cpm
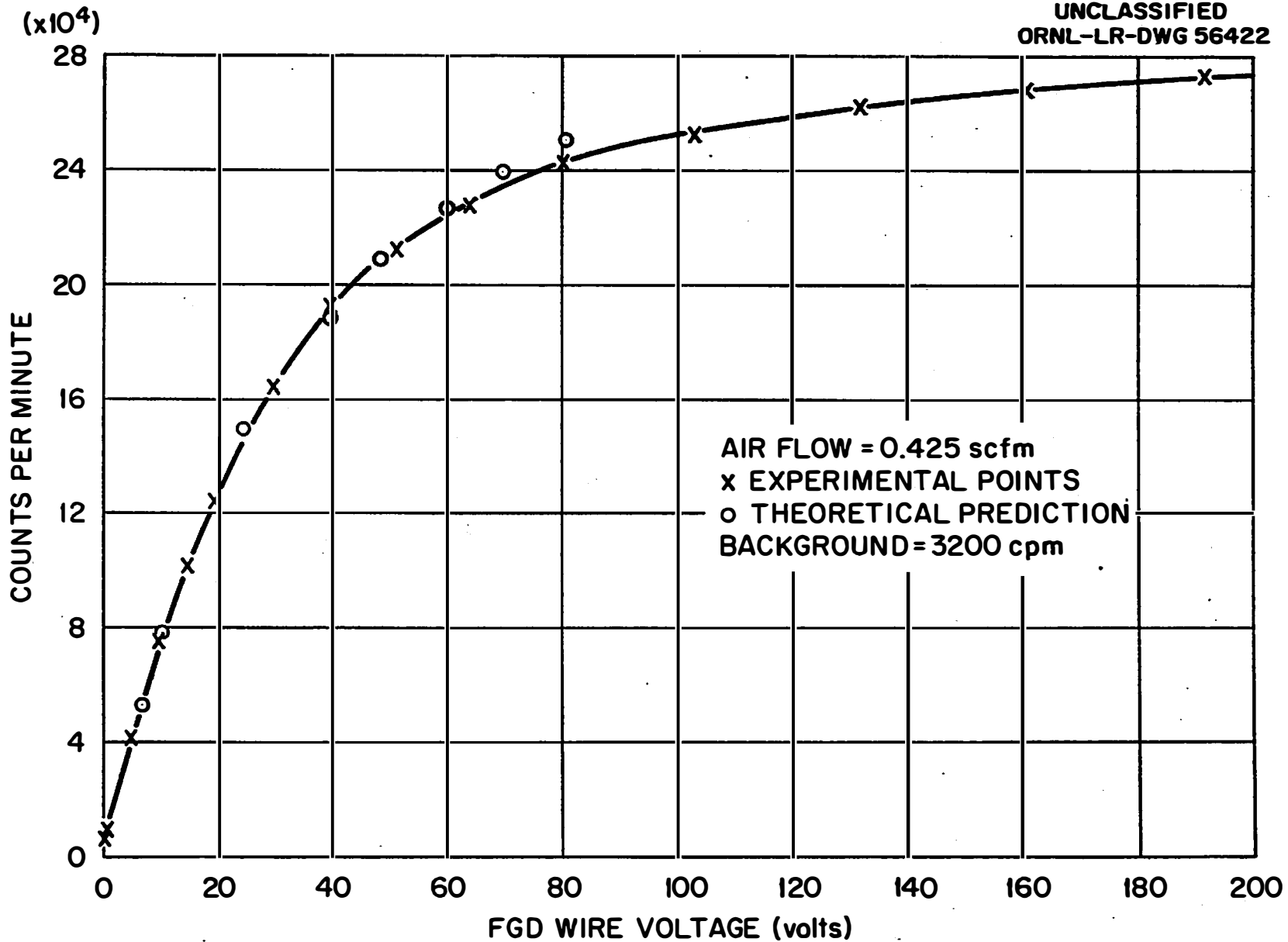
Fig. 18. Count Rate vs Voltage at Low Air Flow. Background, 3200 Counts per Minute, Has Been Subtracted.

mentioned, always operates at slightly negative pressure. Within the pressure limitations of the FGD system, from 0 to about 30 PSIG, the flow change with pressure is relatively small. Figure 19 is a plot of three count-rate versus voltage curves (including the same one used in Figure 18) all taken at 20 per cent flow but at pressures of 2, 10 and 20 PSIG. If we assume that the count rate increase at higher pressure is exactly proportional to the increase in flow, then we can multiply the curves at 2 and 10 PSIG by the appropriate factors and closely approximate the 20 PSIG curve. These factors as determined from Figure 3 are 1.43 for the 2 PSIG curve and 1.18 for the 10 PSIG curve. The results, as shown in Figure 19, are fairly close to the predicted values; when the curves are brought into coincidence at 200 volts, the factors found are 1.34 and 1.14, respectively.

If the data of Figure 12 are replotted, a series of curves of count rate versus flow can be obtained at several values of wire voltage. This is shown in Figure 20. Several features of this group of curves can be correlated with what has been observed previously. The lowest curve, at 10 volts, is linear from about 0.9 SCFM on. This corresponds to the low voltage linear region of the count rate-voltage curves. This is the region where the pattern of ion collection forms a conical volume such as that shown in Figure 14. The volume of this cone as derived in the preceding section was found to be vol. = const. x $V t_o$ where V is the wire voltage and t_o is the length of time a particle remains in the collection chamber. If we now let V be a constant and t_o vary, we note that t_o is inversely proportional to th flow: $t_o \propto \dfrac{1}{F}$ where F is the flow in SCFM.
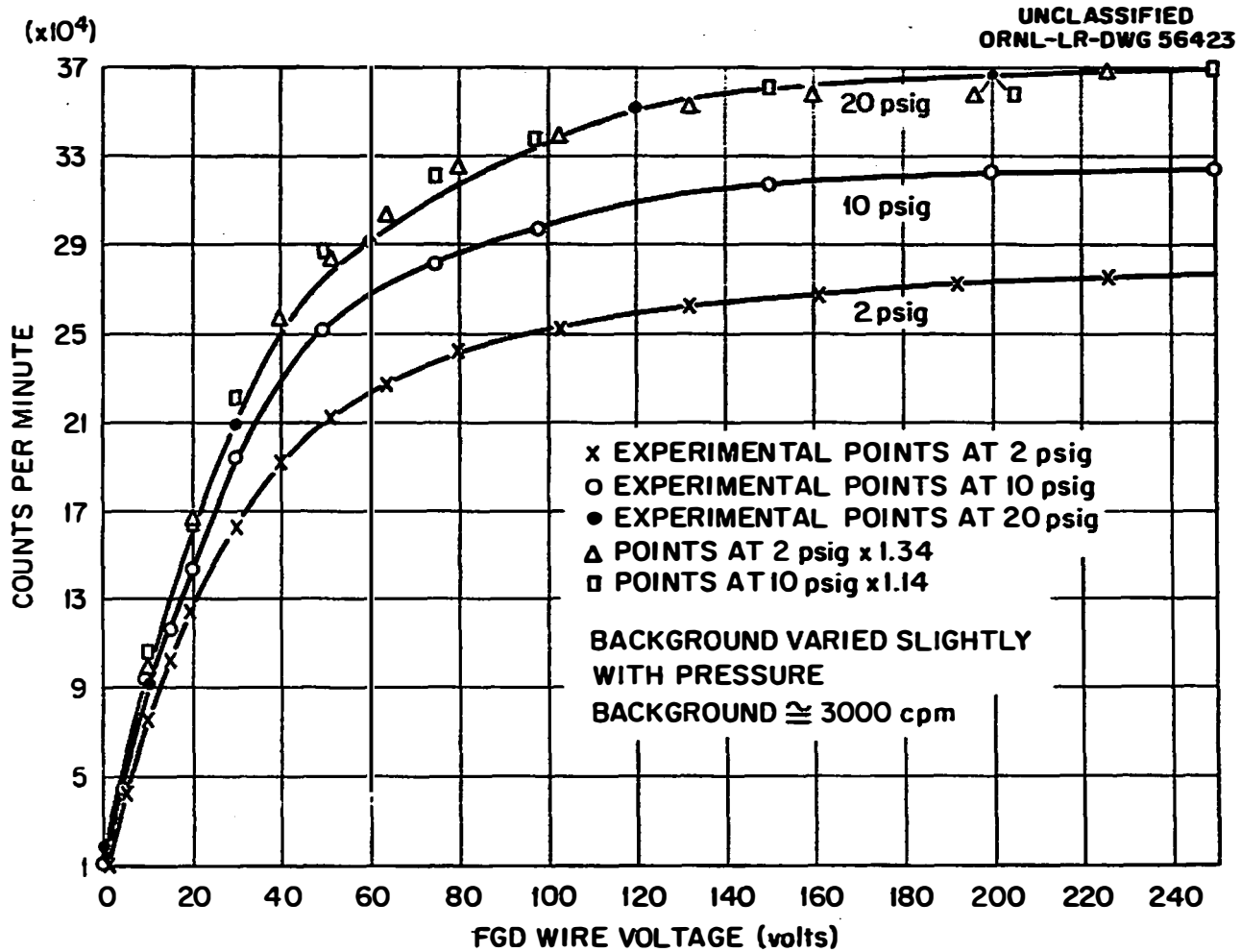
Fig. 19. Count Rate vs Pressure. The Lower Two Curves were Matched
to the Upper Curve at 200 volts. Background Has Been Subtracted for Each Curve.
Fission Product Concentration was Constant.
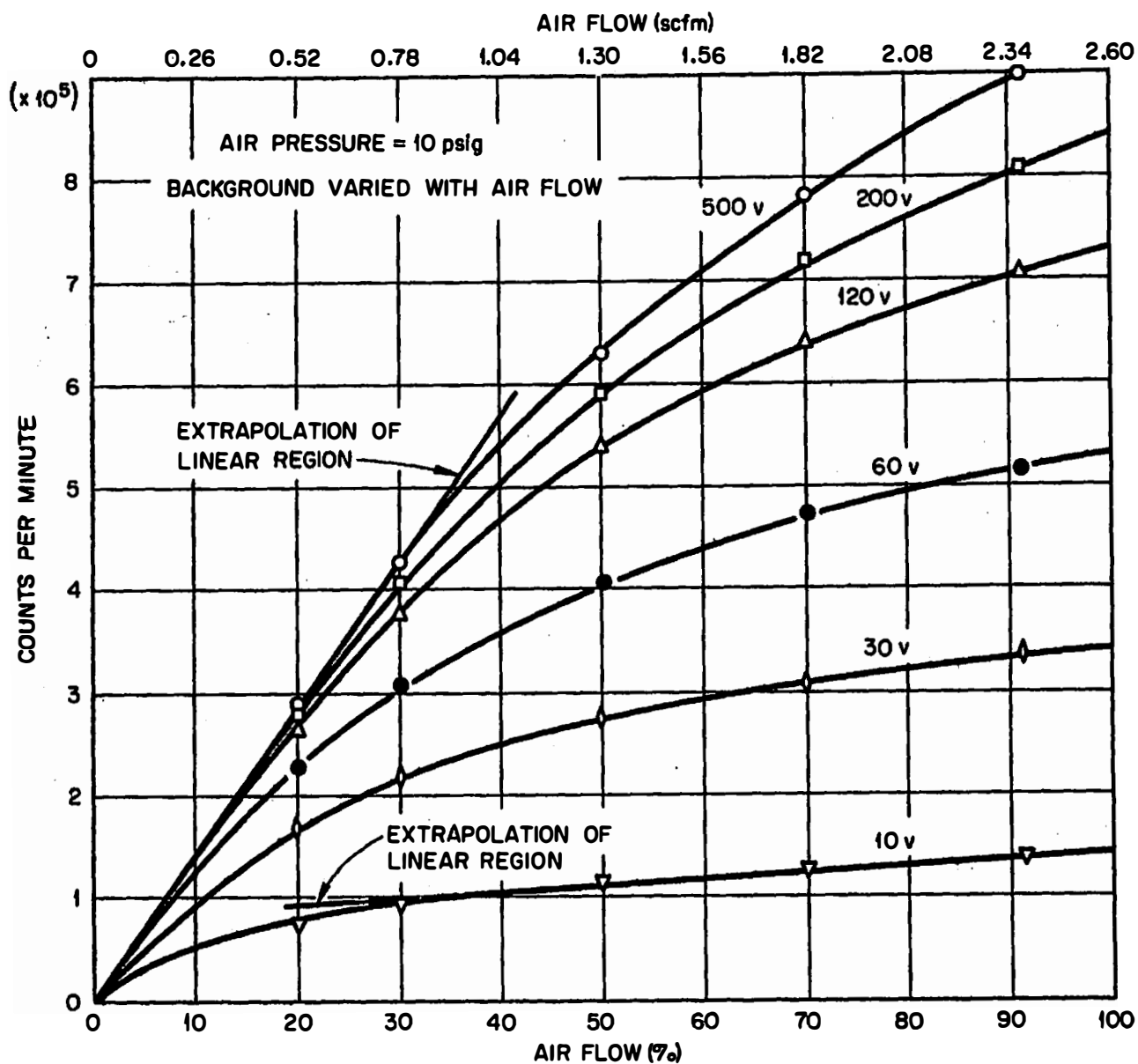
Fig. 20. Count Rate vs Flow at Several Different Voltages, Background has been Subtracted. Fission Product Concentration was Constant.

But whereas in the previous section the count rate could be assumed proportional to the volume of this cone, we now have to consider the added effect of the flow: when the flow doubles, the number of ions passing through the chamber per minute also doubles. Thus we conclude that count rate α F. Combining these two effects, we obtain, count rate = const. x V t_O x F = const. x $\frac{F}{F}$ = const., when the voltage is fixed. This should hold true when the voltage is low enough and flow high enough for the count rate versus voltage relation to be linear.

The actual curve obtained at 10 volts is not constant, but increases slightly with increasing flow. This can probably be attributed to an increase in pressure within the collection chamber; this was assumed to be constant at a value slightly below 1 atmosphere. However, this pressure does increase at high flow rates because the chamber is larger than the exit line (3/8 inch tubing) which connects it to the reactor off-gas system. For instance, it has been observed that for 30 PSIG pressure at the Rotameter, flows above about 80 per cent (2.8 SCFM) on the Rotameter cannot be obtained because the Fission Gas Detector pressure switch (see p. 44) gives an alarm and shuts off the flow. At high pressures, the ratio of flow to linear velocity increases; this should result, when inserted in the formula just derived, in a higher count rate. The linear region at 30 volts starts at a higher flow than for 10 volts; this is in keeping with the observation in the last section that the linear part of count rate-voltage curves was only 30 volts long, even at 2.37 SCFM. Figure 21 is another count rate versus flow plot, showing curves taken at 5 volts, 10 volts and 22.5 volts at differing fission product concentrations. In this plot the
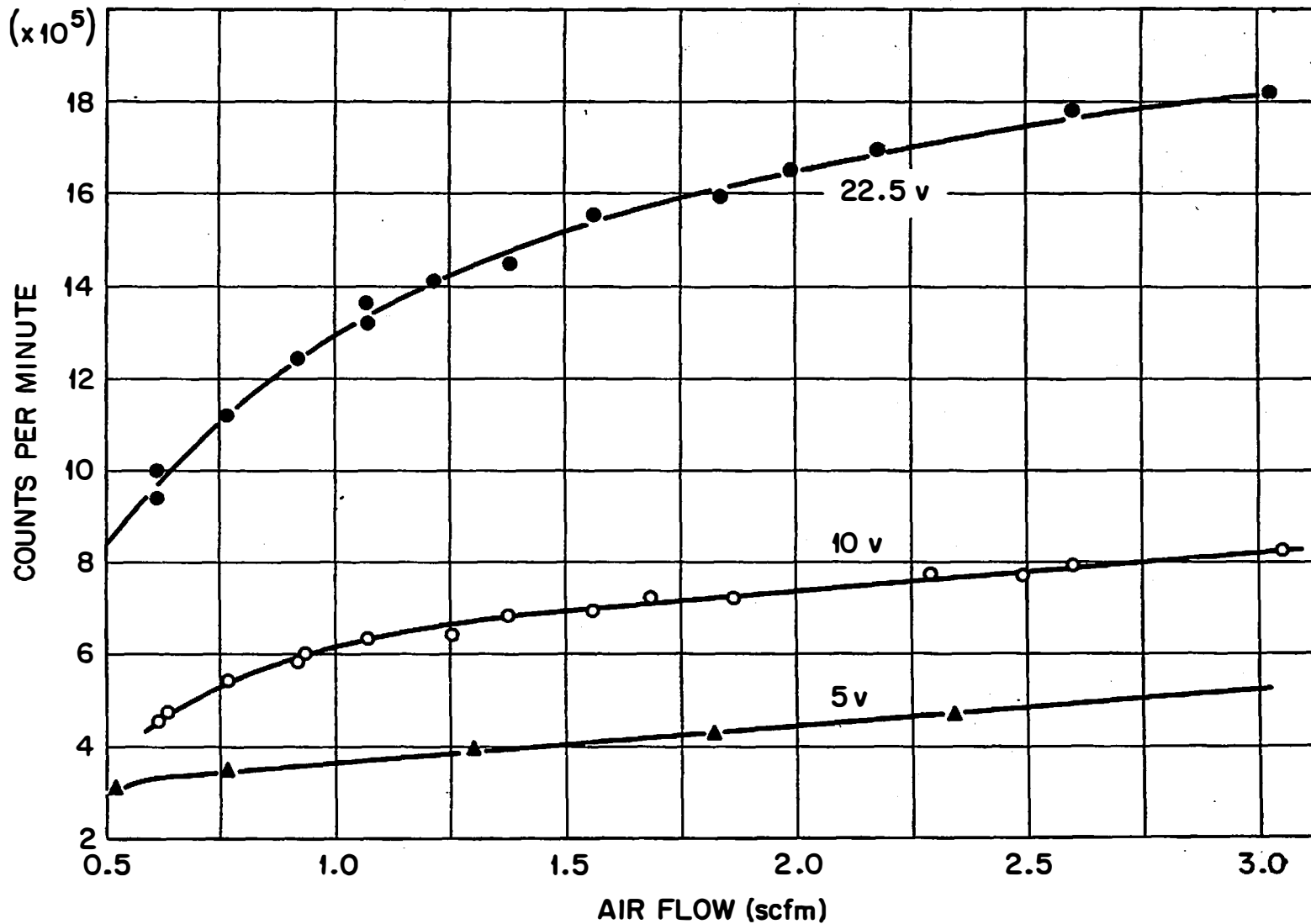
Fig. 21. Count Rate vs Flow for Three Different Voltages. Background has been Subtracted for Each Curve. Fission Product Concentration was Different for Each Curve.

linear portion of the 5-volt curve begins at 0.73 SCFM; for the 10-volt curve this value is again 0.9 SCFM and for the 22.5-volt curve, 1.15 SCFM.

The connecting region of the count rate-voltage curves will again appear at moderate voltages. The measured data for the 60-volt curve, for instance, should lie completely within the connecting region. This curve is plotted separately in Figure 22. Assuming the same mechanism to operate that was postulated in the previous section, we can derive a semi-empirical equation which should follow the curve. The equation which fitted the count rate-voltage curves was $A = K_1 e^{-K_2/\sqrt{V}}$ where K_1 and K_2 were constants determined by matching the equation to the curve. If the same reasoning is used, with voltage held constant instead of flow, we find that the exponential portion of this equation should be changed to $e^{-k_2\sqrt{F}}$ where F is the flow rate. However, we must again insert a factor of F in the equation to show the direct dependence of count rate on the number of ions passing through the chamber. This gives as a final result, $A = k_1 F e^{-k_2\sqrt{F}}$. When this equation is fitted to the curve of Figure 22 at 2.08 and 0.52 SCFM, the resulting equation is $A = 8.12 \times 10^5 F e^{-0.844\sqrt{F}}$. A plot of this equation is included on Figure 22; as can be seen, there is a fairly good fit.

At values of the wire voltage which are not completely within the connecting region, the above formula does not hold over the entire range of flow values. Figure 23 is a plot of a curve taken with 30 volts on the wire. At high flow rates, this curve will be nearly linear; the connecting region is expressed by the equation $A = 8.16 F e^{-1.01\sqrt{F}}$. This gives a good fit from 0.5 to 2.5 SCFM; this curve is also plotted on Figure 23.
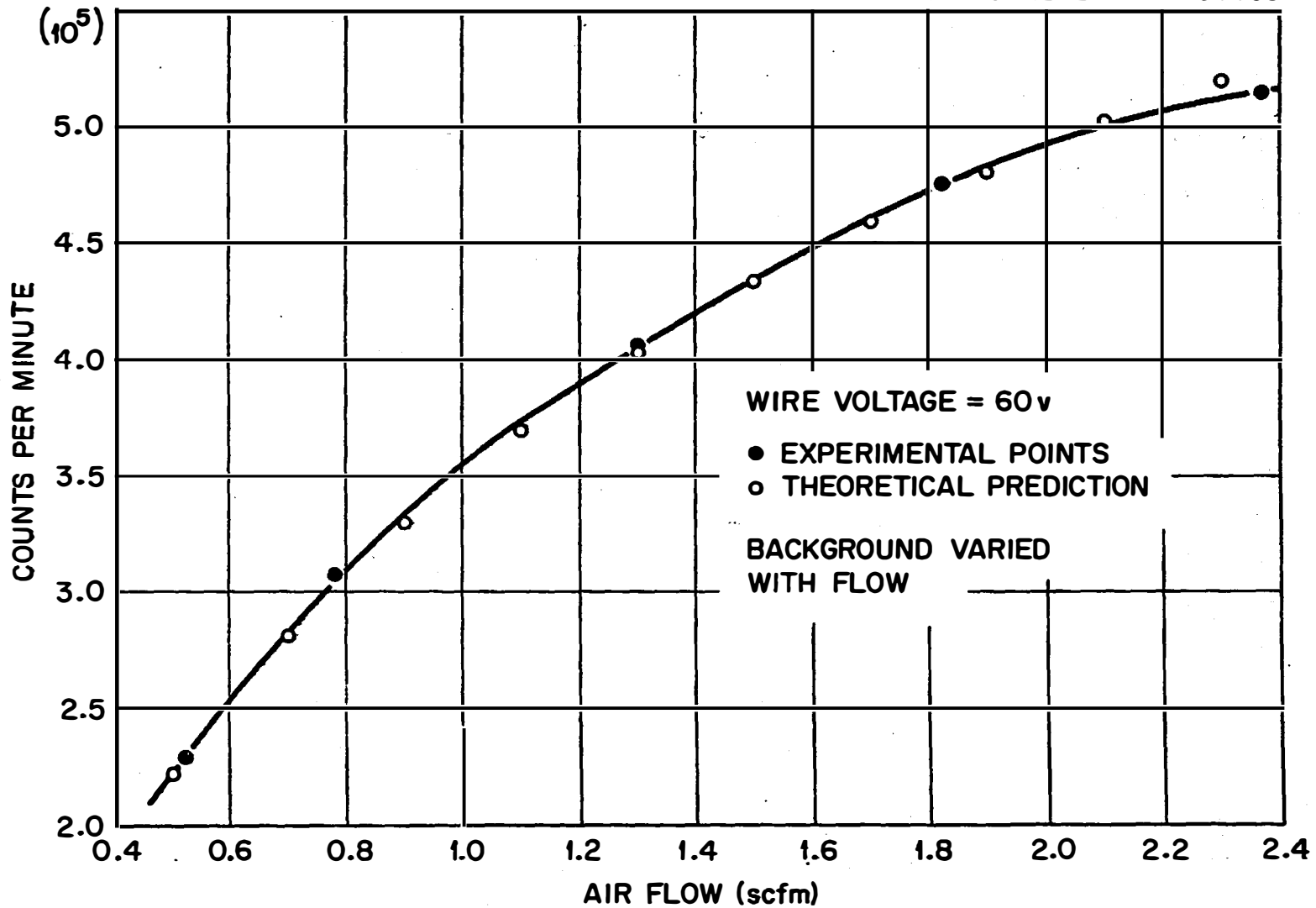
Fig. 22. Count Rate vs Air Flow at a Constant Wire Voltage of 60 Volts. Background has been Subtracted.
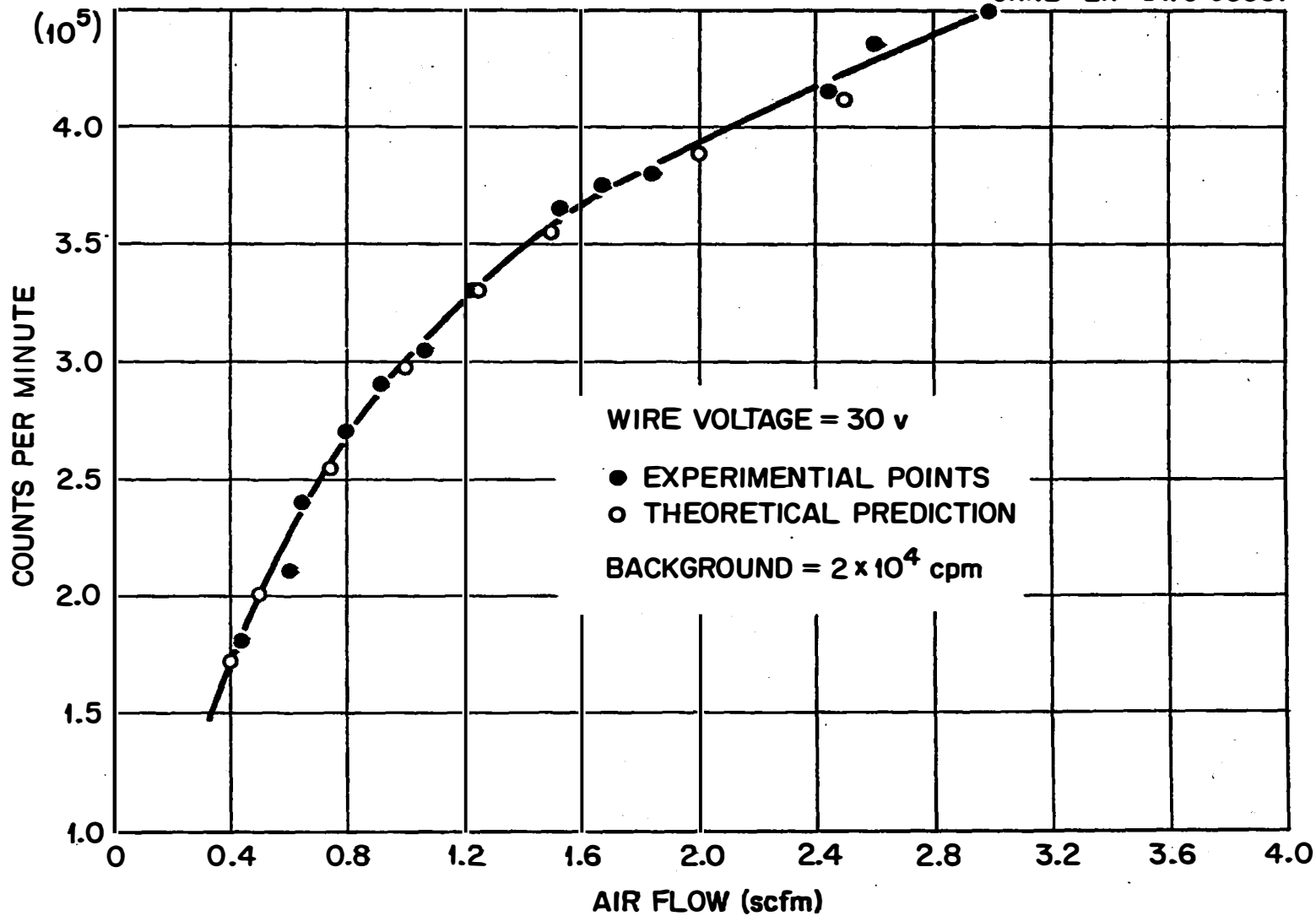
Fig. 23. Count Rate vs Air Flow at a Constant Wire Voltage of 30 volts. Background, 2×10^4 Counts Per Minute, has been Subtracted.

We are now in a position to characterize better the saturation region of the count rate-voltage curves. Saturation occurs when the ions entering the bottom of the chamber are drawn immediately to the collecting wire, so that only the part of the wire (perhaps an inch long) which is just leaving the chamber collects ions. As long as this is true, then the count rate should be directly proportional to the flow; when the flow doubles, the count rate should double. The count rate should follow the equation, count rate = const. x F. From Figure 20 we can see that this is actually followed for low flow rates and high voltages, where the saturation plateau of the count rate-voltage curves was fully developed. Above 1 SCFM, however, even at 500 volts, the count rate deviates from this prediction. This is a consequence of the longer connecting region. The turbulence of the air at higher flow rates probably has an effect in producing deviations from non-linearity.

C. The Variation of Count Rate with Wire Speed

A third variable in the Fission Gas Detector system which will affect the performance is the wire speed. The wire speed was somewhat more difficult to change than the air flow or wire voltage. To accomplish this, the 2 revolution-per-minute Bodine motor on the wire drive was removed and a motor of a different speed substituted. The wire speed through the Fission Gas Detector is directly proportional to the motor RPM. Only a few motors of suitable speed range were available, so the effects of wire speed change were not determined as rigorously as the voltage and flow relations. However, some useful data were obtained.

A determination of the variation in count rate with wire speed was made at constant fission product concentration. For this measurement 1, 2, 6, 9.3 and 23 RPM motors were used. Figure 24 is a plot of the data obtained; the RPM of the motor is plotted as an ordinate and counts per minute as the abcissa. It is apparent that the count rate-wire speed relation will be greatly influenced by the geometry of the Fission Gas Detector. Two effects can be distinguished. When the wire speed is increased, the length of time the wire spends in the collection chamber will be reduced, and the time for the wire to get from the collection chamber to the counter will be reduced. Regarding the first of these effects, let us consider the case of high wire voltage, producing the count rate plateau discussed in Section A. In this case, nearly all of the fission product ions will be collected on the bottom part of wire just as it leaves the collection chamber. If we let C be the concentration of ions collected per centimeter on the wire at wire speed S, then when the wire speed is doubled the ion concentration will be halved (since the same number of ions will be spread over twice the length of wire). Thus we can write $C \propto \dfrac{1}{S}$. Now, the count rate will depend on the total number of ions in the detector shield; since the length of wire in the shield is constant, the count rate varies with the ion concentrations: count rate $\propto \dfrac{1}{S}$. This relation may seem less obvious when the voltage is below the plateau value, but it will still be true because, as will be seen shortly, the count rate-voltage curves have the same shape for all wire speeds.

The second effect of wire speed on count rate will be the decreased delay from the collection chamber to the detector at higher speeds. The
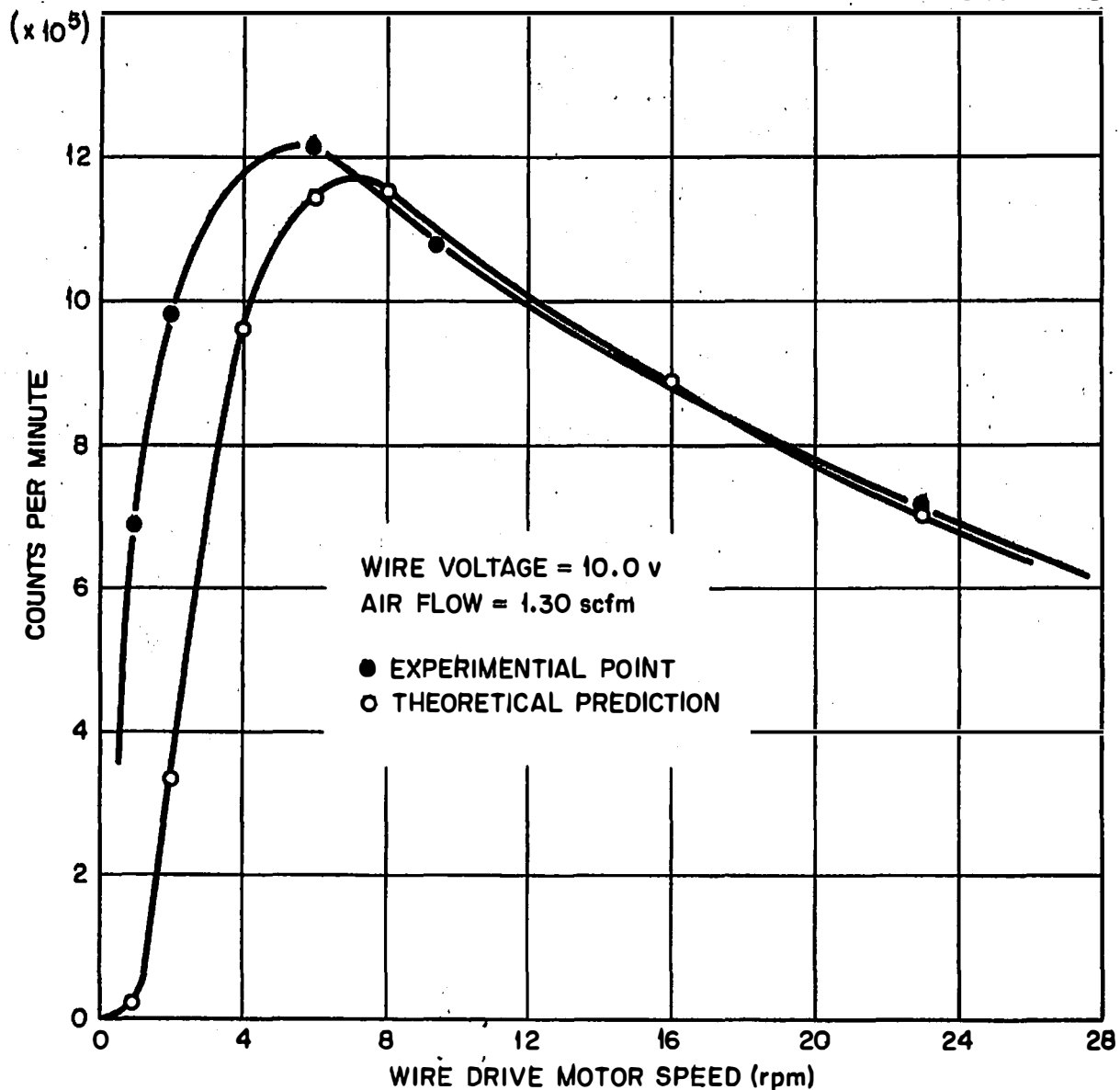
Fig. 24. Count Rate vs Wire Speed for Constant Wire Voltage and Air Flow. Background, 3.2×10^4 Counts Per Minute, has been Subtracted.

measured wire speed of the 2 RPM motor was 5.55 inches per minute. Since

the distance from the bottom of the collection chamber to the inside of

the shield (see Figure 4) is 10-1/8 inches, the time for the wire to

travel this distance will be 1.87 minutes. This delay has been measured;

air flow and voltage through the Fission Gas Detector were started before

the wire drive was turned on and ions were collected on the wire. Then

the wire drive was turned on and the time before a significant count rate

increase occurred was observed. This tended to give a low result, since

the count rate started to climb before the wire actually entered the de-

tector shield, but the measured times were about 1.75 minutes. Table II

is a tabulation of wire speed and time from collection chamber to shield

for each motor speed.

Following the same reasoning that was used in explaining the count

rate-voltage results in Section A of this chapter, we can assume a constant

half-life for the material collected on the wire and postulate that count

rate α $e^{-\lambda T}$ where T is the delay time from the chamber to the detector,

and λ is the decay constant of the material.* The validity of assuming

a constant half-life for decay was not discussed in Section A. This approxi-

mation is not actually valid when more than one fission product nuclide is

collected on the wire, and the activity of the F-2 test system FGD wire

can always be resolved into at least two components. However, at a con-

stant wire speed the initial decay of the mixed fission products is very

close to having a constant half-life. For this reason, the relations worked

_____

*The decay constant λ is related to the half-life $t_{\frac{1}{2}}$ by the expres-
sion = $\dfrac{0.693}{t_{\frac{1}{2}}}$.

TABLE II

FGD WIRE SPEED, DELAY TIME AND MOTOR SPEED

Motor Speed (RPM)	Calculated Delay Time (Minutes)	Measured Delay Time (Minutes)	Calculated Wire Speed (Inches/Min.)
1	3.74	3.1	2.78
2	1.87	1.75	5.55
6	0.623	– –	16.65
9.3	0.402	<1	25.8
23	0.162	~2 sec.	63.8

out for count rate <u>versus</u> flow and voltage at constant wire speed are

valid. When the wire speed is changed, a different situation arises:

at high wire speed, not only is the decay time to the detector shorter,

but short half-life isotopes are emphasized relative to longer half-life

nuclides. The reverse is true at low wire speed. Thus an isotope with

a 1 minute half-life would be decayed hardly at all when the wire speed

is 23 RPM, while it would be over 2/3 decayed at 1-RPM. A 10-minute half-

life isotope on the other hand would be little affected at either wire

speed.

For this reason, λ will not act as a constant, and a simple expres-

sion for the variation of count rate with wire drive cannot be obtained.

Nevertheless, we can derive an equation which has the general features of

the experimental results. Combining the two factors we have just dis-

cussed gives, count rate $= \dfrac{\text{const.}}{S} \times e^{-\lambda T}$ where S is the wire speed or

motor speed. Now T, the delay between collector and detector, is propor-

tional to 1/S; thus we can write, count rate $= \dfrac{C_1}{S} e^{-C_2/S}$ where C_2, con-

taining the decay constant λ, is assumed to be a constant. The constants

C_1 and C_2 can be determined by solving two simultaneous equations using

two experimental points; this was done, using the data at 9.3 and 23 RPM.

The results were adjusted slightly to give a better fit; the equation

plotted in Figure 24 is count rate $= \dfrac{2200}{S} e^{-7/S}$ where S is expressed

in RPM. The effect of a non-constant λ is clearly shown on this plot; at

low RPM, the count rate is higher than predicted because the longer half-

life components did not decay off fast enough. However, the general shapes

of the two curves are the same.

The same data are plotted against decay time as an abcissa in Figure 25. The difference between theory and experiment is accentuated in this graph, since the theoretical equation was arbitrarily forced to fit the short-delay end of the curve. The form of the equation when plotted against time is, count rate $= C_1 T e^{-C_2 T}$. A better fit to the experimental curve should result from a two-group decay expression, such as count rate $= C_1 T e^{-C_2 T} + C_3 T e^{-C_4 T}$. Unfortunately, curve fitting with such a formula is very difficult; simultaneous solution of four such equations can be done only by trial and error, while other methods of curve fitting such as the method of least squares require that the terms be expanded in series and very laborious calculations performed.

Count rate _versus_ voltage curves were run at various wire speeds for several values of air flow. This was done at 1, 2 (already discussed), 9.3 and 23-RPM. These curves are shown in Figures 26, 27 and 28. The count rates are different for the three cases, reflecting the change in count rate at different wire speeds and possibly a change in fission product concentration for the different runs; but the appearance of these curves is generally the same as for the 2-RPM graphs. To determine how closely the curves duplicated each other for equivalent count rate, the data at 30 per cent flow for all wire speeds was normalized to the 2 RPM curve at 200 volts. The results are shown in Table III and Figure 29. As the graph shows, the curves are identical within the limits of experimental error. This also holds true when the same procedure is used for the other flow rates, or if the count rate-flow curves at constant voltage are compared. This seemed somewhat surprising at first, but a review of
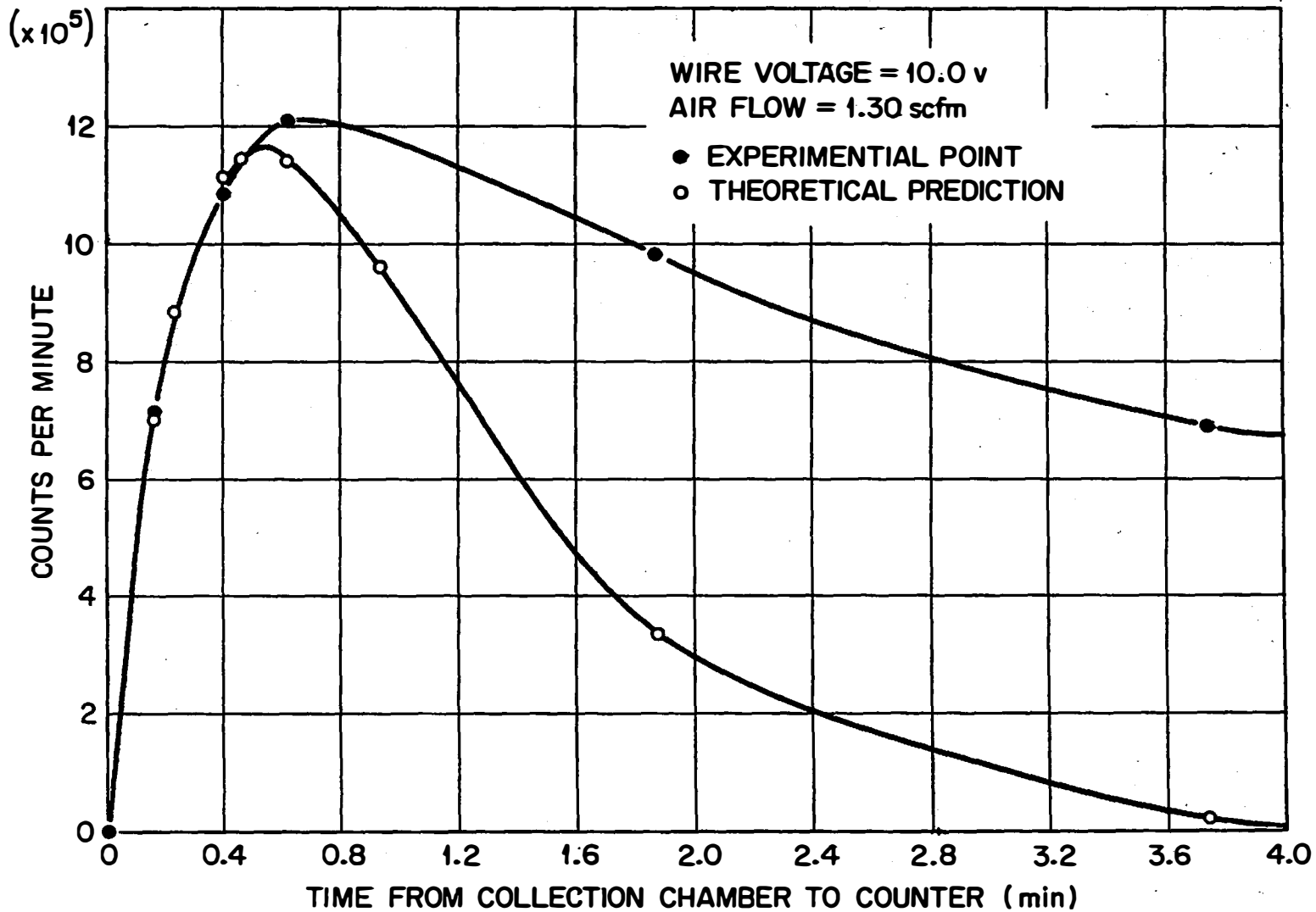
Fig. 25. Count Rate vs Delay Time Between Collection Chamber and Detector. Wire Voltage and Air Flow are Constant. Background, 3.2×10^4 Counts Per Minute, has been Subtracted.
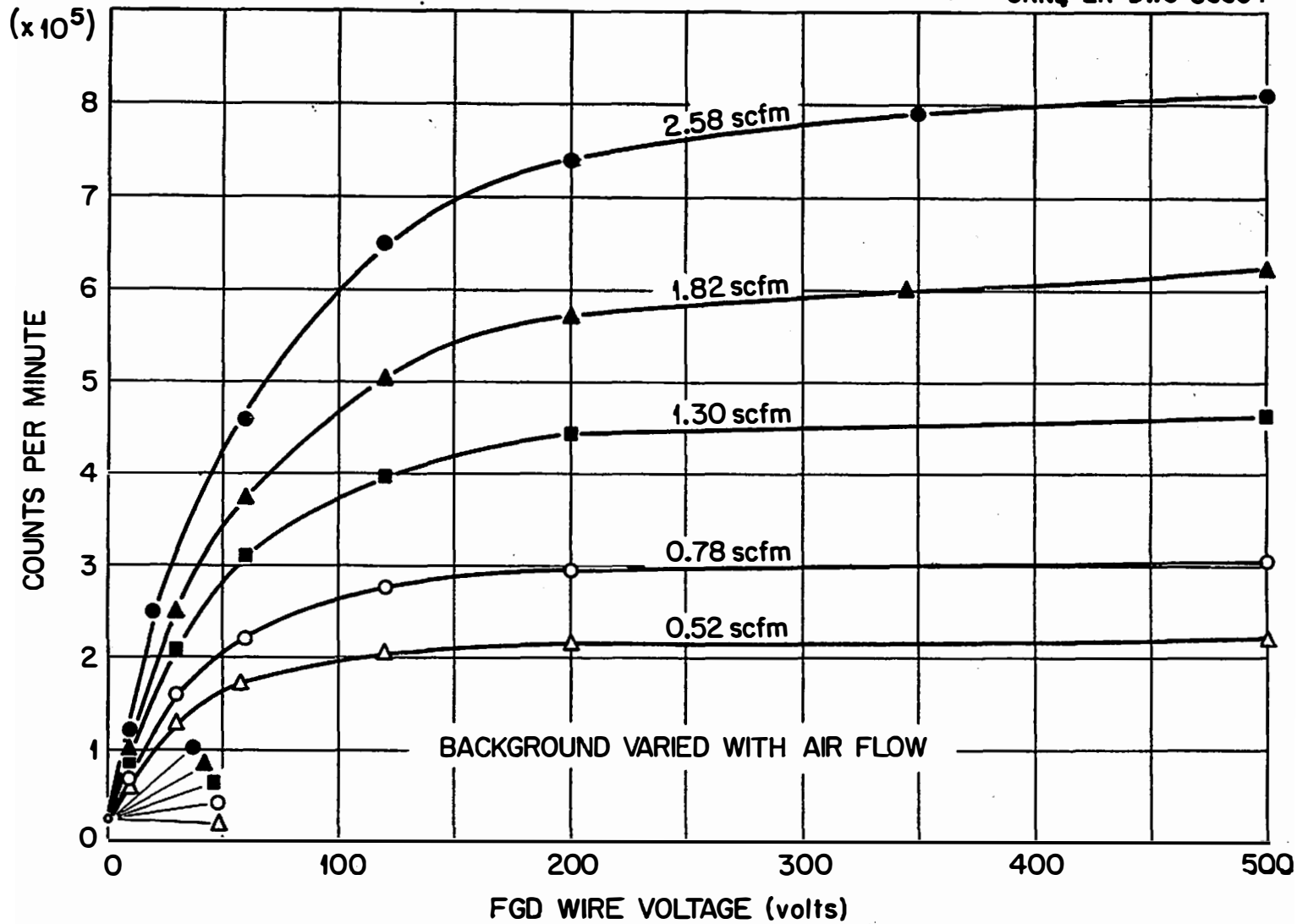
Fig. 26. Count Rate vs Voltage Curves for a Motor Speed of 1rpm. Background has been Subtracted from Each Curve. Fission Product Concentration was Constant.
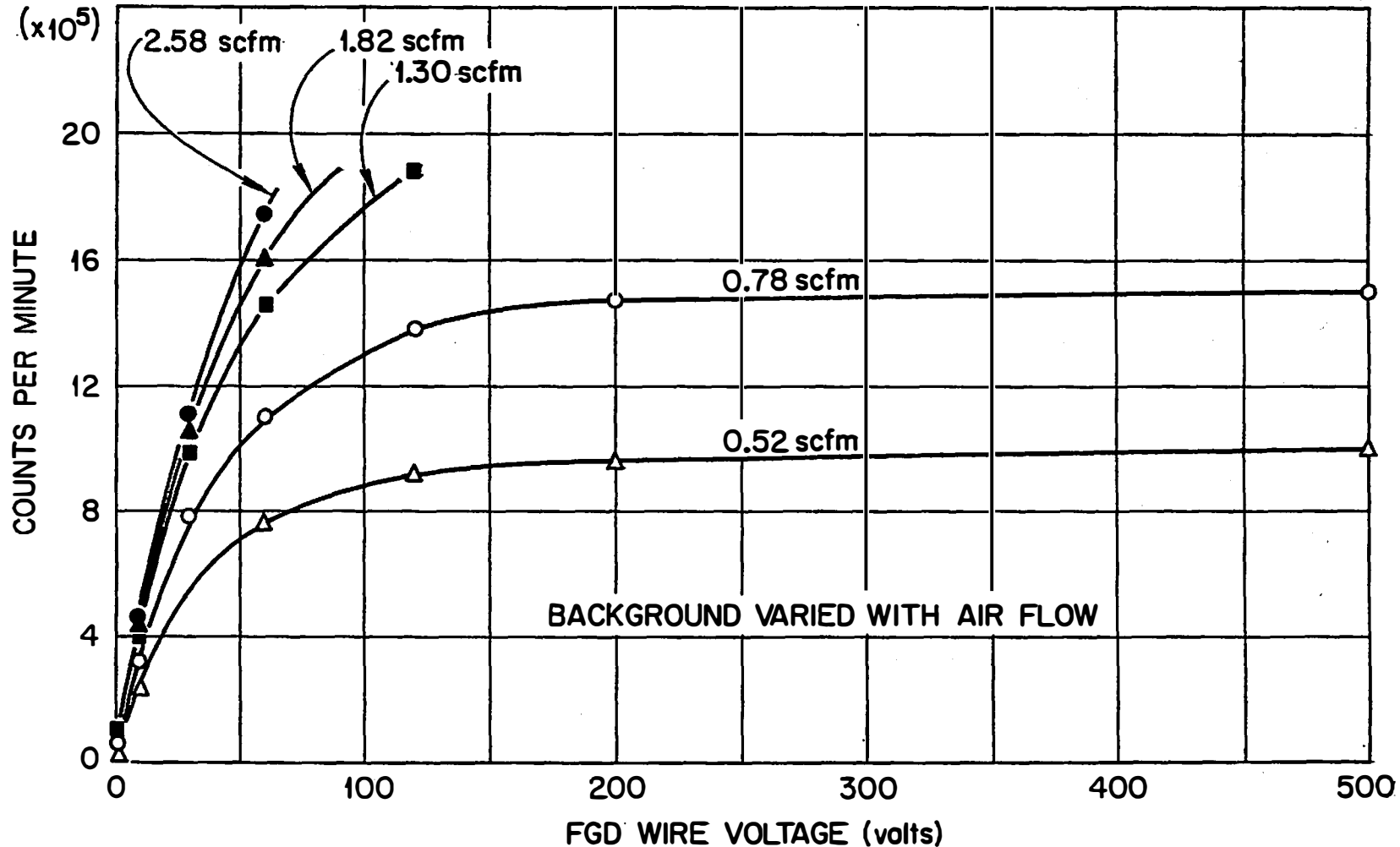
Fig. 27. Count Rate vs Voltage Curves for a Motor Speed of 9.3 rpm. Background has been Subtracted from Each Curve. The Curves at 1.30, 1.82, 2.58 scfm were not Completed Because the Count Rate Meter was Saturated. Fission Product Concentration was Constant.
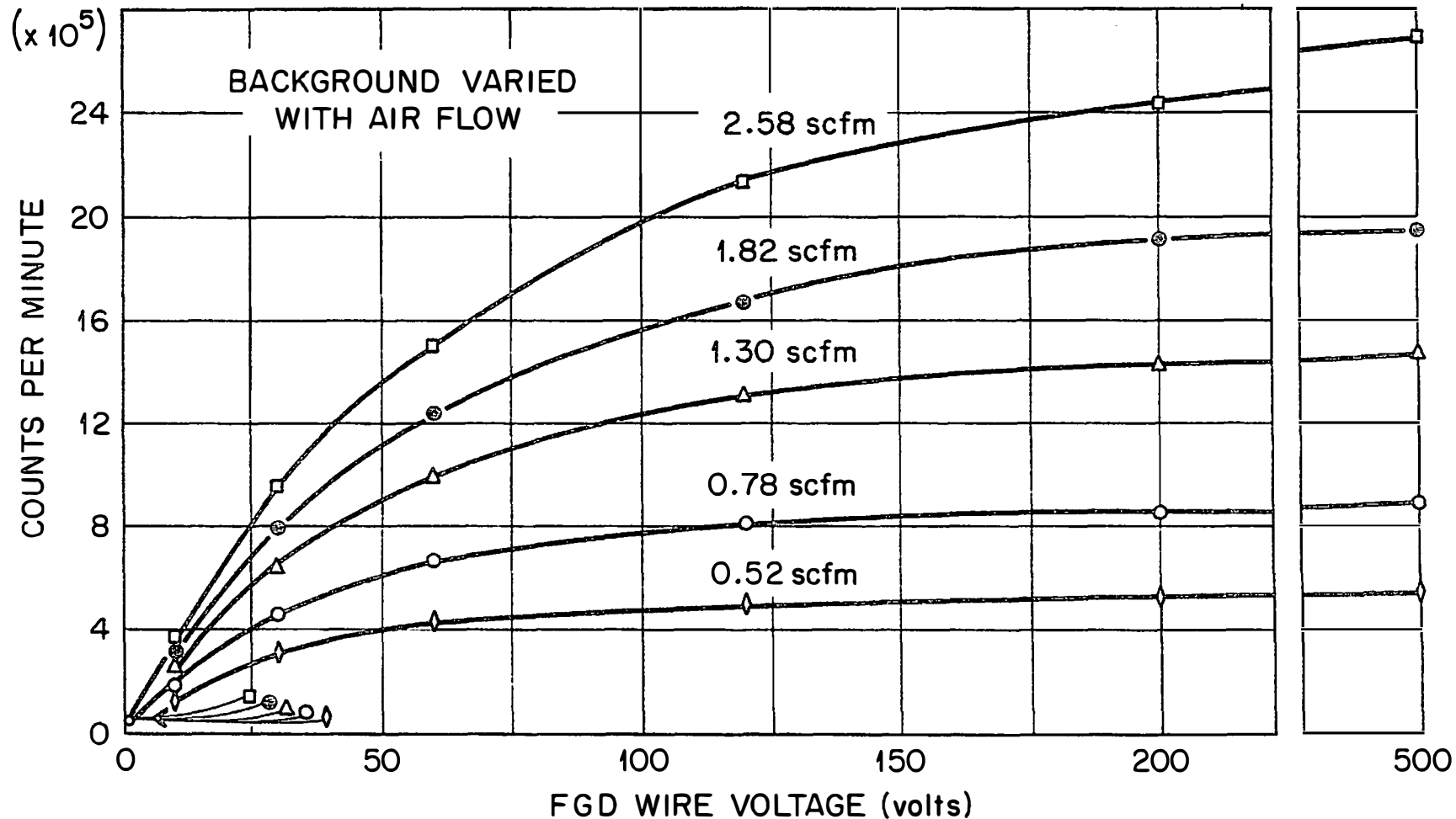
Fig. 28. Count Rate vs Voltage Curves for a Motor Speed of 23 rpm. Background has been Subtracted from Each Curve. Fission Product Concentration was Constant.

TABLE III

NORMALIZED COUNT RATE - VOLTAGE CURVES AT DIFFERENT WIRE SPEEDS

Volts	2 RPM	1 RPM x 1.375	9.3 RPM x 0.278	23 RPM x 0.475
1	1.4×10^4	2.1×10^4	1.5×10^4	1.5×10^4
10	9.4×10^4	9.6×10^4	8.8×10^4	9.0×10^4
30	2.17×10^5	2.21×10^5	2.18×10^5	2.16×10^5
60	3.07×10^5	3.04×10^5	3.06×10^5	3.11×10^5
120	3.77×10^5	3.80×10^5	3.84×10^5	3.82×10^5
200[a]	4.07×10^5	4.07×10^5	4.07×10^5	4.07×10^5
500	4.27×10^5	4.21×10^5	4.2×10^5	4.21×10^5

[a]All curves were normalized to 200 volts.
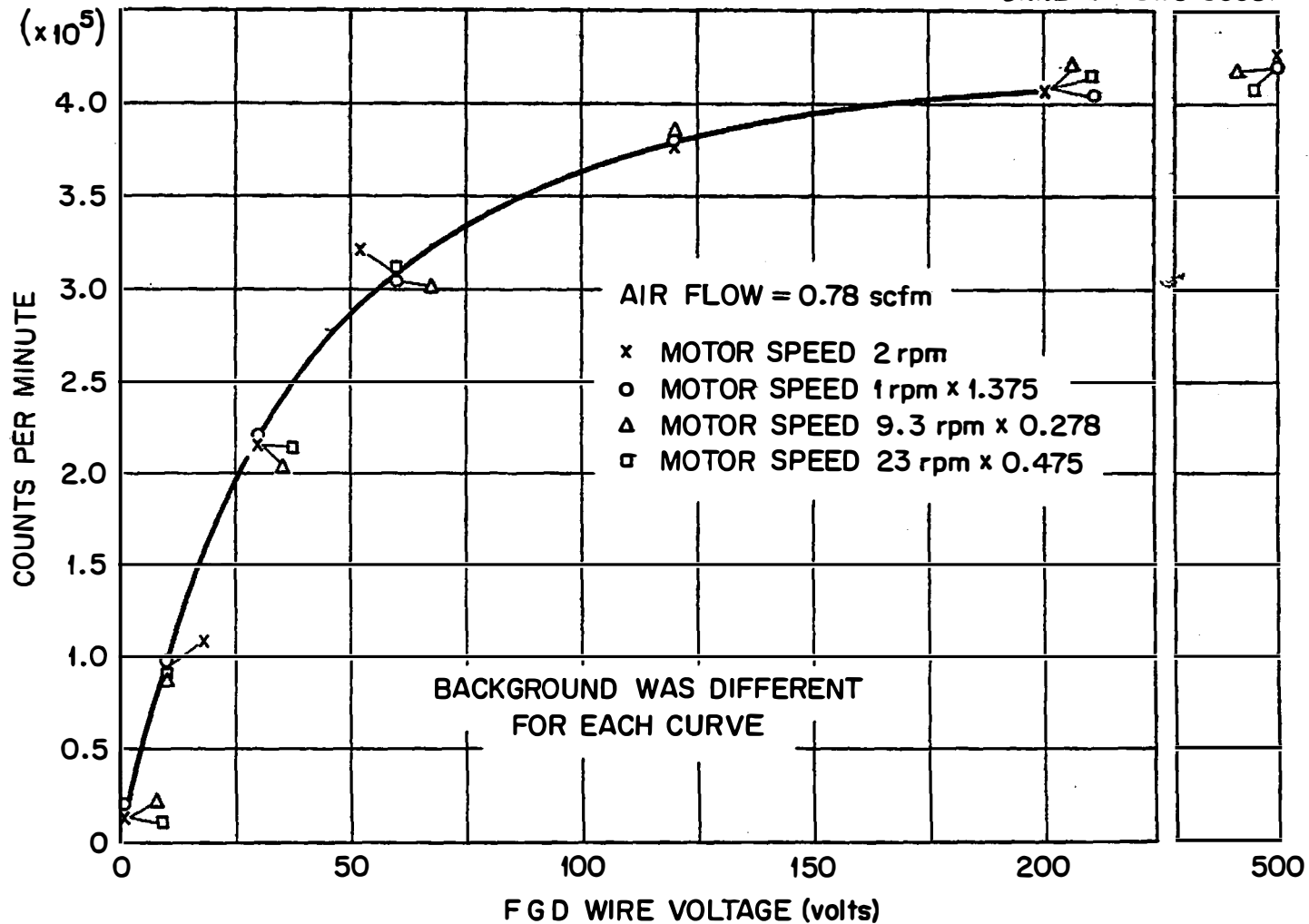
Fig. 29. Comparison of Count Rate-Voltage Curves Taken at Different Wire Speeds. All Curves are Normalized to the Same Value at 200 volts. Background has been Subtracted from all Curves. Each Curve was run at a Different Fission Product Concentration.

the theories advanced in Sections A and B disclosed no reason to suppose that wire speed would influence the shape of these curves. Thus, the linear low-voltage region depends primarily on the air velocity and collection chamber diameter; the connecting region will persist until saturation is reached, and the voltage required for saturation does not depend on wire speed. From this we can infer that the distance from the collection chamber to the detector will influence the count rate but not the shape of the count rate-voltage or count rate-air flow curves. The usefulness of the data presented in these three sections will be discussed after an examination of the capabilities of the Fission Gas Detector for identifying isotopes.

D. Isotope Identification

1. Introduction

In principle, it is possible to characterize and identify any single gamma-emitting radionuclide from a measurement of its gamma spectrum and half-life for decay. This is true even with the relatively poor resolution available from scintillation spectrometry, because the total number of radionuclides is limited (about 1026 presently known). The best method for accomplishing identification is to obtain a pure unknown sample, run a gamma spectrum, and compare this with the curves in Heath[121] or Crouthamel.[122] If the isotope is one whose spectrum does not appear in these sources, it is still possible in many cases to identify the unknown isotope by comparing the measured gamma energies with a tabulation of known gamma energies for the various radionuclides.

This, coupled with a half-life determination will identify the nuclide present. A chart to aid in such identifications was recently published in Nucleonics.[123] When more than one nuclide is present the problem is more difficult, but resolution is still possible in some cases. Quantitative measurements of mixtures, however, require favorable conditions such as widely disparate half-lives or gamma energies. Work is presently being conducted, especially in the field of activation analysis, on unfolding the spectra of radionuclide mixtures;[124,125] as previously mentioned, these unfolding methods are still incompletely developed and often require the aid of a large computer.

It is apparent that if the gamma energies of a nuclide are unknown, then identification of the nuclide by this method will be impossible. The decay of the material collected on the FGD wire is fairly rapid; most of the activity exhibits a half-life between 30 minutes and 30 seconds. Very little information on gamma energies for fission products with half-lives shorter than 30 minutes is available. Furthermore, the half-life of many of these fission products has not been established with any certainty. In spite of this difficulty, a knowledge of the operation of the Fission Gas Detector permits the list of possible isotopes involved to be narrowed considerably. The following criteria were set up for a preliminary investigation of the fission products being detected on the FGD wire:

1. The half-life of the fission product nuclide must be between 30 seconds and 1 hour.

2. The nuclide must be a gamma emitter.

3. The nuclide must have a predecessor, i.e., it cannot be the first member of a decay chain.

4. The predecessor must have a half-life comparable to the time required for it to reach the collection chamber, or shorter. The reason for this restriction will be explained later.

5. The fission yield of the nuclide must be greater than 0.1 per cent.

Several tabulations of the properties of fission products are available. One of these is by J. O. Blomeke,[126] which has several convenient tables of nuclear properties of the fission products. A more recent compilation was published in Nucleonics;[127] this gives prominent gamma energies for all nuclides and lists the fission product decay chains. The "standard" tabulation of gamma-ray energies is found in the April 1958 issue of the Reviews of Modern Physics,[128] which gives a very complete literature survey of the nuclear properties of all radioisotopes known up through February 1958. Another source of gamma energies is Appendix IV of Crouthamel's book.[129] For quick reference, the Trilinear Chart of the Nuclides[130] provides much information, including half lives; this information is kept current by periodic revisions which are issued at least twice a year. Unless otherwise stated, the data published in Nucleonics will be used here.

When the fission products with half-lives between 30 seconds and 1 hour are checked against the criteria listed above, many of them can be eliminated. Those that remain can be fitted into one of the following mass chains: 84, 85, 87, 89, 90, 91, 92, 93, 94, 95, 99, 101, 104, 105, 107, 130, 131, 132, 133, 134, 137, 138, 139, 140, 141, 142, 143, 147 and 148. This constitutes 29 mass chains of the 81 listed for fission products. These mass chains as given in Nucleonics are shown in Table IV.

TABLE IV

SELECTED DECAY CHAINS AND YIELDS FOR THERMAL NEUTRON FISSION OF U^{235}

Mass No.

84

$6.0\text{-m } Br^{84m}$
$\underline{0.019}$

$3.3\text{-m } Se^{84} \longrightarrow \quad 31.8\text{-m } Br^{84} \quad \nearrow \rightarrow \text{Stable } Kr^{84}$
$1.1 \qquad\qquad\qquad \underline{0.92} \qquad\qquad\qquad \underline{1.00}$

85

$4.4\text{-h } Kr^{85m} \quad 0.775$

$39\text{-s } Se^{85} \longrightarrow \quad 3.00\text{-m } Br^{85} \nearrow \quad \bigg| 0.225 \quad \searrow \text{Stable } Rb^{85}$
$\underline{\sim 1.1} \qquad\qquad\qquad 1.5 \qquad\qquad 10.6\text{-y } Kr^{85} \qquad \underline{1.30}$
$\qquad\qquad\qquad\qquad\qquad\qquad\qquad \underline{0.293}$

87

$\sim 0.03 \nearrow \text{Stable } Kr^{86}$
$+ \text{ Neutron}$

$16\text{-s } Se^{(87)} \longrightarrow \quad 5.45\text{-s } Br^{87}$
$\underline{\sim 2} \qquad\qquad\qquad 2.7 \qquad \sim 0.97 \searrow$
$\qquad\qquad\qquad\qquad\qquad\qquad 78\text{-m } Kr^{87} \longrightarrow 5 \times 10^{10}\text{-y } Rb^{87}$
$\qquad\qquad\qquad\qquad\qquad\qquad 2.7 \qquad\qquad\qquad \underline{2.49}$

89

$2.8\text{-h } Kr^{88}$
$\sim 0.15 \nearrow + \text{ Neutron}$

$4.4\text{-s } Br^{89}$
$(3) \quad \sim 0.85 \searrow \qquad\qquad\qquad\qquad\qquad\qquad\qquad \sim 0.0002 \nearrow \quad 16\text{-s } Y^{89m}$

$3.2\text{-m } Kr^{89} \longrightarrow 15.4\text{-m } Rb^{89} \longrightarrow 50.5\text{-d } Sr^{89}$
$\underline{4.59} \qquad\qquad\qquad 4.8 \qquad\qquad\qquad \underline{4.79} \quad \sim 0.9998 \searrow \text{Stable } Y^{89}$

90

$3.2\text{-m } Kr^{89}$
$\sim 0.15 \nearrow + \text{ Neutron}$

$1.6\text{-s } Br^{(90)}$
$(1.7) \qquad \searrow$
$\qquad\qquad 33\text{-s } Kr^{90} \longrightarrow 2.7\text{-m } Rb^{90} \longrightarrow 28\text{-y } Sr^{90} \longrightarrow 64.3\text{-h } Y^{90} \longrightarrow \text{Stable } Zr^{90}$
$\qquad\qquad \underline{5.0} \qquad\qquad\qquad 5.9 \qquad\qquad\qquad \underline{5.77} \qquad\qquad\qquad \underline{5.77}$

TABLE IV (CONTINUED)

Mass No.

91   10-s Kr^{91} $\longrightarrow$ 72-s Rb^{91} $\longrightarrow$ 9.7-h Sr^{91} $\xrightarrow{0.60}$ 51-m Y^{91m} $\dashrightarrow$ Stable Zr^{91}
   $\underline{3.45}$ $\underline{5.43}$ $\underline{5.81}$ $\xrightarrow{0.40}$ 58-d Y^{91} $\underline{5.84}$

                                          $\underline{\sim 5.4}$

92   3.0-s Kr^{92} $\longrightarrow$ (80s?) 5.3-s Rb^{92} $\longrightarrow$ 2.7-h Sr^{92} $\longrightarrow$ 3.6-h Y^{92} $\longrightarrow$ Stable Zr^{92}
   $\underline{1.87}$ 5.5 $\underline{5.3}$ ·   6.1 $\underline{6.03}$

93   2.0-s Kr^{93} $\longrightarrow$ 5.6-s Rb^{93} $\longrightarrow$ 7.9-m Sr^{93} $\longrightarrow$ 10.3-h Y^{93} $\longrightarrow$
   $\underline{0.48}$ 4.4   6.4 $\underline{6.1}$

     1.1 x 10^{6}-y Zr^{93} $\xrightarrow{\sim 1.00}$ 12-y Nb^{93m}
        $\underline{6.45}$ $\dashrightarrow$ Stable Nb^{93}

94   1.4-s Kr^{94} $\longrightarrow$ 2.9-s Rb^{94} $\longrightarrow$ 1.3-m Sr^{94} $\longrightarrow$ 20-m Y^{94} $\longrightarrow$ Stable Zr^{94}
   $\underline{0.10}$ 2.9   5.8 $\underline{5.4}$ $\underline{6.40}$

95   Short Kr^{95} $\longrightarrow$ (Short Rb) $\longrightarrow$ 40-s Sr^{95} $\longrightarrow$ 10-m Y^{95} $\longrightarrow$
   $\underline{0.007}$ 1.6   4.7   6.4

                $\xrightarrow{0.02}$ 90-h Nb^{95m}
     65-d Zr   Stable Mo^{95}
     $\underline{6.2}$ $\xrightarrow{0.98}$ 35-d Nb^{95} $\nearrow$ $\underline{6.27}$
                  $\underline{6.4}$

TABLE IV (CONTINUED

Mass No.

99   33-s Zr^{99} $\longrightarrow$ 2.4-m Nb^{99} $\longrightarrow$ 66.5-h Mo^{99} $\nearrow^{0.87}$ 6.0-h Tc^{99m}
  (4.3)   (6.0)   6.06   0.13 $\searrow$
  Stable Ru^{99}
  2.1 x 10^{5}-y Tc^{99}
  6.1

101   1.0-m Nb^{101} $\longrightarrow$ 14.6-m Mo^{101} $\longrightarrow$ 14.0-m Tc^{101} $\longrightarrow$ Stable Ru^{101}
  (4.0)   ~5.6   5.0   5.0

104   (< 2.5-m Mo^{104}) $\longrightarrow$ 18-m Tc^{104} $\longrightarrow$ Stable Ru^{104}
  (1.2)   (1.8)   1.8

105   (< 2-m Mo^{105}) $\longrightarrow$ 9-m Tc^{105} $\longrightarrow$ 4.45-h Ru^{105} $\nearrow$ 38-s Rh^{105m}
  0.6   0.9   0.9   Stable Pd^{105}
  36-h Rh^{105}
  0.9

107   (< 1-m Tc^{107}) $\longrightarrow$ 4.6-m Ru^{107} $\nearrow$ 45-s Rh^{107m}
  0.16   0.2   7 x 10^{6}-y Pd^{107} $\longrightarrow$ Stable Ag^{107}
  22-m Rh^{107} 0.2
  0.19

130   2.6-m Sn^{130} $\longrightarrow$ 7.1-m Sb^{130} $\longrightarrow$ Stable Te^{130}
  2.0   2

131   3.4-m Sn^{131} $\longrightarrow$ 23-m Sb^{131} $\nearrow^{0.15}$ 30-h Te^{131m} $\searrow^{0.80}$ 0.008 $\nearrow$ 12-d Xe^{131m}
  (2.6)   2.6   0.44   8.05-d I^{131}
  0.85 $\searrow$ $\downarrow$ 0.20   ~3.1   0.992 $\searrow$
  24-m Te^{131} Stable Xe^{131}
  2.9   2.93

TABLE IV (CONTINUED)

Mass No.

132   2.2-m Sn^{132} $\longrightarrow$ 2.1-m Sb^{132} $\longrightarrow$ 77-h Te^{132} $\longrightarrow$ 2.30-h I^{132} $\longrightarrow$ Stable Xe^{132}
       (3.4)   3.4   ~4.7   4.4   4.38

133   4.1-m Sb^{133} —0.72→ 52-m Te^{133m} —0.87→ 20.8-h I^{133} —0.024→ 2.3-d Xe^{133m} → Stable Cs^{133}
      4.0   4.9   0.13   6.9   0.976   5.27-d Xe^{133} 6.59
        0.28 → 2-m Te^{133} 6.62

134   (50-s Sb^{134}) $\longrightarrow$ 43-m Te^{134} $\longrightarrow$ 52.5-m I^{134} $\longrightarrow$ Stable Xe^{134}
        3.0   6.9   7.8   8.06

137   24.4-s I^{137} —~0.04→ Stable Xe^{136} + Neutron
       4.9   ~0.96 → 3.9-m Xe^{137} $\longrightarrow$ 30-y Cs^{137} —0.92→ 2.57-m Ba^{137m}
                          6.00   6.15 0.08 → Stable Ba^{137}

138   6.3-s I^{138} —~0.03→ 3.9-m Xe^{137} + Neutron
       3.4 ~0.97 → 17-m Xe^{138} $\longrightarrow$ 32.2-m Cs^{138} $\longrightarrow$ Stable Ba^{138}
                       5.49   5.8   5.74

139   2.0-s I^{139} —~0.04→ 17-m Xe^{138} + Neutron
       1.8 ~0.96 → 41-s Xe^{139} → 9.5-m Cs^{139} $\longrightarrow$ 83-m Ba^{139} $\longrightarrow$ Stable La^{139}
                      5.4   6.47   6.55

TABLE IV (CONTINUED)

Mass No.					

140   16-s Xe^{140} $\rightarrow$ 66-s Cs^{140} $\rightarrow$ 12.8-d Ba^{140} $\rightarrow$ 40.2-h La^{140} $\rightarrow$ Stable Ce^{140}
            <u>3.8</u>   <u>6.0</u>   <u>6.35</u>   <u>6.35</u>   <u>6.44</u>

141   1.7-s Xe^{141} $\rightarrow$ 25-s Cs^{141} $\rightarrow$ 18-m Ba^{141} $\rightarrow$ 3.8-h La^{141} $\rightarrow$ 33-d Ce^{141} $\rightarrow$
            <u>1.33</u>   <u>4.6</u>   <u>6.3</u>   <u>6.4</u>   <u>~6.0</u>

      Stable Pr^{141}

142   ~1.5-s Xe^{142} $\rightarrow$ <8-s Cs^{142} $\rightarrow$ 10-m Ba^{142} $\rightarrow$ 81-m La^{142} $\rightarrow$ Stable Ce^{142}
            <u>0.35</u>   3.4   5.6   5.9   <u>6.01</u>

143   1-s Xe^{143} $\rightarrow$ (Short Cs) $\rightarrow$ 13-s Ba $\rightarrow$ 18-m La^{143} $\rightarrow$ 33-h Ce^{143} $\rightarrow$
            <u>0.051</u>   1.9   4.9   6.2   <u>6.0</u>

      13.7-d Pr^{143} $\rightarrow$ Stable Nd^{143}
         6.2   6.03

147   1.2-m Ce^{147} $\rightarrow$ 12.0-m Pr^{147} $\rightarrow$ 11.1-d Nd^{147} $\rightarrow$ 2.6-y Pm^{147} $\rightarrow$ 1.3 x 10^{11}-y Sm^{147}
            (2.4)   (2.4)   <u>~2.7</u>   <u>2.36</u>

148   40-s Ce^{148} $\rightarrow$ 1.95-m Pr^{148} $\rightarrow$ Stable Nd^{148}
            (1.7)   (1.7)   <u>1.71</u>

Note: Underlined yield values have been measured. Those yield values in parentheses are estimated by the method of the Appendix. All other yield values are taken from the compilation by Blomeke.[126]

Dashed arrows indicate branching which is suspected but has not been experimentally observed. Nuclides in parenthesis are suspected but have not been observed.

A list of the isotopes from each chain which would be counted by the FGD, with their gamma energies, is in Table V.* Note that in thus restricting the fission products to be considered, no mention has yet been made of the gamma energies of the fission products nor of the probability of their release from the fuel element. Before we proceed further, the gamma energy measurements of the FGD wire will be presented; this will permit elimination of a few isotopes whose gamma spectra are known. Then an estimation of the relative release of material from the fuel matrix will be made, so that the isotopes to be expected on the wire can be more accurately specified.

2. Gamma Energy Determinations

The counting equipment for the Fission Gas Detector was designed so that the gamma energy of the fission products could be determined as an aid to the identification of the isotopes being counted. The factors to be considered in designing a scintillation spectrometer are discussed by P. R. Bell[131] and Heath.[121] A relatively large scintillation crystal was used to increase the fraction of a gamma ray adsorbed in the crystal. The internal cavity of the detector shield was made as large as space would permit to reduce lead X-rays and backscattering. The resolution obtained from the spectrometer, as previously mentioned, was about 7.5 per cent. Backscattering and other interferences were comparable with the values observed by Heath for the same isotopes and using a 3 inch x 3 inch crystal in a shield of comparable dimensions.

---

*This list will be referred to as the "expected isotopes" or "expected nuclides".

TABLE V

A LIST OF EXPECTED NUCLIDES ON THE FGD WIRE

Nuclide	Half-Life (Minutes)	Predecessor Nuclide	Half-Life (Seconds)	First Predecessor Nuclide	Half-Life (Seconds)
Kr^{89}	3.2	Br^{89}	4.5	- -	
Kr^{90}	0.55	Br^{90}	1.6	- -	
Rb^{90}	2.74	Kr^{90}	33	Br^{90}	1.6
Rb^{91}	14	Kr^{91}	9.8	- -	
Rb^{91m}	1.67	Kr^{91}	9.8	- -	
Sr^{93}	8.2	Rb^{93}	5.6[a]	Kr^{93}	2.0
Sr^{94}	1.3	Rb^{94}	2.9[a]	Kr^{94}	1.4
Sr^{95}	0.7	Rb^{95}	Short	- -	
Y^{94}	16.5	Sr^{94}	78	Rb^{94}	2.9[a]
Y^{95}	10.5	Sr^{95}	~42	Rb^{95}	Short[b]
Nb^{99}	2.4	Zr^{99}	35	- -	
Tc^{104}	18	Mo^{104}	<150[a]	- -	
Tc^{105}	10	Mo^{105}	<120	- -	
Sb^{130m}	7	Sn^{130}	156	- -	
Sb^{131}	22	Sn^{131}	204	- -	
Sb^{132}	1.9	Sn^{132}	132	- -	
Te^{133}	2	Sb^{133}	246	- -	
Te^{133m}	60	Sb^{133}	246	- -	
Te^{134}	44	Sb^{134}	45	- -	

TABLE V (CONTINUED)

Nuclide	Half-Life (Minutes)	Predecessor Nuclide	Half-Life (Seconds)	First Predecessor Nuclide	Half-Life (Seconds)
Xe^{137}	3.9	I^{137}	22.0	– –	
Xe^{139}	0.684	I^{139}	2.7	– –	
Cs^{139}	9.5	Xe^{139}	41	I^{139}	2.7
Cs^{140}	1.1	Xe^{140}	16	– –	
Ba^{141}	18	Cs^{141}	25[a]	Xe^{141}	1.7
La^{143}	19	Ba^{143}	13[a]	Cs^{143}	Short[b]
Pr^{148}	2.0	Ce^{148}	42	– –	

[a]Half-life taken from decay chain tabulation of Nucleonics.[123]

[b]These expected nuclides have more than two predecessors. One predecessor nuclide is assumed to have 0 half-life.

Note: Half-lives were taken from the Trilinear Chart of the Nuclides[130] except where specified.

The position of a well-defined peak on the chart could be determined to within 0.1 inch in a 10-inch long scan. Thus, the energy of a peak could be determined to within $\pm$ 0.01 Mev for a 1.00-Mev scan. This precision was verified by running scans of known standards. After the detector calibration procedure had been worked out, a number of gamma scans of the material on the FGD wire were run under varying conditions. Since fresh material is continuously being brought before the detector, the time required to complete a scan is immaterial; there is no effective decay of the gamma source. It is for this reason that a single channel analyzer can be employed instead of the more complex multichannel analyzers. A typical gamma scan of the FGD wire is shown in Figure 30. The gamma energies of the large peaks are identified. Scans were run during the operation of several different tests, at various flows and at different wire speeds. Table VI is a listing of all the gamma energies observed during these scans, and the number of scans on which they were observed. Five of the peaks listed were very prominent under most conditions, namely, those at 0.030, 0.098, 0.193, 0.601 and 0.827 Mev. No significant gamma peak was ever found with energy greater than 1.02 Mev, although several scans at the higher energies were run. This fact made it possible to eliminate a number of isotopes having gamma energies above 1.0 Mev. The significance of being able to resolve any gamma peaks at all should not be overlooked; attempts to count gross fission products in this range of half-lives usually produce a smeared-out spectrum across the entire energy span. So some degree of separation has been obtained.
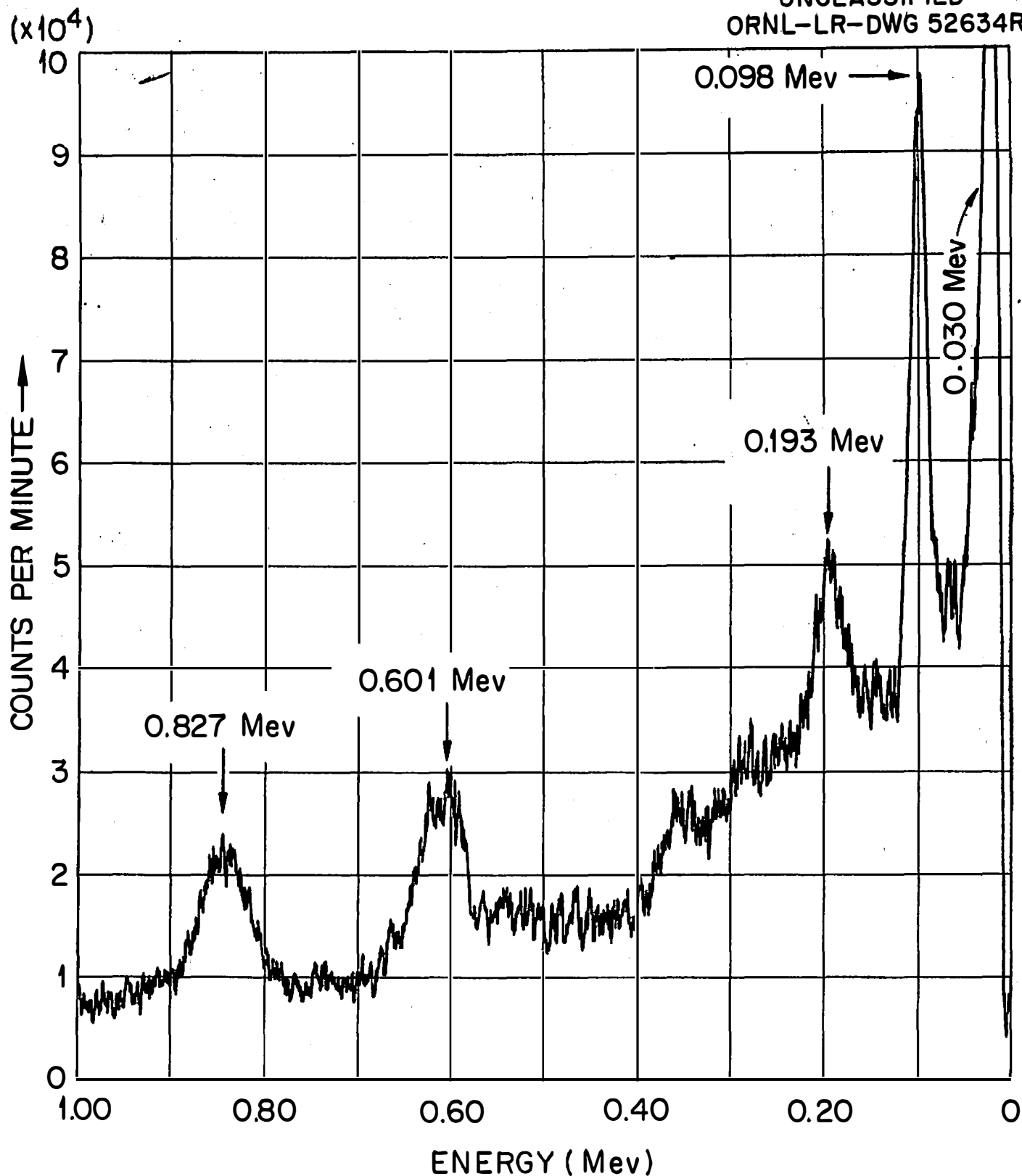
Fig. 30. A Typical Gamma Scan on the Fission Gas Detector.

TABLE VI

GAMMA ENERGY PEAKS OBSERVED ON THE FGD WIRE

Energy	Average Deviation	Number of Observations
0.030	± 0.005	15
0.098	± 0.002	25
0.193	± 0.002	15
0.281	± 0.002	2
0.352	± 0.002	4
0.601	± 0.006	28
0.827	± 0.009	26
1.02	± 0.02	3

The conditions under which the gamma energies in Table VI were obtained will be important in determining the isotope which emitted them. For the present, however, we will simply place the restriction on all nuclides listed in Table V as possible species being counted, that their gamma spectra if known should not conflict with the measured gamma energies. This would not necessarily mean that these nuclides were not present on the wire, but only that their contribution to the total count rate was small compared to the peak-producers. When the nuclides of Table V are examined on this basis, the following species can be eliminated: bromine-84, 85 and 87; bromine-84m, rubidium-89, yttrium-94, molybdenum-101, ruthenium-107, xenon-138, barium-142 and praseodymium-147. This leaves 25 nuclides to be considered.

3. Prediction of FGD Count Rate

The constant or nearly-constant fission product release rate of the fuel samples involved in this study has already been mentioned. However, this does not imply that all fission products are released equally well, or that there might not be a delay from the time of fission until the fission product leaves the fuel sample. It is apparent that there could not be a very long delay between origination and release, because of the short half-lives of the nuclides appearing on the FGD wire. As a first approximation, we will assume that there is no delay or holdup of fission products in the sample. This will be true if the fission product activity is produced entirely by direct recoil into the coolant of fission nuclei from fissioning atoms at the surface of the fuel. If there is an additional component of the fission product activity from slow diffusion of atoms generated in the interior of the fuel sample, then the Fission

Gas Detector will be relatively insensitive to these isotopes because of their longer half-lives. Fast diffusion of atoms from the interior will contribute to the count rate in the same manner as direct recoils.

The release rate of a fuel sample is defined as the per cent of a given isotope formed by fission which escapes from the sample. The absolute release rates for the fuel samples being tested in the Oak Ridge Research Reactor are not known; but if some estimate of the relative release can be made, then the relative count rates of nuclides collected on the wire can be determined. For purposes of calculation, the following release rates will be used,[132] relative to strontium as 1:00: tellurium, 150; bromine and iodine, 100; xenon and krypton, 35; rubidium, ruthenium, and cesium, 15; antimony and tin, undetermined; strontium, barium and all others, 1.0. This listing assumes that all isotopes of a given element are released equally well. It is unfortunate that none of the mass chains containing tellurium as a predecessor have short-lived (iodine) daughters; also, the half-life of the tellurium isotopes is generally not short, and it is an unsuitable predecessor from that standpoint. Therefore it is improbable that isotopes from the tellurium chains will be observed by the FGD, even though they are known to be present in high concentration.

After an atom has migrated out of the fuel material, it still has to traverse over 40 feet of piping before it reaches the FGD collection chamber. The less volatile isotopes have shown a tendency to "plate out" on the piping before they reach the FGD. This does not occur to the rare gases, but plate-out of ruthenium(of the elements just mentioned) is especially high. However, ruthenium does not occur as a predecessor to any of the nuclides remaining to be considered. Further discussion of the plateout problem will be deferred

until the next section.

We can now describe the FGD count rate as a combination of 6 terms: (1) the number of predecessor atoms released from the fuel sample per minute; (2) the number of ions formed by decay of the predecessor which reach the collection chamber;* (3) the collection efficiency of the wire; (4) the disintegration rate of the material collected by the wire; (5) the counting efficiency of the detector; (6) the decay characteristics of the nuclide. Of these terms, (6) will depend on the decay scheme of the expected isotope, (5) can be determined from the calibration of the detector, and (3) was determined by the count rate - voltage and count rate - flow measurements. Term (1), the number of predecessor atoms released, we will designate by the letter R; then we can write,

$$R = 60 \text{ GYEQ}$$

where

R = number of atoms of a given nuclide escaping the fuel per second.

G = number of fissions in the fuel sample per second (assumed to be constant).

Y = fission yield for the nuclide considered.

E = absolute release rate for strontium isotopes, in atoms released per atom formed.

Q = relative release of nuclide in question as compared to strontium.

Now we need to compute the number of these predecessor atoms which form ions by the time they reach the collection chamber. Comparing the table of isotopes expected on the wire with the mass chains from which they were derived, we see that certain of these nuclides have two or more

*Term (2) can be derived from term (1); however, the two terms cannot be written as factors whose product will give term (2) in every case.

predecessors. Since the transit time from the fuel sample to the collection chamber is rather short, these predecessor chains must be taken into account. In order to do this the correct yield of the predecessors must be known. The early members of a decay chain are produced directly from fission; in addition, all nuclides in the chain except the first are produced by decay of preceding members. The last members of a chain are produced almost entirely from decay of predecessors. This is illustrated by mass chain 141, which has been well worked out. The first three members of the chain are produced directly from fission, with barium-141 having a yield from fission and decay of predecessors of 6.3 per cent. The last three members of the chain arise almost solely from decay of barium-141. Barium-141 is the isotope in this chain which will appear on the wire, but only the fraction which does not arise from direct fission will be counted.

The first member of the chain is xenon-141, with a yield of 1.33 per cent arising wholly from fission. This decays to cesium-141, whose yield is augmented by direct fission. Cesium-141 is the predecessor of the isotope expected on the wire, and has a total yield of 4.6 per cent. It is the number of ions formed by decay of cesium-141 that we wish to calculate; this will be equal to the number of barium-141 atoms formed. Consider the decay chain, $a \xrightarrow{\lambda_a} b \xrightarrow{\lambda_b} c \xrightarrow{\lambda_c}$. When the differential equations for growth of daughters from decay of a parent are solved, the amount of c (which is barium-141 in this case) is given by,

$$c = c_0 e^{-\lambda_c t} + b_0 \frac{\lambda_b}{\lambda_c - \lambda_b} (e^{-\lambda_b t} - e^{-\lambda_c t}) +$$

$$a_0 \left[\frac{\lambda_a}{\lambda_b - \lambda_a} \cdot \frac{\lambda_b}{\lambda_c - \lambda_a} e^{-\lambda_a t} + \frac{\lambda_a}{\lambda_a - \lambda_b} \cdot \frac{\lambda_b}{\lambda_c - \lambda_b} e^{-\lambda_b t} \right.$$

$$\left. + \frac{\lambda_a}{\lambda_a - \lambda_c} \cdot \frac{\lambda_b}{\lambda_b - \lambda_c} e^{-\lambda_c t} \right]$$

where

a_0 = amount of a at time 0 ($\rightleftharpoons$ release rate of a per second)

b_0 = amount of b at time 0 ($\rightleftharpoons$ release rate of b per second)

c_0 = amount of c at time 0 (= 0, since only the amount of c formed by decay of a and b is being considered), and

λ_a, λ_b and λ_c are the radioactive decay constants for decay of a, b and c.

The time t to be used in the equation is the delay time from the fuel sample to the FGD collection chamber. From this equation and a knowledge of the yields of a and b and the decay constants λ_a, λ_b and λ_c, the number of predecessor ions formed can be calculated; or more correctly, instead of the yields we should employ the factor R previously defined for the release rate of each predecessor nuclide. The equation would then become

$$c = R_b \frac{\lambda_b}{\lambda_c - \lambda_b} (e^{-\lambda_b t} - e^{-\lambda_c t}) + R_a \left[\frac{\lambda_a}{\lambda_b - \lambda_a} \cdot \frac{\lambda_b}{\lambda_c - \lambda_a} e^{-\lambda_a t} + \frac{\lambda_a}{\lambda_a - \lambda_b} \cdot \frac{\lambda_b}{\lambda_c - \lambda_b} e^{-\lambda_b t} + \frac{\lambda_a}{\lambda_a - \lambda_c} \cdot \frac{\lambda_b}{\lambda_b - \lambda_c} e^{-\lambda_c t} \right]$$

Where only a single predecessor is known, that is, when we are interested in the amount of b formed, then the growth-rate equation becomes

$$b = \frac{\lambda_a R_a}{\lambda_b - \lambda_a} (e^{-\lambda_a t} - e^{-\lambda_b t})$$

where the symbols have the same meanings as before, and b is the amount of "b" formed only from decay of a predecessor. We are now in a position to state the quantities involved in term (2), which we shall designate

by the letter U:

$$U = \frac{P\ (1-D)\ B}{F}$$

where

U = concentration of ions of the expected isotope which are present at the collection chamber, in ions per SCF.

P = plateout factor = fraction of atoms escaping plateout between fuel sample and FGD $\cong$ 1.0 for all mass chains considered.

D = recombination factor = fraction of ions of expected isotope which recombine before reaching the collection chamber.

B = number of ions of an expected nuclide which are formed between the fuel sample and the collection chamber. This factor depends on the values of b or c, which in turn depend on the values of R for each predecessor nuclide.

F = total air flow over the sample, SCFM.

The plateout factor has already been mentioned; plateout is not known to be a serious problem for any of the elements existing as predecessors for the FGD system with the possible exception of iodine. The recombination factor can be estimated from a knowledge of the ion concentration in the exit air system.

The recombination rate of ions is given by the equation,[133] $\frac{dn_+}{dt} = \frac{dn_-}{dt} = \alpha\ n_+\ n_-$ where n_+ and n_- are the density of the positive and negative charges (ions per cm.^{3}), α is the recombination coefficient and $\frac{dn_+}{dt}$ is the number of recombinations per cm.^{3} per second. In air, α is about 10^{-10} cm.^{3} per second when the negative charges exist as electrons. Positive ion and electron concentrations will, of course, be equal

($n_+ = n_-$) since they are formed as pairs. The ionic concentration can be determined from measurements of the activity of the FGD sample lines; this reaches a maximum of 0.1 roentgen per hour. The activity inside the lines, then, should not exceed 10 roentgens per hour. A roentgen is defined as the amount of radiation which will produce one electrostatic unit of charge in a cubic centimeter of air.[*] Using this value, we can calculate the ions per cm.^{3} of the FGD sample line air:

$$10 \text{ roentgens/hr.} = 10 \text{ esu/cm.}^3\text{/hr.} = \frac{10}{3600} \text{ esu/cm.}^3\text{/sec.}$$

$$\text{atoms ionized/cm.}^3\text{/sec.} = n_+ = \frac{10}{3600} \times \frac{1}{4.8 \times 10^{-10}} \text{ esu/cm.}^3\text{/sec.} \times$$

$$\text{electrons/esu}$$

$$= 5.8 \times 10^6$$

$$\text{Recombinations per second} = \frac{dn_+}{dt} = 10^{-10} \times (5.8 \times 10^6)^2 = 34$$

$$\text{Fraction recombining per second} = \frac{34}{5.8 \times 10^6} = 5.8 \times 10^{-6}$$

This will be the initial rate of recombinations; as the ion concentration builds up, the recombination rate will rise until equilibrium with ion production is established. Since the time from the fuel specimen to the collection chamber is relatively short, the fraction of ions recombining will be small. In 10 seconds, only 5.8×10^{-5} of the ions formed (0.0058 per cent) will have recombined. Thus the factor D in the equation for U will be ~ 0.

---

[*]This definition strictly applies only to electromagnetic radiation, but is commonly used for mixed gamma and beta radiation fields.

This puts into explicit form all of the factors influencing the count rate except (4), the disintegration rate of the material collected on the wire. If the number of ions of a nuclide b collected per centimeter of wire is N_b (calculated from the wire speed, wire voltage, air flow and ion concentration U) then the number of atoms remaining after the time T required for the wire to reach the counter is given by $N_b e^{-\lambda_b T}$, where λ_b is the decay constant of b. Then the disintegration rate of b is obtained by multiplying the number of atoms times the decay constant. Thus, $d = \lambda_b N_b e^{-\lambda_b T}$ where d = disintegrations per minute of material on each cm. of wire, and λ_b = decay constant of b in minutes^{-1}.

The total count rate of each expected nuclide as a function of all the variables we have discussed will be examined in the next chapter. At the present, we wish to isolate those factors which will cause one expected nuclide to differ from another in count rate. The following assumptions will be made:

1. Relative release rates are to be used as previously given.

2. The variation in detector response with gamma ray energy is neglected.

3. Any variable not appearing in the equation below is assumed to be constant, including term (6), the gamma branching ratio.

With these assumptions, the count rate for any expected nuclide with a single predecessor will be given by,

$$\text{count rate} = K \lambda e^{-\lambda T} \cdot \frac{Q Y \lambda_a}{\lambda - \lambda_a} (e^{-\lambda_a t} - e^{-\lambda t})$$

where

K is a constant, the same for all nuclides.

λ is the decay constant for the expected nuclide.

T is the time required for the FGD wire to move from the collection chamber to the detector.

Q is the relative release rate of the predecessor nuclide, with strontium isotopes set at 1.00.

Y is the fission yield of the predecessor, in per cent.

λ_a is the decay constant of the predecessor.

t is the time required for $\underline{a}$ to travel from the fuel sample to the collection chamber.

When more than one predecessor is present, the expression is more complicated:

$$\text{count rate} = K \lambda e^{-\lambda T} \left[Q_b(Y_b-Y_a) \frac{\lambda_b}{\lambda - \lambda_b} (e^{-\lambda_b t} - e^{-\lambda t}) + \right.$$

$$Q_a Y_a \left(\frac{\lambda_a}{\lambda_b - \lambda_a} \cdot \frac{\lambda_b}{\lambda - \lambda_a} e^{-\lambda_a t} + \frac{\lambda_a}{\lambda_a - \lambda_b} \cdot \frac{\lambda_b}{\lambda - \lambda_b} e^{-\lambda_b t} + \right.$$

$$\left. \left. \frac{\lambda_a}{\lambda_a - \lambda} \cdot \frac{\lambda_b}{\lambda_b - \lambda} e^{-\lambda t} \right) \right] .$$

Here, the subscripts a and b refer to the first and second predecessors, respectively. Using the two equations we have just described and solving for count rate/K, we can get an indication of the relative count rates for the various expected isotopes. In these equations the values of T and t will be known from the operating conditions of the testing system; the λ's and the measured fission yields can be found in the data from Nucleonics. In giving the fission yields in Table IV, the measured yields are underlined. A number of additional values for fission yield can be found in the tabulation by Blomeke;[126] these are based on theoretical

considerations advanced by Glendenin and coworkers.[134] The remainder of the fission yields were determined by a graphical process which is described in Appendix I. Yields determined in this manner are indicated in Table IV by being in parenthesis.

The results of the calculations just described are shown in Table VII for a single value of T and t. The value of T was set at 2.0 minutes, which corresponds to a wire-drive motor speed of 2 RPM. The value of t, 2.8 seconds, corresponds to an air flow of 1.30 SCFM. The half-lives for each isotope are listed; most of these were taken from the Trilinear Chart of the Nuclides,[130] but a few values are from the decay chain data of Nucleonics.[123] Where the only half-life listed was "short", a value of 1 second was used. A relative release rate of 1 was used for tin and antimony isotopes. The case of mass chain 91 is somewhat unusual; the predecessor, krypton-91, can presumably branch into the two isotopes rubidium-91 and rubidium-91m, both of which are known. This branching is shown in Blomeke,[126] but the branching ratio is not given. However, the branching is not shown in the Nucleonics tabulation, and the short half-life rubidium isomer is specified. In any event, the branching ratio is unknown.

The value in the last column of each part of the table represents the relative disintegration rate of that nuclide. The significant detection level for isotopes will be set at 1.00, since most of the values below 1.00 are quite low. Examination of the table on this basis shows that all of the chains with tin and antimony predecessors have been eliminated, mostly because of their relatively long half-lives. Mass chains with even longer half-life predecessors were previously eliminated in setting up the

TABLE VII

PREDICTED RELATIVE COUNT RATE

PART I: NUCLIDES WITH A SINGLE PREDECESSOR

Expected Nuclide	$T_{\frac{1}{2}}$ (Min.)	λ (Min.$^{-1}$)	Predecessor Nuclide	λ_a (Sec.$^{-1}$)	λ_a (Min.$^{-1}$)	Q	Y	Predicted Count Rate
Kr^{89}	3.2	0.216	Br^{89}	0.154	9.24	100	3	14.6
Kr^{90}	0.55	1.25	Br^{90}	0.433	26.0	100	1.7	11.8
Rb^{91}	14	0.0495	Kr^{91}	0.071	4.26	35	3.45	0.974 ← Branching ratio
Rb^{91m}	1.67	0.415	Kr^{91}	0.071	4.26	35	3.45	3.91 ← unknown
Sr^{95}	0.7	0.99	Rb^{95}	~0.7	42	15	1.6	2.74
Nb^{99}	2.4	0.289	Zr^{99}	0.0198	1.188	1	4.3	0.037
Tc^{104}	18	0.0385	Mo^{104}	0.007	0.42	1	1.2	8.3×10^{-4}
Tc^{105}	10	0.0693	Mo^{105}	0.007	0.42	1	0.6	7.0×10^{-4}
Sb^{130m}	7	0.099	Sn^{130}	0.00444	0.266	1	2.0	2.0×10^{-3}
Sb^{131}	22	0.0315	Sn^{131}	0.0034	0.204	1	2.6	7.3×10^{-4}
Sb^{132}	1.9	0.364	Sn^{132}	0.00525	0.315	1	3.4	8.9×10^{-3}
Te^{133}	2	0.347	Sb^{133}	0.0028	0.168	1	4.0	5.4×10^{-3}
Te^{133m}	63	0.011	Sb^{133}	0.0028	0.168	1	4.0	3.4×10^{-4}
Te^{134}	44	0.0157	Sb^{134}	0.0154	0.924	1	3.0	1.93×10^{-3}
Xe^{137}	3.8	0.182	I^{137}	0.0315	1.89	100	4.9	5.21
Xe^{139}	0.684	1.01	I^{139}	0.256	15.36	100	1.8	12.0
Cs^{140}	1.1	0.630	Xe^{140}	0.0433	2.60	35	3.8	2.22
Pr^{148}	2.0	0.347	Ce^{148}	0.0165	0.990	15	1.7	1.98

TABLE VII (CONTINUED)

PART II.   NUCLIDES WITH TWO PREDECESSORS

Expected Nuclide	$T_{\frac{1}{2}}$ (Min.)	λ_c (Min.$^{-1}$)	1st Predecessor Nuclide, a	$T_{\frac{1}{2}}$ (Sec.)	λ_b (Sec.$^{-1}$)	2nd Predecessor Nuclide, b	$T_{\frac{1}{2}}$ (Sec.)	λ_b (Sec.$^{-1}$)	Q_a	Y_a	Q_b	$Y_b - Y_a$	Predicted Count Rate Total
Rb^{90}	2.74	0.253	Br^{90}	1.6	0.433	Kr^{90}	33	0.0210	100	1.7	35	3.3	6.92
Sr^{93}	8.2	0.0845	Kr^{93}	2.0	0.346	Rb^{93}	5.6	0.124	35	0.48	15	3.9	20.8
Sr^{94}	1.3	0.533	Kr^{94}	1.4	0.495	Rb^{94}	2.9	.0.239	35	0.10	15	2.8	20.4
Y^{95a}	10.5	0.0660	Rb^{95}	(1)^b	0.693	Sr^{95}	42	0.0165	15	1.6	1	3.1	2.90
Cs^{139}	9.5	0.0729	I^{139}	2.7	0.257	Xe^{139}	41	0.0169	100	1.8	35	3.6	44.3
Ba^{141}	18	0.0385	Xe^{141}	1.7	0.408	Cs^{141}	25	0.0277	35	1.33	15	3.3	3.87
Ba^{142}	6	0.1155	Xe^{142}	1.5	0.462	Cs^{142}	60	0.0116	35	0.35	15	3.0	3.89
La^{143a}	19	0.0365	Xe^{143}	1	0.693	Ba^{143}	13	0.0533	35	0.051	1	3.0	0.454

[a]These nuclides have three predecessors; one of the predecessors in each case is assumed to have zero half-life.

[b]Half-life unknown; 1 second assumed.

preliminary criteria for examining the decay chains. The remaining mass chains have either rare gas, halogen or rubidium predecessors, with the exception of mass chain 148.

Unfortunately, the relative disintegration rates are not widely enough separated to reduce the number of expected isotopes greatly. This is especially true in view of the considerable uncertainty present in the relative release rates and in the assumption that there is no plateout of the predecessor isotopes. Thus the decay of the material collected on the wire will be the result of several components decaying simultaneously. Also, none of the nuclides with high relative count rate has a half life greater than 30 minutes, although the decay curves contain at least one component with a half-life greater than 30 minutes.

B. Half-Life Measurements

The decay of material collected on the Fission Gas Detector wire can be followed by stopping the wire and continuing to count the activity within the shield. The gross activity decay can be followed on the log count rate meter. The decay of a single nuclide on this recorder produces a linear count rate decrease; the observed decay curve was not linear, signifying the presence of two or more nuclides on the wire. In view of the large number of nuclides predicted to be present on the wire, no attempt was made to resolve the gross count rate curve. However, the decay at various energy values could be followed by using the linear count-rate meter. This was done by placing the linear count rate meter in the

Differential, Internal position and setting the desired energy on the Pulse-Height Setting dial. The scale selector and window width were adjusted to give a count rate near 100 on the Brown Recorder chart. Then the wire drive was stopped and the decay at the selected energy followed.

The decays of the four peaks most prominent at a wire speed of 2 RPM were measured, along with the troughs adjacent to these peaks. The spectrum being studied was essentially identical to that of Figure 30, except the peak at 0.193 Mev was more strongly accentuated. These decay curves were replotted on semi-log graph paper and graphically resolved into their component activities, using the method described by Friedlander and Kennedy.[135] Most of these curves could be resolved, within the limit of experimental accuracy, into three components. A tabulation of the half-lives found in this process for each energy examined is presented in Table VIII. In general, the half-lives fall into three groups; one slightly more than 1 minute, one about 7 minutes and one about an hour. The average of values in these regions is given at the bottom of the table. The accuracy of resolution decreases with increasing half-life; this is partly a consequence of the poorer counting statistics after long decay, when the count rate began to approach background. An idea of the precision of these measurements can be obtained from comparing the two sets of values found for the trough at 0.130 Mev; two different decays were used in this case. In general, the accuracy is estimated to be better than ± 50 per cent for all half-lives, and within ± 20 per cent for the short half-life measurement.

TABLE VIII

HALF-LIFE MEASUREMENTS AT VARIOUS GAMMA ENERGIES

	Energy (Mev)	Half-Life (Minutes)	Per Cent of Initial Count Rate Due to Each Component
1.	Trough at 0.05 Mev	46.7	6.97
		4.60	17.83
		1.02	75.2
2.	Peak at 0.098 Mev	56.8	1.79
		6.56	6.21
		1.01	91.9*
3.	Trough at 0.130 Mev	91	3.45
		7.47	26.3
		1.08	70.2
4.	Trough at 0.130 Mev	83	4.06
		9.72	28.1
		1.43	67.9
5.	Peak at 0.193 Mev	73.2	2.68
		13.2	48.4*
		1.33	49.0
6.	Trough at 0.235 Mev	108	2.75
		8.08	31.1
		1.26	66.2
7.	Trough at 0.530 Mev	60	4.10
		5.63	14.3
		1.28	81.6
8.	Peak at 0.601 Mev	69	1.49
		6.79	12.8
		1.12	85.7*
9.	Trough at 0.630 Mev	41.7	7.73
		5.95	19.1
		1.30	73.2
10.	Trough at 0.760 Mev	81.6	4.25
		7.6	25.3
		1.21	70.5

TABLE VIII (CONTINUED)

	Energy (Mev)	Half-Life (Minutes)	Per Cent of Initial Count Rate Due to Each Component
11.	Peak at 0.827 Mev	38.3	5.26
		4.23	59.3*
		0.71	35.4
12.	Trough at 0.900 Mev[a]	16.5	27.2
		1.63	72.8

[a]Decay too short for good resolution.

Note: The half-life most prominent in each peak is indicated by an * sign.

Average half-life, short = 1.20 $\pm$ 0.11 or 1.2 min. (10 values)
medium = 6.93 $\pm$ 1.14 or 7 min. (8 values)
long = 55 min. and 87 min. (2 groups)
average of both groups = 70 min. (11 values).

The reason for taking the decay of a peak and its adjacent troughs can be seen in Figures 31, 32 and 33. These are the resolved decay curves for the peak at 0.098 Mev and the troughs at 0.050 and 0.130 Mev. It is apparent that the short half-life component contributes more to the 0.098 Mev peak than to the adjacent troughs. Thus, the peak energy is associated with a half-life of about 1 minute. This was confirmed by running a decay at a wire speed of 9.3 RPM; the peaks at 0.098 and 0.601 Mev were greatly emphasized. This is put on a more quantitative basis in Table VIII, where the per cent of the decay during the first hour due to each half-life is listed. In every case the count rate had begun to approach background after one hour. The half-life associated with each peak energy is indicated in the table.

Another type of measurement which yielded information on the half-life of a nuclide producing a given peak involved gamma scans at different wire speeds. Recalling the effect of wire speed on count rate for a given nuclide, discussed in Section C, we have count rate = $K_1 T e^{-\lambda T}$ where T is the delay time between the collection chamber and the counter. Differentiating this with respect to T gives $\frac{\partial CR}{\partial T} = K_1 e^{-\lambda T} - K_1 \lambda T e^{-\lambda T}$. Setting this equal to zero to find the maximum count rate gives $1 - \lambda T = 0$ or $\lambda T = 1$. Since $\lambda = \frac{0.693}{T_{\frac{1}{2}}}$ where $T_{\frac{1}{2}}$ is the half life, we see that $T = \frac{T_{\frac{1}{2}}}{0.693}$. Thus the size of a peak will reach a maximum, relative to the other peaks, when its half-life is 0.693 times the delay time. Scans were run at 23, 9.3, 2 and 1 RPM. These four scans are shown in Figures 34 and 35. Table IX gives the relative sizes of the peaks in these four scans, compared to the peak at 0.098 Mev as 1.00. This was the most prominent
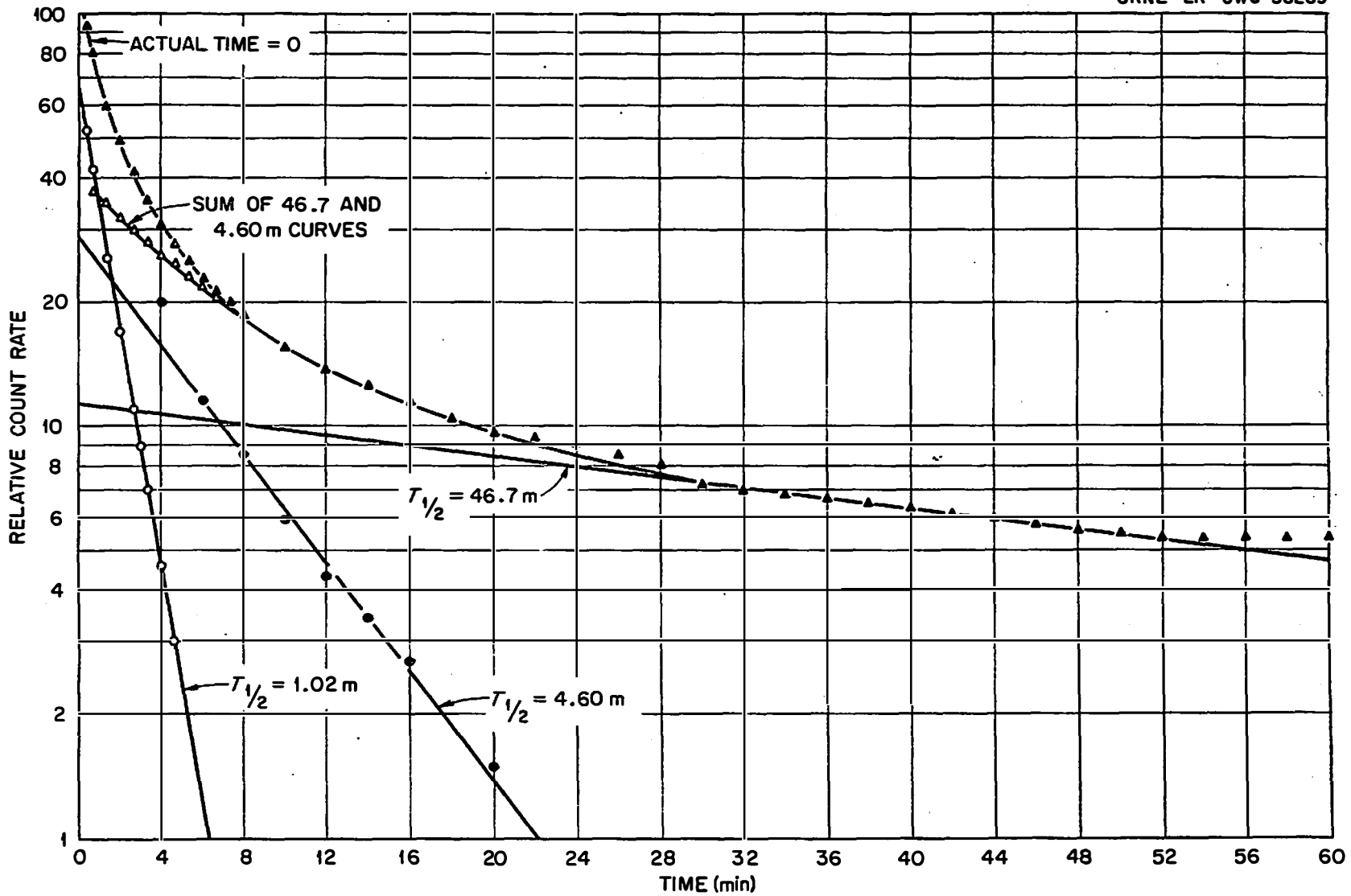
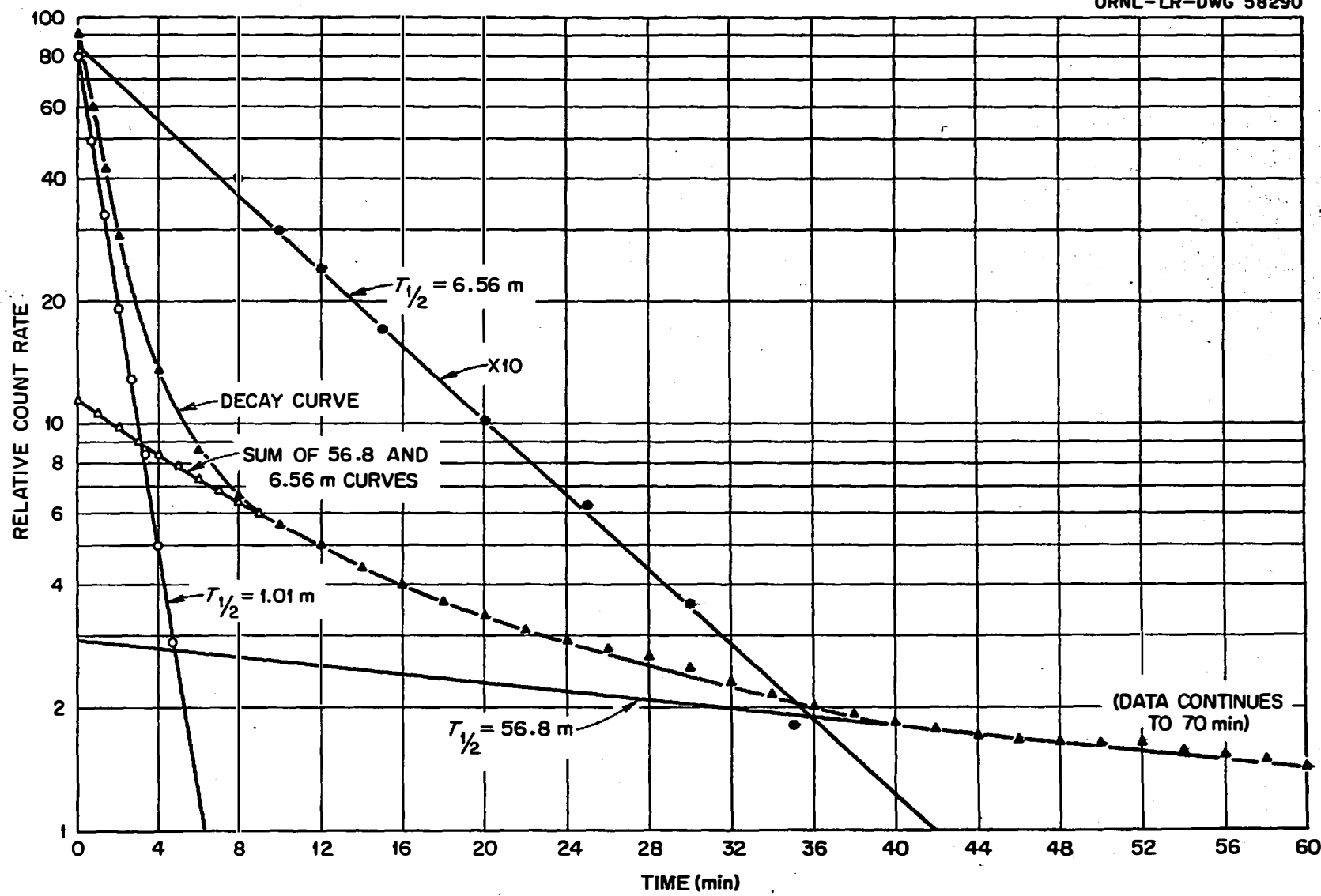Fig. 31. Decay of Trough at 0.05 Mev.
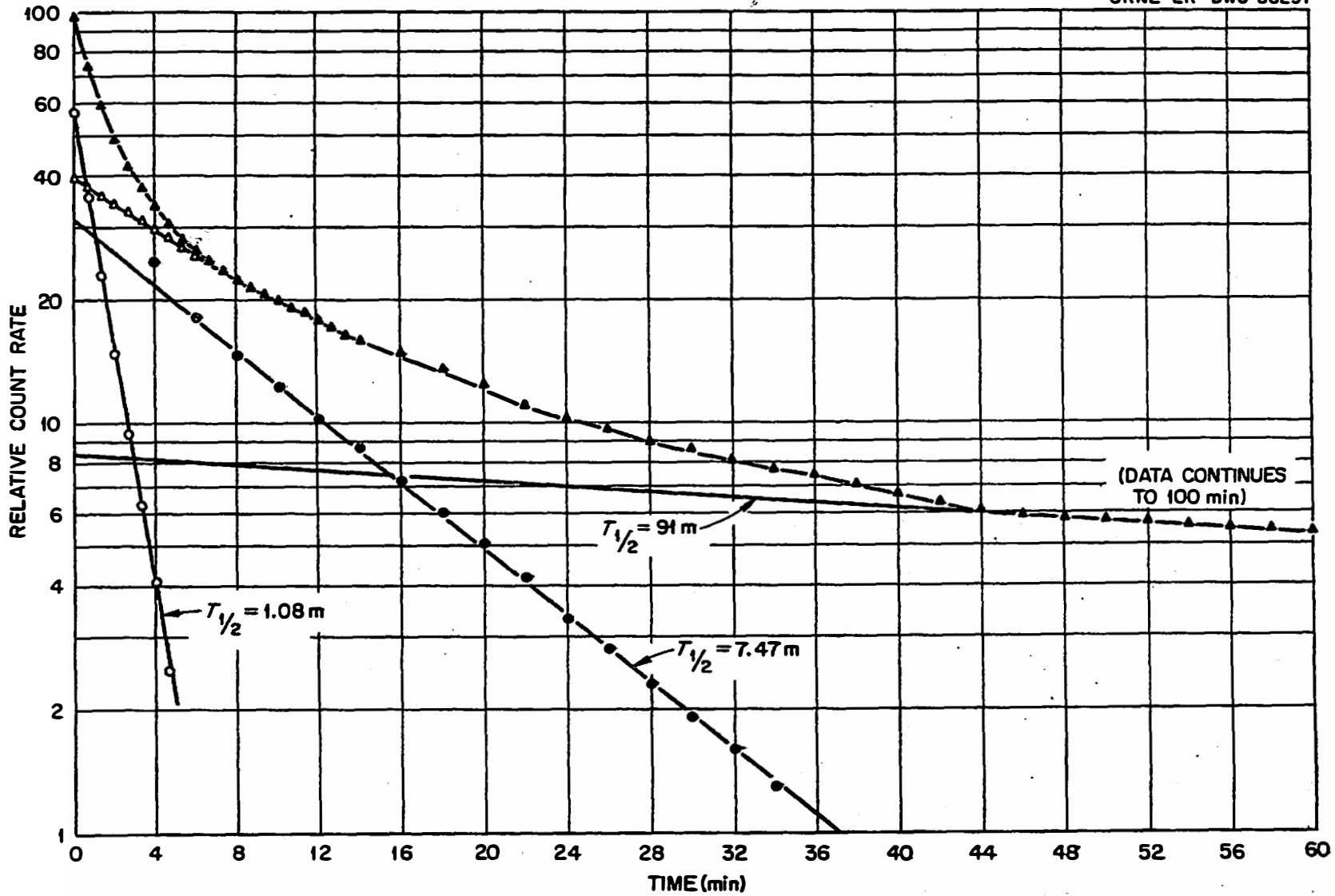
Fig. 32. Decay of Peak at 0.098 Mev.

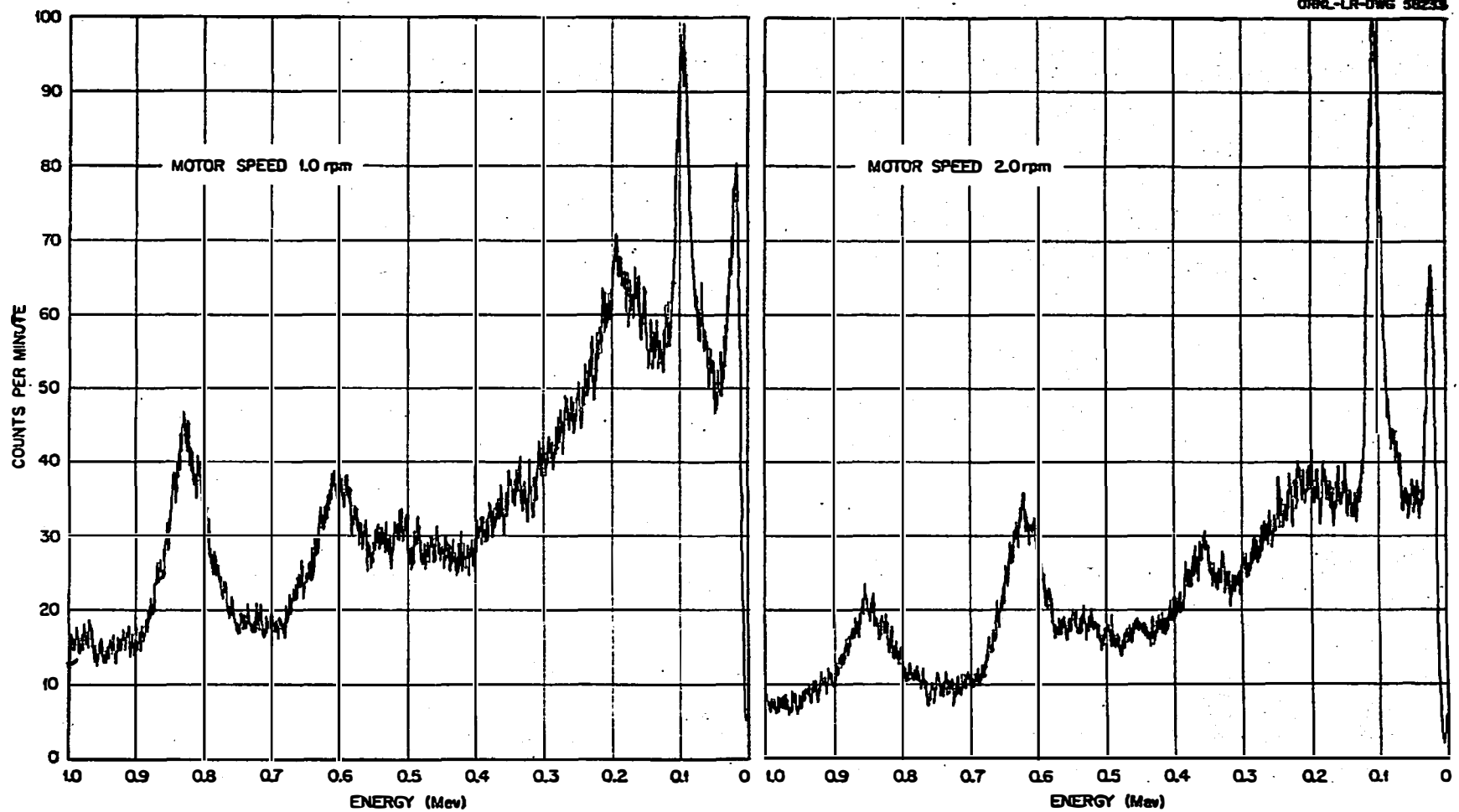Fig. 33. Decay of Trough at 0.130 Mev.
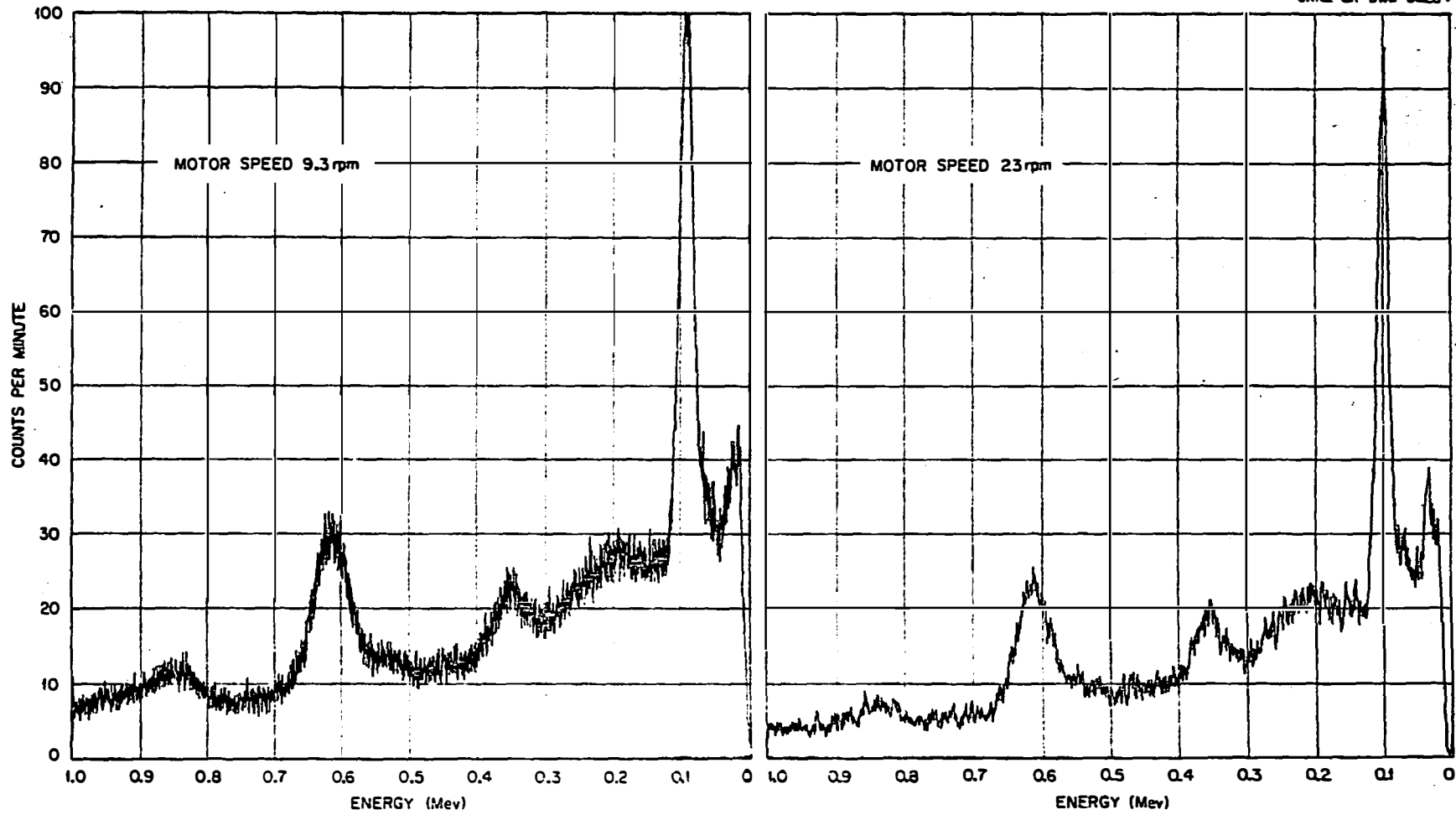
Fig. 34. Gamma Energy Scans at 1.0 and 2.0 rpm.

Fig. 35. Gamma Energy Scans at 9.3 and 23 rpm.

TABLE IX

RELATIVE PEAK SIZES AT VARIOUS WIRE SPEEDS

Motor Speed (RPM)	Delay Time (Minutes)	Peak Energy (Mev)	Relative Peak Size[a]	Predicted Absolute Magnitude
1	3.74	0.030	0.83	0.357
		0.098	1.00	0.430
		0.193	0.72	0.310
		0.601	0.385	0.166
		0.827	0.47	0.202
		0.352	- -	No peak
2	1.87	0.030	0.60	0.382
		0.098	1.00	0.636
		0.193	0.38	0.242
		0.601	0.35	0.222
		0.827	0.21	0.1335
		0.352	0.29	0.184
9.3	0.402	0.030	0.43	0.137
		0.098	1.00	0.319
		0.193	0.28	0.089
		0.601	0.31	0.099
		0.827	0.12	0.038
		0.352	0.24	0.077
23	0.162	0.030	0.41	0.131
		0.098	1.00	0.148
		0.193	0.23	0.073
		0.601	0.26	0.083
		0.827	0.08	0.026
		0.352	0.21	0.067

[a]Peak at 0.098 Mev was set as 1.00 in each case.

peak in all scans, and the one whose half-life (1.20 minutes) is best known from the decay data.

Assuming the measured half-life for the 0.098 Mev peak to be correct, we can obtain an estimate of the half-lives of the other peaks. In Table IX the calculated values of $Te^{-\lambda T} = CR/K_1$ are tabulated for $\lambda = \frac{0.693}{1.2} =$ 0.577 minutes^{-1}. These values are listed as "Predicted Absolute Magnitudes". The other values in this column were obtained by multiplying the relative peak sizes by the predicted absolute magnitudes for the 0.098 Mev peak. The results of this analysis are plotted in Figure 36. From the points plotted on this graph we see that the curves at 0.601 and 0.030 Mev have maxima in the region covered (0 to 4 minutes) while the other two energy curves are monotonic. This is an indication that the peaks at 0.601 and 0.030 Mev decay with approximately the same half-life as the 0.098 Mev peak, on the order of 1-2 minutes. The other two peaks have longer half-lives. This is in accord with the half-life measurements from decay. Unfortunately, no decays were run on the peak at 0.030 Mev.

This method of determining half-life showed considerable promise, but was limited in this study because only a few different wire speeds were available. A continuously variable wire drive would allow enough points to be collected for a good curve; a fairly good value of the half-life could then be obtained by fitting the theoretical equation to the curves.

By comparing the measured half-lives with the predicted relative count rates in Table VII, we can make tentative assignments of gamma energies to certain nuclides. Table X lists the expected nuclides in the
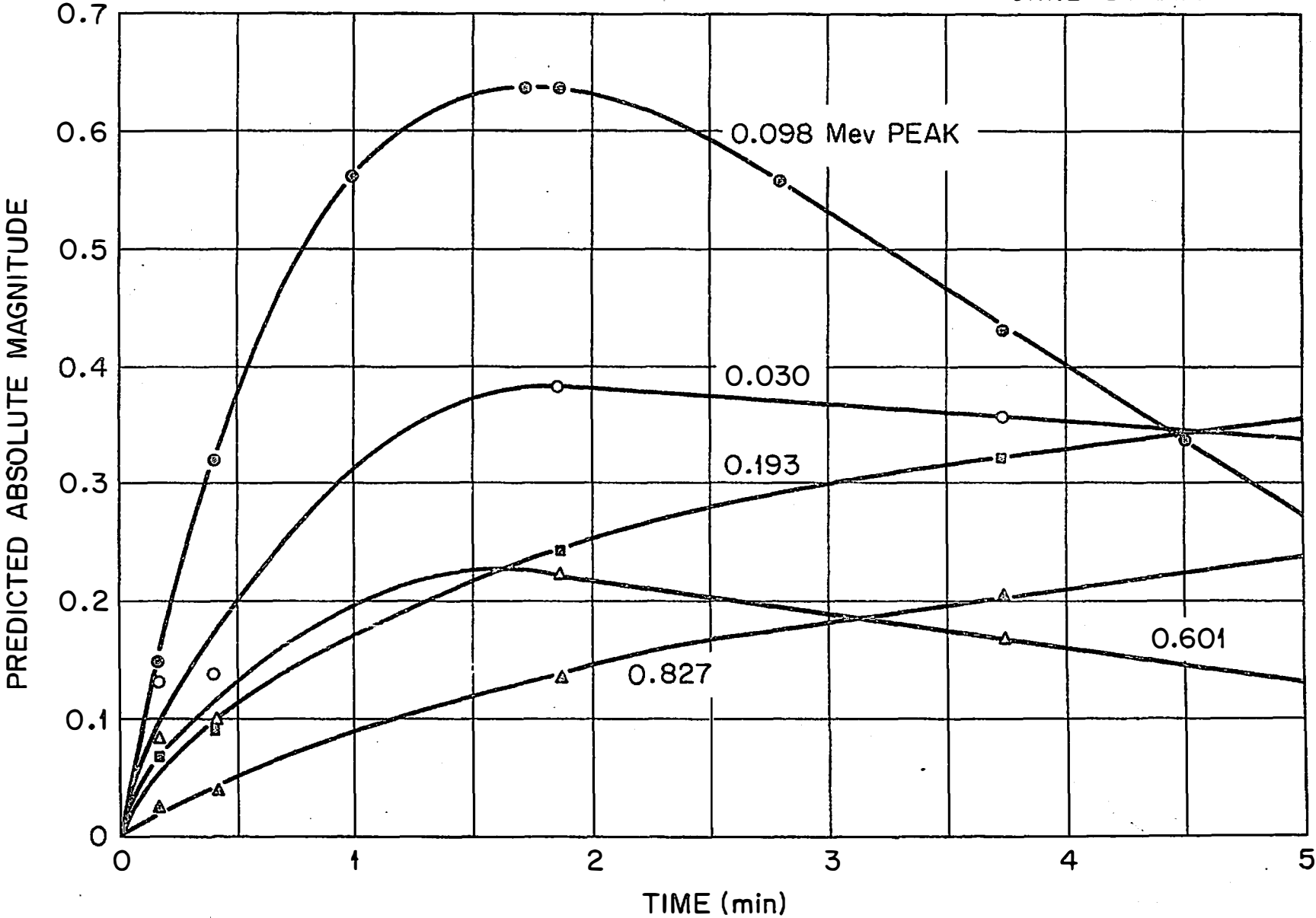
Fig. 36. Peak Sizes as a Function of Delay Time.

TABLE X

NUCLIDES IN ORDER OF PREDICTED RELATIVE COUNT RATE

Nuclide	Half Life (Minutes)	Predicted Relative Count Rate
Cs^{139}	9.5	44.3
Sr^{93}	8.2	20.8
Sr^{94}	1.3	20.4
Kr^{89}	3.2	14.6
Xe^{139}	0.684	12.0
Kr^{90}	0.55	11.8
Rb^{90}	2.74	6.92
Xe^{137}	3.8	5.21
Rb^{91m}	1.67	3.91[a]
Ba^{142}	6	3.89
Ba^{141}	18	3.87
Y^{95}	10.5	2.90
Sr^{95}	0.7	2.74
Cs^{140}	1.1	2.22
Pr^{148}	2.0	1.98

[a]Or less. See note on Table VII.

order of their predicted count rates, for those nuclides where this value is above 1.0. It is immediately apparent that only one nuclide of high relative count rate has a half-life near 1.2 minutes, namely, strontium-94. The only other nuclide with this approximate half-life is cesium-140, whose predicted count rate is only 1/10 that of strontium-94. Therefore, the identity of the isotope producing the peaks at 0.098 and 0.601 Mev is suspected to be strontium-94. The assignment for the other half-lives found is not so clear-cut. The peak at 0.193 Mev appears to be of slightly longer half-life than the average for the median half-life region. This could be possible if the peak were due to cesium-139, while the background arose mostly from strontium-93.*

Two of the rare gases with high predicted count rates have half-lives somewhat shorter than 1 minute. No half-lives were found in this region, with the exception of a very small "tail" on the 0.827 Mev peak. This leads to the possibility that the rare gas atoms do not cling to the FGD wire; that they are drawn there as ions and neutralized, but do not adhere to the charged stainless steel surface. If this hypothesis is correct, then krypton-89, xenon-139, krypton-90 and xenon-137 will not appear in the counting chamber in significant concentrations. This also means that the peak at 0.827 Mev, with a measured half-life of 4.23 minutes, would have to be ascribed to rubidium-90, with a reported half-life of 2.74 minutes. The resolution of this decay curve was not as

---

*It is interesting to note in this connection that the peak at 0.193 Mev is more variable than the others being studied; it is quite strong at times, as in Figure 30, but weak at other times, as in Figure 34 (2 RPM scan). This would seem to indicate that the nuclide responsible for this peak is released more strongly at certain times, i.e., after long irradiation, than at others.

satisfactory as most of the others, so this matchup does not seem improbable.

Of the other isotopes listed, there is some indication that barium-141 might be detected above 0.827 Mev, where other low energy activities do not mask it. The other nuclides, rubidium-91m, yttrium-95, strontium-95, cesium-140 and praseodymium-148, have relatively low count rates and half-lives that are close to those of the higher count-rate nuclides. Their presence would probably be masked by those species. However, it should be recalled that of the nuclides listed, only barium-141 and barium-142 have known gammas; the count rate computed is actually proportional to the disintegration rate or the beta emission rate. The fraction of disintegrations which result in gammas can vary widely, from zero to more than 1. This unknown factor introduces an additional uncertainty into the assignment of gamma energy values to specific nuclides. Also, the half-life data on these nuclides is not very reliable. No attempt will be made to identify the longer-life isotopes present on the wire. A multi-channel analyzer would be very helpful in determining the identify of these constituents.

CHAPTER V

THE QUANTITATIVE USE OF THE FGD

A. Determination of Absolute Release Rates

The original purpose of the Fission Gas Detector was to act as a leak detection device which would give warning of the first failure of cladding material on a metal-clad fuel element. The purpose of this research has been to extend this capability to measure the amount of fission product leakage from either a cladding defect or an unclad specimen. The desired result is the absolute release rate for a given mass chain under the conditions of test operation. This number we have already labeled EQ in section D of Chapter IV. In order to obtain an absolute release rate, we must identify and count some particular isotope; we have seen that with some degree of confidence we can detect strontium-94 and probably strontium-93 and cesium-139. These nuclides should be representative of the decay chains originating as halogens or rare gases, which account for a large part of the fission product activity given off by fuel under irradiation.

By considering the case of a single-predecessor nuclide, we can describe the count rate as the product of 6 factors, analogous to the terms of section D, Chapter IV: (1) The number of predecessor atoms released from the fuel sample per minute; (2) the fraction of atoms released which have formed ions by decay of the predecessor at the time they reach the collection chamber; (3) the collection efficiency of the wire; (4) the disintegration rate of the material collected by the wire; (5) the counting

efficiency of the detector for the gamma peak being measured; (6) the gamma branching ratio of the nuclide being counted. The case for more than one predecessor is somewhat more complicated, in that the first two terms cannot be written as factors; the other factors will be the same.

Considering these factors in order, we recall from section D, Chapter IV that factor (1) was given by (1) = R = 60 GYEQ. In this formula, G is the number of fissions in the fuel sample per second, Y is the fission yield, and EQ is the absolute release rate. The fission rate G can be calculated from the fuel weight using the formula,

$$G = \frac{W \times 6.02 \times 10^{23}}{235} \times 590 \times 10^{-24} \times \phi = 1.51\ W\ \phi$$

where W is the weight in grams of uranium-235 in the sample, ϕ is the reactor neutron flux in neutrons/cm.^{2}/sec., 590×10^{-24} is the fission cross section for uranium-235 and a factor of 60 is put in to convert to fissions per minute. The fission yield Y can be obtained from the data tabulations mentioned earlier.

The second term is given by, (2) = U = $\frac{P\ (1 - D)\ B}{F}$ where P is the plateout factor, D is the recombination factor and F is the total air flow over the sample in SCFM. The factor B is given by,

$$B = \frac{\lambda_a}{\lambda_b - \lambda_a}\ (e^{-\lambda_a t} - e^{-\lambda_b t})$$

using the notation of the previous chapter. For normal operation, the recombination factor D will approach 0, as has been shown. The plateout factor P should be near 1 for the isotopes of interest, but more radiochemical studies of the exit air piping are needed to establish accurate values for this factor. The product of factors (1) and (2) gives the number of ions per standard cubic foot of air entering the FGD chamber.

Factor (3), the collection efficiency of the wire, was discussed at length in sections A and B of the last chapter. From the measurements presented there, an optimum set of conditions can be specified for FGD operation. These conditions are high wire voltage (500 volts) and low air flow (less than 1 SCFM). Under these conditions, the ions just entering the chamber will be drawn immediately to the wire with a collection efficiency near 1. The wire voltage in this region is not critical, as the count rate changes slowly with voltage. However, the count rate varies directly with air flow in this region; thus the third factor will reduce to (3) = 1 x f. When a lower wire voltage is desired for some reason such as detector saturation at high voltages, then the count rate-voltage curves of Chapter IV can be used to obtain the fraction of the plateau counting rate corresponding to the voltage in use.

The product of the three factors just discussed will give the number of ions per minute of a given nuclide being collected by the FGD wire. This will, of course, be independent of the wire speed; to get the ion concentration per inch of wire, we must divide by the wire speed. At 2 RPM, this is 5.55 inches per minute. If we let N = number of ions per inch of wire, then $N = \frac{(1) \cdot (2) \cdot (3)}{5.55}$. The disintegration rate of N atoms is obtained by multiplying by the decay constant, λ: dpm = λN when λ is in minutes^{-1}. This is the initial decay rate of the ions as they are collected on the wire. A time T of 1.87 minutes elapses before these ions enter the counting shield, so the disintegration rate per inch of wire at this point is given by, dpm = $\lambda N e^{-\lambda T}$. Now, there are 11 inches of wire exposed in the counting shield, so the total disintegration rate of material in the chamber is dpm = 11 x $\lambda N e^{-\lambda T}$ or dpm = $\frac{11 \times \lambda e^{-\lambda T}}{5.55}$ x (1)·(2)·(3) =

$2\lambda e^{-\lambda T}$ (1)·(2)·(3) at a wire speed of 2 RPM. This treatment makes one important assumption which has not been stated: That the half-life of the material being counted is long compared to the time the wire is in the counting shield, which is 2 minutes. This, of course, is not true for several of the nuclides being considered.*

For short half-life nuclides, the dpm per inch as the wire enters the shield is dpm = $\lambda Ne^{-\lambda T}$ and as the wire leaves, 2 minutes later, it is dpm = $\lambda Ne^{-\lambda(T + 2)}$. To convert this to dpm per minute of wire exposure, we must multiply by 5.55. The total disintegration rate of a given nuclide within the shield can be obtained by integrating between the above limits:

$$dpm = \int_{t=0}^{2} 5.55 \ \lambda \ Ne^{-\lambda(T + t)} \ dt =$$

$$5.55 \ \lambda Ne^{-\lambda T} \int_{0}^{2} e^{-\lambda t} \ dt = -5.55 \ Ne^{-\lambda T} \ e^{-\lambda t} \Big|_{0}^{2}$$

so dpm = $5.55 \ Ne^{-\lambda T} (1 - e^{-2\lambda})$. Substituting for N gives

$$dpm = (1)\cdot(2)\cdot(3) \ e^{-\lambda T} (1 - e^{-2\lambda}).$$

When the half-life is long relative to 2 minutes (so that λ is small), this reduces to dpm = $(1)\cdot(2)\cdot(3) \ e^{-\lambda T}\cdot 2\lambda$, which is the expression previously derived assuming no depletion of material on the wire. An error of about 10 per cent results from using a half-life of 7 minutes with the

---

*In Chapter IV, section D, this problem did not appear because only the disintegration rate per cm. of wire was calculated. This introduces an error into the relative count rate tabulations, but this error should be less than the uncertainty in relative release rate Q. The error will cause the calculated values of count rate for short half lives to be too high.

simplified formula; the error increases rapidly as the half-life becomes
shorter. Factor (4) can thus be written as, $(4) = e^{-\lambda T} (1 - e^{-2\lambda})$ for
a wire speed of 2 RPM. In general, if the time spent in the shield is
designated by θ, we can say $(4) = e^{-\lambda T} (1 - e^{-\lambda\theta}) =$ disintegration rate
of material in the detector shield.

The detector efficiency, factor (5), has been determined experi-
mentally for cobalt-60 to be 16.3 disintegrations per count (above 0.05
Mev). The efficiency for the two gamma peaks of cobalt-60, at 1.16 and 1.33
Mev, can be determined from a gamma scan of the cobalt standard.[136] This
efficiency determination consists essentially of measuring the area under
the gamma peak of interest and relating this to the disintegration rate.
Then when a different source having the same geometry is used, the efficiency
for detection of the emitted gammas will depend only on the energy of the
gamma. A good approximation for gammas above 0.2 Mev can be obtained solely
from knowledge of the sodium iodide gamma cross section $\mathcal{T}$ at various energies.
The efficiency for one of the cobalt peaks could be related to a gamma peak
of different energy by this method. For more accurate work, the effect of
the particular geometry of the FGD would have to be taken into account.
This is a rather complicated problem; elementary cases have been discussed
by P. R. Bell[131] and Heath.[121] The assistance of a computer is required to
solve any but the simplest of these calculations. Of course, by using ad-
ditional standards other than cobalt-60 in the FGD geometry, the crystal
efficiency for different gamma energies could be measured experimentally.

Note that in the case of constantly-decaying material on the wire,
that is when the half-life of the nuclide being counted is less than $\sim$7
minutes, the geometry is no longer approximated by the cobalt wire standard.

This is because the wire has a higher disintegration rate near the top of the shield. One way this difficulty could be circumvented is by using a high wire speed, so that the decay taking place as the wire crosses the chamber is small, and determining the efficiency at this speed. Then the peak size could be experimentally related to that at a slower speed. Another problem in the quantitative application of peak measuring to yield efficiency is the background created by nuclides on the wire other than the one of interest. By running a decay of the peak being measured, the fraction of decay due to the gamma of interest can be measured, as in Table VIII. However, because of all the quantities requiring individual attention for any given gamma, no simple expression for the crystal efficiency can be written. Therefore factor (5), the fraction of gammas emitted which are detected, will be designated as $J(\gamma)$, where γ is the sodium iodide gamma cross section at the energy of interest.

The last factor in determining the count rate is the gamma branching ratio of the nuclide whose peak is being counted, that is, the fraction of disintegrations which result in a particular gamma energy. In the case of cobalt-60, both gammas are emitted with every disintegration; in the majority of nuclides, however, the per cent of disintegrations producing a given gamma is less than 100 per cent and can be less than 1 per cent. The tabulation of nuclear data in Nucleonics[127] gives some idea of the variations in gamma branching ratio for different nuclides. Obviously, since the gamma energies for most of the expected isotopes are not known, no gamma branching ratios will be known. Therefore, at the present time factor (6) cannot be determined; this lack of information also produces uncertainties in nuclide

identification, as mentioned in the last chapter. Factor (6) will be designated by the letter L, which denotes the gamma branching ratio for the nuclide under consideration.

As our analysis of the use of FGD for determination of absolute release rates now stands, the first 5 factors which influence the count rate can be determined (although more experimental work may be needed on factor (5)); but no information is available on the gamma branching ratios of the expected isotopes. When the decay schemes for these short-lived nuclides have been worked out, direct calculation of release rates should be feasible. Gathering all of our terms into one equation gives,

$$\text{Count Rate} = 90.6 \text{ W } \phi \text{ Y EQ} \cdot \frac{P(1-D)}{F} \cdot \frac{\lambda_a}{\lambda_b - \lambda_a} (e^{-\lambda_a t} - e^{-\lambda_b t}) \cdot$$

$$f \cdot e^{-\lambda T} (1 - e^{-\lambda \theta}) \cdot J(\gamma) \cdot L$$

where

W = weight of uranium-235, grams.

ϕ = reactor neutron flux, neutrons/cm.^{2}/sec.

Y = fission yield for nuclide being counted.

EQ = absolute release rate for given nuclide =

fraction of atoms produced by fission which escape the fuel material

P = plateout factor = fraction of atoms released from fuel which reach the collection chamber.

D = recombination factor = fraction of ions produced by decay of predecessor which recombine before reaching collection chamber ($\cong$ 0).

F = total air flow over fuel specimen, SCFM.

λ_a = decay constant of predecessor, minutes^{-1}.

$\lambda = \lambda_b$ = decay constant of expected nuclide, minutes^{-1}.

t = air flow time from fuel specimen to collection chamber, minutes.

f = air flow through the collection chamber, SCFM

T = delay time from collection chamber to counting shield, minutes.

θ = time that FGD wire remains within counting shield, minutes.

J (Υ) = detector efficiency for the gamma peak being counted, in

counts per emitted gamma.

L = gamma branching ratio = fraction of disintegrations which result

in a gamma of the energy being counted.

This equation assumes high voltage-low flow operating conditions; when these conditions are not present, additional corrections must be made. The equation for two predecessors differs from this in the exact form of terms (1) and (2) in a manner discussed in the last chapter.

B. Measurement of Release Rates as a Function of Time

Even though the FGD cannot, at present, be used to give an independent value for the absolute release rate, it can be used in conjunction with other release measurement methods such as charcoal trapping to determine release rates. For this purpose it should be sufficient to monitor only the total count rate, as recorded by the log count rate meter. The count rate equation given in the last section was for a single nuclide; if we isolate those factors which are common for all nuclides and imagine that the remainder is summed over all nuclides present, we can write

$$\text{Total Count Rate} = K \, W \, \phi \, \frac{f}{F} \cdot EQ$$

where K is a constant under constant operating conditions. Here the term
EQ represents a quantity proportional to total fission product release for
short half-life isotopes. This equation allows immediate application of
the FGD to measurement of relative fission product release. If some par-
ticular test condition employing reproducible fuel specimens is set as a
standard, then the release rate for other specimens under changed conditions
(such as longer irradiation, different temperature or humidity) can be
compared. In this sense, the FGD can measure progress in fuel element de-
velopment where a reduction in fission product release is the desired re-
sult.

These relative release rates can be converted to absolute release
measurements if the relative count rate can be shown to follow one of the
components determined by charcoal trap analysis. Thus far, no attempt has
been made to correlate the two measurements; since the isotopes determined
by charcoal trap analysis have much longer half-lives than those found on
the FGD, it may be that the release mechanisms are different and the re-
lease rates do not follow each other. However, there is a good chance that
at least some mass chains can be measured by this technique. There is also
the possibility that one of the isotopes found in charcoal trap analysis
will correspond to the relative count rate of one of the gamma energy peaks
on the FGD, instead of the gross count rate. Periodic scans under standard
conditions will show any change in the nature of the material being re-
leased when total count rate is being measured.

C. The Use of the FGD as a Research Instrument

The usefulness of the FGD both as a research tool and for fission product release measurements could be greatly enhanced by making several changes in the system. These changes are:

1. Extend the air flow control system so that flows down to one-tenth those presently used would be available, or provide a delay tank so that the air would require up to 10 times as long to travel to the collection chamber when the tank was in the line.

2. Employ a wire drive mechanism with continuously variable wire speed, remotely controlled and measured. This should provide delay times from about 1 second to 1 hour or longer.

3. Employ a multichannel pulse height analyzer in the place of the presently installed single channel analyzer.

Consider first the use of long delay times coupled with gamma energy measurements. A delay time of 1 hour would allow the 1.2 and 7 minute components to decay essentially completely, and the gamma peaks remaining would be from longer-lived nuclides. Now, the gamma energies and decay schemes for many of these longer-lived nuclides are known, so that absolute release rates for some isotopes should be available.

To examine the effect of expanded flow rates and wire speed, recall the factors in the count rate equation which involve the air transit time t and delay time T:

$$\text{Count Rate } \alpha \ (e^{-\lambda_a t} - e^{-\lambda_b t}) \ \frac{\lambda_a}{\lambda_b - \lambda_a} \ (\lambda_b T e^{-\lambda_b T})$$

where the problem of decay within the shield has been neglected and use was made of the fact that wire speed $\alpha \frac{1}{T}$. This expression is for the case of a single-predecessor nuclide; the more complicated case of two predecessors can be treated in an analogous fashion. What we wish to do is find values of T and t which will produce a maximum count rate for a given value of λ_a and λ_b. We have already seen that the term $\lambda_b Te^{-\lambda_b T}$ reaches a maximum when $\lambda_b T = 1$. The wire speed can be adjusted to give a delay time T satisfying this equation. Considering now the term dependent on t, we have

$$\text{Count Rate} = \text{CR} \ \alpha \ (e^{-\lambda_a t} - e^{-\lambda_b t}) \ \frac{\lambda_a}{\lambda_b - \lambda_a} \ .$$

The choice of a nuclide will fix the values of λ_a and λ_b. Differentiating with respect to t, we have

$$\frac{\partial \text{CR}}{\partial t} = \frac{\lambda_a}{\lambda_b - \lambda_a} (- \lambda_a e^{-\lambda_a t} + \lambda_b e^{-\lambda_b t}) = 0$$

at the maximum. This means that $\lambda_a e^{-\lambda_a t} = \lambda_b e^{-\lambda_b t}$ or $\frac{\lambda_a}{\lambda_b} = e^{(\lambda_a - \lambda_b)t}$. A value of t can be found to satisfy this equation, when λ_a and λ_b are given.

As an example of how these equations can be used, consider the case of cesium-140, which is of interest because barium-140 in the same mass chain can be determined by charcoal trapping. The decay constant for cesium-140 is 0.630 minutes^{-1}. Imposing the conditions that $\lambda T = 1$ gives $T = \frac{1}{0.630} = 1.59$ minutes. This is fairly close to the delay time at 2 RPM of 1.87 minutes. The predecessor for cesium-140 is xenon-140, with a decay constant of 2.60 minutes^{-1}. Inserting this value of λ_a with $\lambda_b = 0.630$ into the equation $\frac{\lambda_a}{\lambda_b} = e^{(\lambda_a - \lambda_b)t}$ gives $4.13 = e^{1.97t}$ so that

t = 0.720 minutes or 43 seconds. This value of the air transit time is quite a bit longer than the 3.8 seconds used in the scans which have been analyzed. However, with these values of t and T made available through modification of the FGD system, the prospect of measuring release rates in mass chain 140 is good.

The main advantage to be realized from the use of a multichannel analyzer over a single channel is the ease of treating quantitative data. This has been discussed by Heath[121] and other sources. A multichannel analyzer would also permit scans of the gamma spectrum of the wire at any point during a decay, so that the decay of the entire spectrum could be followed at once, instead of by separate decays at isolated energy values. However, multichannel analyzers, as mentioned previously, are more expensive and require more maintenance work than single channel analyzers; they would be less desirable for routine measurement of fission product release.

CHAPTER VI

SUMMARY

One of the devices which has found use in the measurement of fission products in the exit stream from a gas-cooled reactor or in-pile test is the wire-precipitation Fission Gas Detector (FGD). The operational characteristics of a fission gas detector of this type installed in a test loop utilizing position F-2 of the Oak Ridge Research Reactor have been studied in order to adapt this device to quantitative fission product release measurements. The operation of the FGD is as follows: Fission products released into the coolant air will become positively charged by emission of a beta particle; a sample of the air is conducted into a collection chamber through which runs a negatively charged wire. The positive fission product ions are drawn to the wire, which continuously moves through the chamber. Particles adhering to the wire are carried before a scintillation detector, where subsequent decays are counted. Since fission products often have multiple beta decays while other interfering nuclides have only one, this produces an effective separation of fission products from neutron activation products.

Fuel samples of uniform release rate were used to obtain data on the response of the FGD with wire voltage, sample air flow and wire speed. At low voltage the count rate is linear with wire voltage; as the voltage increases an equation of the form, count rate $= K_1 e^{-K_2\sqrt{V}}$ is followed; at about 200 volts the count rate reached a plateau and did not increase as the voltage was raised further. At low wire voltage and high air flows (about 2 SCFM)

the count rate was independent of air flow; at high voltages and low flows (less than 1 SCFM) the count rate is directly proportional to the flow. Between these extremes the count rate follows the equation, count rate = $C_1Fe^{-C_2\sqrt{F}}$. The count rate-wire speed measurements gave a curve which was approximated by the equation, count rate = $\dfrac{C_1}{S}\, e^{-C_2/S}$ where S is the wire speed.

The gamma spectrum and decay of material on the FGD wire were determined under varying conditions, in an effort to identify the nuclides present. Lack of information on the gamma energies of short half-life fission products prevented firm identification, but constituents with 1.2, 7 and about 60 minute half-lives were found. The 1.2 minute activity was found associated with gamma peaks at 0.098 and 0.601 Mev, and tentatively identified as strontium-94. Other nuclides thought to be major contributors to the wire activity were strontium-93 and cesium-139. With minor changes, the FGD can be adapted to give a high relative count rate for any of the several nuclides expected to be present on the wire in moderate concentrations.

BIBLIOGRAPHY

BIBLIOGRAPHY

1. H. S. Isbin, in H. Etherington, Ed., "Nuclear Engineering Handbook," McGraw-Hill Book Co., Inc., New York, 1958, p. 124.

2. _Ibid._, pp. 124-141.

3. _Nucleonics_, 14, No. 2, 45 (1956).

4. 86th Congress, 1st session, "Aircraft Nuclear Propulsion Program: Report of the Joint Committee on Atomic Energy," U. S. Government Printing Office, Washington, D. C., p. 10.

5. W. J. Price, "Nuclear Radiation Detection," McGraw-Hill Book Co., Inc., New York, 1958, p. 152.

6. J. T. Kummer, _Nucleonics_, 3, No. 1, 27 (1943).

7. R. J. Kokes, H. Tobin, Jr. and P. H. Emmett, _J. Am. Chem. Soc._, 77, 5860 (1950).

8. A. G. Engelkeimer, W. H. Hamill, M. H. Inghram, W. F. Libby, _Phys. Rev._, 75, 1825 (1950).

9. C. V. Robinson, _Rev. Sci. Instr._, 22, 353 (1951).

10. C. V. Robinson, _Nucleonics_, 13, No. 11, 90 (1955).

11. R. Wolfgang and F. S. Rowland, _Anal. Chem._, 30, 2908 (1958).

12. R. Wolfgang and C. F. Mackay, _Nucleonics_, 16, No. 12, 69 (1958).

13. R. F. Glascock, _Nucleonics_, 9, No. 5, 28 (1951).

14. A. V. G. Grosse and co-workers, _Science_, 113, 1 (1951).

15. L. Melander, _Acta Chem. Scand._, 2, 440 (1948).

16. M. L. Eidinoff and J. E. Knoll, _Science_, 112, 250 (1948).

17. D. F. White, I. G. Campbell and P. R. Payne, _Nature_, 166, 629 (1950).

18. G. Nilsson and G. Aniansson, _Nucleonics_, 13, No. 2, 38 (1955).

19. J. B. Birks, "Scintillation Counters," McGraw-Hill Book Co., Inc., New York, 1953.

20. S. A. Korff, "Electron and Nuclear Counters," 2nd Ed., D. Van Nostrand Co., Princeton, N. J., 1955.

21. M. A. Dillis and D. H. Taysum, Nucleonics, 13, No. 2, 68 (1955).

22. H. P. Kallmann, M. Furst and F. H. Brown, Nucleonics, 14, No. 4, 48 (1956).

23. C. Eggler and C. M. Huddleston, Phys. Rev., 95, 600 (1954).

24. C. Eggler and C. M. Huddleston, Nucleonics, 14, No. 4, 34 (1956).

25. J. A. Northrup and R. Nobles, Nucleonics, 14, No. 4, 36 (1956).

26. A. Sayres and C. S. Wu, Rev. Sci. Instr., 28, 758 (1957).

27. L. H. Tung and H. G. Drickamer, J. Chem. Phys., 20, 6 (1952).

28. H. G. Drickamer, K. D. Timmerhaus and L. H. Tung, Chem. Eng. Progr., 49, 503 (1953).

29. L. L. Mai and A. L. Babb, Nucleonics, 13, No. 2, 52 (1955).

30. J. B. Evans and J. E. Willard, J. Am. Chem. Soc., 78, 2908 (1956).

31. B. B. Rossi and Hans H. Staub, "Ionization Chambers and Counters," McGraw-Hill Book Co., Inc., New York, 1949.

32. D. H. Wilkinson, "Ionization Chambers and Counters," Cambridge University Press, London, 1950.

33. F. C. Henriques, Jr. and Charles Margnetti, Ind. Eng. Chem. Anal. Ed., 18, 417 (1946).

34. W. P. Jesse, L. A. Hannum, H. Forstat and A. L. Hart, Phys. Rev., 71, 478 (1946).

35. K. E. Wilzbach, A. R. Van Dyken and L. Kaplan, Anal. Chem., 26, 880 (1954).

36. C. D. Janney and B. J. Moyer, Rev. Sci. Instr., 19, 667 (1948).

37. G. L. Brownell and H. S. Lockhart, Nucleonics, 10, No. 2, 26 (1952).

38. M. A. Bullen, Nucleonics, 11, No. 12, 15 (1953).

39. P. Reisz and K. E. Wilzbach, J. Phys. Chem., 62, 6 (1958).

40. A. T. Wilson and M. Calvin, J. Am. Chem. Soc., 77, 5948 (1955).

41. W. R. Kanne, U. S. Patent 2,625,657 (Jan. 1953).

42. J. J. Fitzgerald and B. W. Borelli, Knolls Atomic Power Laboratory, Publication KAPL-1231 (1954).

43. B. M. Tolbert, University of California Radiation Laboratory at Berkley, Publication UCRL-3499 (1956).

44. C. J. Borkowski, USAEC Doc. MDDC 1099 (declassified June 12, 1947).

45. H. F. Schulte, in H. Blatz, Ed., "Radiation Hygiene Handbook," McGraw-Hill Book Co., Inc., New York, 1959, pp. 20-22.

46. B. C. Eutsler, G. L. Evans, R. D. Hieber, R. N. Mitchell, M. C. Robbins and R. J. Watts, Nucleonics, 14, No. 9, 114 (1956).

47. C. E. Lapple, in J. H. Perry, Ed., "Chemical Engineers Handbook," 3rd Ed., McGraw-Hill Book Co., Inc., New York, 1950, p. 1013.

48. I. Langmuir, OSRD Rept. 865 (1942).

49. E. A. Ranskill and W. L. Anderson, J. Colloid Sci., 6, 416 (1951).

50. C. Y. Chen, Chem. Rev., 55, 595 (1955).

51. Private communication from H. C. Butler.

52. D. R. Sawle, Nucleonics, 14, No. 8, 90 (1956).

53. J. B. H. Kuper, E. H. Foster and W. Bernstein, Nucleonics, 6, No. 4, 44 (1950).

54. T. H. Mansfield, Nucleonics, 10, No. 9, 55 (1952).

55. H. V. Watts, A. R. Brauner, G. M. Burgwald and L. Rieffel, Nucleonics, 13, No. 1, 51 (1955).

56. J. B. Hursh, University of Rochester Atomic Energy Project, Publication UR-258 (undated).

57. J. B. Hursh and A. A. Gates, Nucleonics, 7, No. 1, 46 (1950).

58. W. E. Browning and C. C. Bolta, Oak Ridge National Laboratory, Publication ORNL-2116 (1956).

59. R. E. Adams and W. E. Browning, Oak Ridge National Laboratory, Publication ORNL-CF-58-4-14 (1958).

60. R. E. Adams and W. E. Browning, Oak Ridge National Laboratory, Publication ORNL-CF-58-5-59 (1958).

61. R. E. Adams and W. E. Browning, Oak Ridge National Laboratory, Publication ORNL-CF-58-7-71 (1958).

62. R. E. Adams and W. E. Browning, Oak Ridge National Laboratory, Publication ORNL-CF-58-12-10 (1958).

63. W. E. Browning, R. E. Adams and R. D. Ackley, Oak Ridge National Laboratory, Publication ORNL-CF-59-6-47 (1959).

64. J. B. Trice, Ed., General Electric-Aircraft Nuclear Propulsion Department, Publication XDC 58-9-16 (1958).

65. G. W. C. Tait, Nucleonics, 14, No. 1, 53 (1956).

66. K. R. May, J. Sci. Instr., 22, 187 (1945).

67. H. F. Johnstone and M. H. Roberts, Ind. Eng. Chem., 41, 2417 (1949).

68. S. Laskin, R. H. Wilson and K. Lauterbach, "Encyclopedia of Instrumentation for Industrial Hygiene," University of Michigan, Ann Arbor, Michigan, 1956.

69. P. Drinker and T. Hatch, "Industrial Dust," 2nd Ed., McGraw-Hill Book Co., Inc., New York, 1954.

70. R. D. Thomas, Nucleonics, 17, No. 5, 134 (1959).

71. D. R. Whittel, National Gas Turbine Establishment, Great Britain, Publication NGTE-R-139 (1953).

72. M. Pobereskin, D. N. Sunderman, et al., Battelle Memorial Institute, Publication BMI-1146 (Del.) (1956).

73. R. A. Dewes, Knolls Atomic Power Laboratory, Publication KAPL-M-RAD-2 (1957).

74. G. N. Kinchin, United Kingdom Atomic Energy Authority Research Group, Atomic Energy Establishment, Publication FRDC/P-165 (1956).

75. C. M. Gordon and J. I. Hoover, Nucleonics, 15, No. 1, 91 (1957).

76. H. C. Rieck, C. A. Ratcliffe and L. C. Schwendiman, Hanford Atomic Products Operation, Publication HW-61117 (1959).

77. L. C. Schwendiman, A. C. Kieck and R. A. Harvey, Proc. U. N. Intern. Conf. Peaceful Uses Atomic Energy, 2nd Geneva, 1958, Vol. 23, A/CONF 23/P-394, p. 414 (1958).

78. R. L. Heath, Phillips Petroleum Co., Atomic Energy Division, Idaho Falls, Idaho, Publication IDO-16213 (1956).

79. R. L. Heath, Nucleonics, 15, No. 12, 54 (1957).

80. J. E. Howes, Jr., T. S. Elleman and D. N. Sunderman, Battelle Memorial Institute, Publication BMI-1432 (1960).

81. F. J. Witt, Knolls Atomic Power Laboratory, Publication KAPL-M-SMS-72 (1957).

82. P. R. Tunnicliffe and A. C. Whittier, Chalk River Project, Report RDP-51 (1953).

83. I. L. Fowler, A. Pearson and L. A. K. Watt, Nucleonics, 17, No. 1, 78 (1959).

84. N. P. Palladino, Westinghouse Atomic Power Division, Report WAPD-RD-87 (1955).

85. Atomic Energy of Canada, Ltd., British Patent No. 793,905 (April 23, 1958): Nuclear Power, 3, 298 (1958).

86. Nuclear Power, 3, 298 (1958).

87. D. Aliaga-Kelly, Nuclear Power, 4, 77 (1959).

88. Private communication from C. D. Cagle.

89. J. A. Cox and H. E. Seagren, Oak Ridge National Laboratory, Publication ORNL-2286, p. 1 (1957).

90. W. R. Kanne, United States Patent 2,599,922 (June 10, 1952).

91. J. Labeynie and A. Poguin, Proc. Intern. Conf. Peaceful Uses Atomic Energy, Geneva, 1955, Vol. 3, p. 85 (1955).

92. J. M. Markowitz, R. C. Koch and J. A. Roll, Westinghouse Atomic Power Division, Publication WAPD-180 (1957).

93. M. Fox, Proc. Intern. Conf. Peaceful Uses Atomic Energy, Geneva, 1955, Vol. 2, p. 353 (1955).

94. H. K. Ferguson Co., New York, "Brookhaven National Laboratory Design Manual," Publication M4412, Book I, Vol. 3, Part 4 (Declassified 1956).

95. J. Chernick and I. Kaplan, Brookhaven National Laboratory, Report BNL-20 (1948, declassified 1955).

96. F. W. Fenning and R. F. Jackson, United States Patent 2,807,580 (Sept. 24, 1957).

97. R. Livingston and H. A. Levy, United States Patent 2,576,616 (1949).

98. R. F. Jackson, Proc. Intern. Conf. Peaceful Uses Atomic Energy, Geneva, 1955, Vol. 2, p. 266 (1955).

99. Nucleonics, 14, No. 12, 520 (1956).

100. D. D. Bowen, Nuclear Power, 2, 91 (1957).

101. E. Long, J. M. Laithwaite and K. W. Cunningham, J. Brit. Nuclear Energy Conf., 2, 197 (1957).

102. F. Harlen, Nucl. Eng., 3, 158 (1958).

103. P. Barr and L. G. Ralfe, H. T. R. Division of Atomic Energy Research Establishment, Harwell, England, Publication AERE-M593 (1959).

104. J. Kaufman, Nuclear Safety, 1, No. 3, 33 (1960).

105. E. S. Collins, P. K. Conn and J. B. Trice, Nucl. Sci. and Eng. Supl., 2, No. 1, 209 (1959).

106. W. Lee, U. S. Naval Radiological Defense Laboratory, Publication USNRDL-TR-246 (1958).

107. N. E. Schofield, U. S. Naval Radiological Defense Laboratory, Publication USNRDL-TR-447 (1960).

108. J. A. Cox, F. T. Binford, C. D. Cagle, R. A. Costner and W. H. Tabor, Nucl. Sci. and Eng. Supl., 1, No. 1, 72 (1959).

109. P. R. Bell, in K. Siegbahn, "Beta and Gamma Ray Spectroscopy," Interscience Publishers, Inc., New York, N. Y., 1955, p. 132.

110. E. Fairstein, Rev. Sci. Instr., 27, 475 (1956).

111. F. E. Kinard, Nucleonics, 15, No. 4, 92 (1957).

112. L. A. Webb, U. S. Naval Radiological Defense Laboratory, Publication USNRDL-TR-48 (1955).

113. R. B. Murray and J. J. Manning, in Oak Ridge National Laboratory Report ORNL-2842, 193 (1959).

114. W. J. Price, "Nuclear Radiation Detection," McGraw-Hill Book Co., Inc., New York, 1958, p. 183.

115. F. P. Brauer and M. B. Laboeuf, Hanford Atomic Products Operation, Publication HW-28263 (1953, declassified Jan. 6, 1956).

116. R. L. Heath, Phillips Petroleum Co., Atomic Energy Division, Idaho Falls, Idaho, Publication IDO-16408, pp. 1-24-2 (1957).

117. B. B. Rossi and H. H. Staub, "Ionization Chambers and Counters," McGraw-Hill Book Company, Inc., New York, 1949, p. 18.

118. W. J. Price, "Nuclear Radiation Detection," McGraw-Hill Book Company, Inc., New York, 1958, p. 122.

119. J. D. Cobine, "Gaseous Conductors," McGraw-Hill Book Company, Inc., New York, 1941, Chap. 2.

120. National Research Council, "International Critical Tables, Volume VI," McGraw-Hill Book Company, Inc., New York, 1929, p. 111.

121. R. L. Heath, Phillips Petroleum Company, Atomic Energy Division, Idaho Falls, Idaho, Publication IDO-16408 (1957).

122. C. Crouthamel, "Applied Gamma-Ray Spectrometry," Pergamon Press, New York, 1960.

123. Nucleonics, 18, No. 11, 204 (1960).

124. W. E. Kuykendall and R. E. Wainerdi, Texas Engineering Experiment Station, Texas A and M College, Publication TEES-2565-1 (1960).

125. W. Zobel and G. M. Estabrook in R. E. Brocklehurst, Ed., Wright Air Development Center Report WADC TN 57-298, Pt. I, p. 189.

126. J. O. Blomeke, Oak Ridge National Laboratory, Report ORNL-1783 (1956).

127. Nucleonics, 18, No. 11, 186-210 (1960).

128. D. Strominger, J. M. Hollander and G. T. Seaborg, Rev. Mod. Phys., 30, 585 (1958).

129. C. Crouthamel, "Applied Gamma-Ray Spectrometry," Pergamon Press, New York, 1960, p. 343.

130. W. H. Sullivan, "Trilinear Chart of the Nuclides," Oak Ridge National Laboratory, Oak Ridge, Tennessee (1957).

131. P. R. Bell in K. Siegbahn, Ed., "Beta and Gamma-Ray Spectroscopy," Interscience Publishers, Inc., New York, 1955, pp. 132-165.

132. Private communication from Dr. P. K. Conn.

133. W. J. Price, "Nuclear Radiation Detection," McGraw-Hill Book Company, Inc., New York, 1958, p. 68.

134. L. E. Glendenin, C. D. Coryell and R. R. Edwards, in "Radiochemical Studies: The Fission Products," National Nuclear Energy Series, Div. IV, Vol. 9, McGraw-Hill Book Company, Inc., New York, 1951, p. 489.

135. G. Friedlander and J. W. Kennedy, "Nuclear and Radiochemistry," John Wiley and Sons, Inc., New York, 1955, p. 128.

136. R. L. Heath and F. Schroeder, Phillips Petroleum Co., Atomic Energy Division, Idaho Falls, Idaho, Publication IDO-16149 (1955).

APPENDIX

APPENDIX

ESTIMATION OF YIELDS FOR FISSION PRODUCT DECAY CHAINS

The calculations presented in Table VII require that the fission yields for the various predecessor nuclides be known. Some of these values have been measured; these are presented in the Nucleonics tabulation[123] and indicated in Table IV by underlining. Other yield values are listed in Blomeke;[126] these values were recommended by Glendenin and Steinberg on the basis of the "Equal Charge Distribution" rule.[133] From these two sources, cumulative yield values were found for most of the nuclides in Table IV. The remaining yields were estimated by a simple graphical procedure; these are indicated in the table by parentheses. The graphs used for this purpose are shown in Figures 37 through 39. On these graphs are plotted the known fission yields versus the mass number for a number of different elements. By simple extrapolation of the curves where no yields are known, either to parallel a measured element or as an extension of incomplete data, the yields of unmeasured nuclides can be estimated.

Fig. 37. Fission Yields for Mass Numbers 83-97.
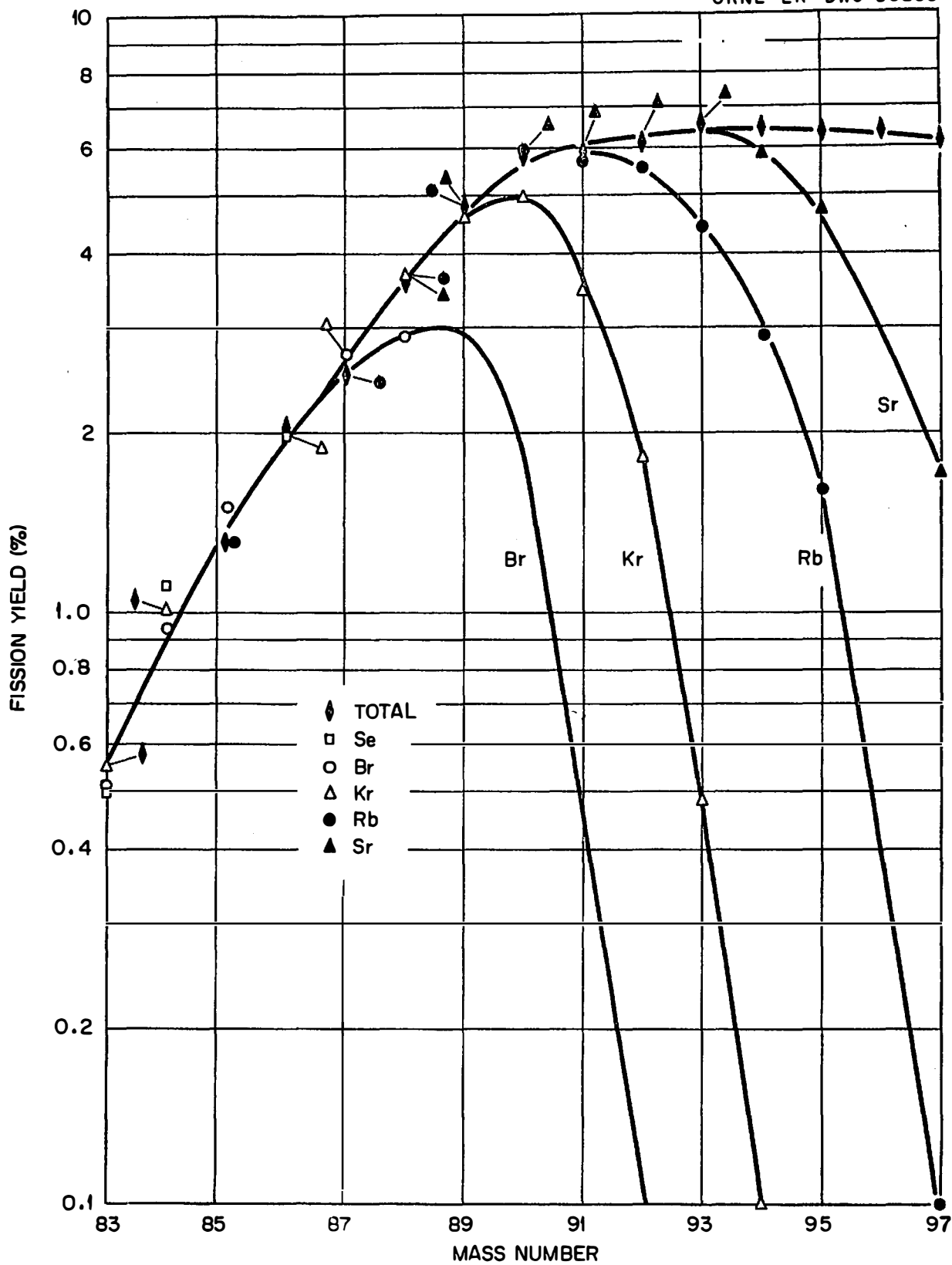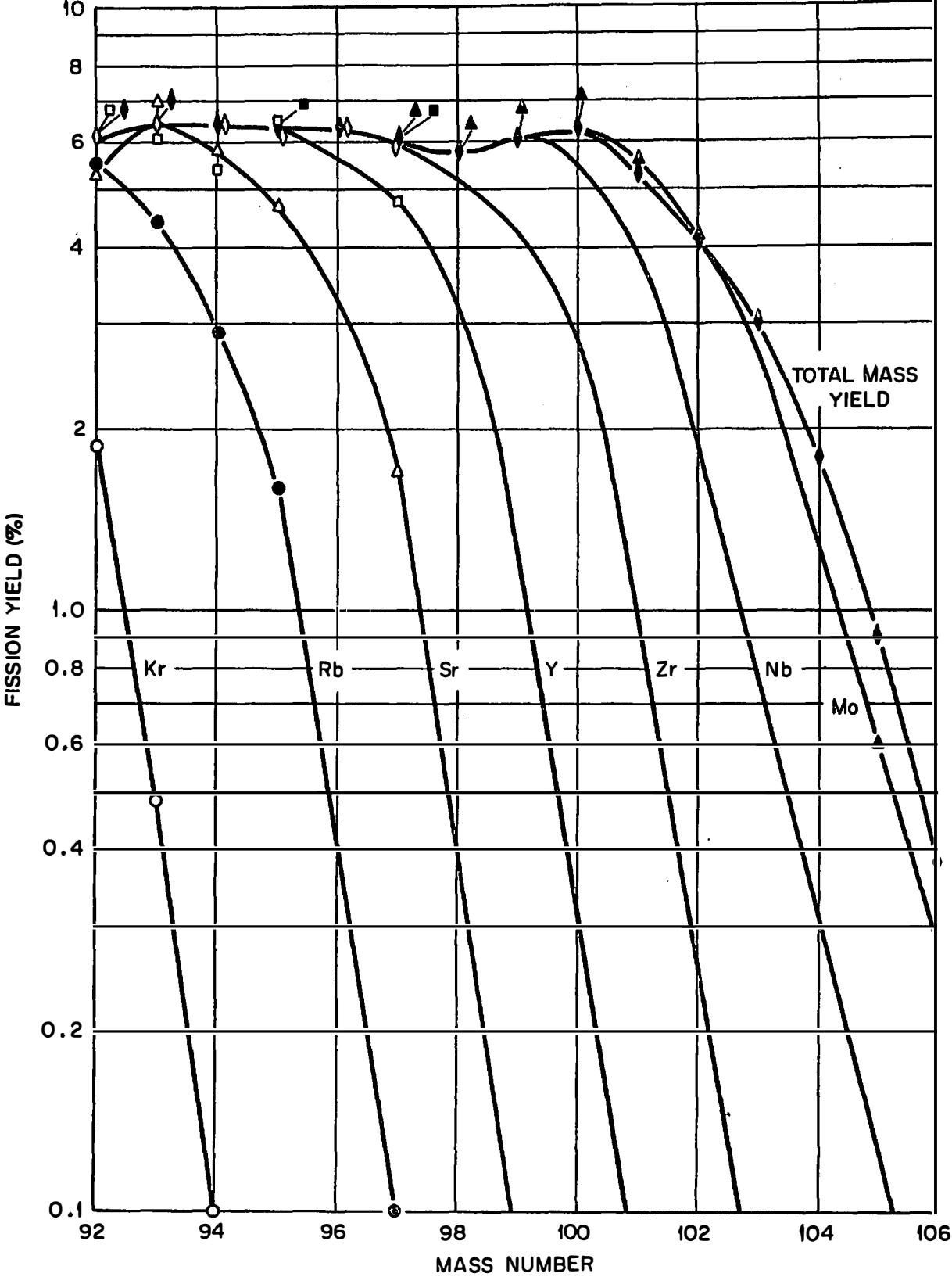
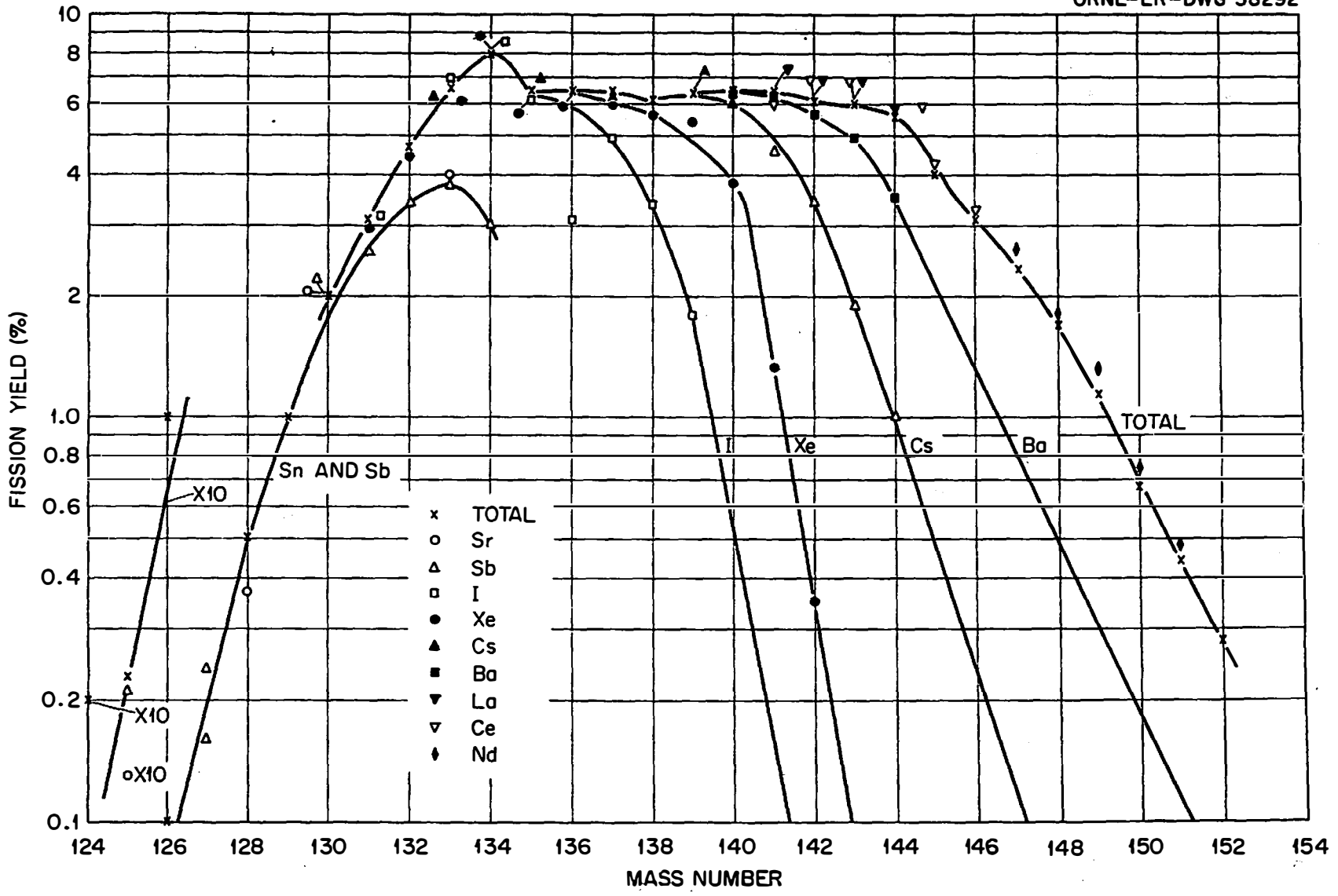Fig.38. Fission Yields for Mass Numbers 92 – 106.

Fig. 39. Fission Yields for Mass Numbers 124 − 152.

VITA

Raymond Curtis Lee was born in Dallas, Texas on October 22, 1929. He was educated in the public school system of Henderson, Texas, and was graduated from high school in May 1946. The following September he entered The Rice Institute in Houston, Texas and was graduated with a B. A. degree in June 1950. He continued his graduate work at Rice and received an M. A. before being called into the Navy in June 1953. He was discharged from the Navy three years later and took a job with the General Electric-Aircraft Nuclear Propulsion Department in Oak Ridge, Tennessee. He entered the Graduate School of The University of Tennessee, Oak Ridge Branch, in January 1957 while continuing his employment with General Electric.

The author is a member of the American Chemical Society, American Nuclear Society, Phi Lambda Upsilon and Sigma Xi.